UPPSALA
UNIVERSITET

Digital Comprehensive Summaries of Uppsala Dissertations from the Faculty of Science and Technology 191

Studies of Nuclear Fuel Performance Using On-site Gamma-ray Spectroscopy and In-pile Measurements

INGVAR MATSSON

ACTA
UNIVERSITATIS
UPSALIENSIS
UPPSALA
2006

ISSN 1651-6214
ISBN 91-554-6582-X
urn:nbn:se:uu:diva-6912

Dissertation presented at Uppsala University to be publicly examined in Sal 2001, Ångströmlaboratoriet, Uppsala, Wednesday, June 7, 2006 at 13:30 for the degree of Doctor of Philosophy. The examination will be conducted in English.

Abstract

Matsson, I. 2006. Studies of Nuclear Fuel Performance Using On-site Gamma-ray Spectroscopy and In-pile Measurements. Acta Universitatis Upsaliensis. *Digital Comprehensive Summaries of Uppsala Dissertations from the Faculty of Science and Technology* 191. 103 pp. Uppsala. ISBN 91-554-6582-X.

Presently there is a clear trend of increasing demands on in-pile performance of nuclear fuel. Higher target burnups, part length rods and various fuel additives are some examples of this trend. Together with an increasing demand from the public for even safer nuclear power utilisation, this implies an increased focus on various experimental, preferably non-destructive, methods to characterise the fuel.

This thesis focuses on the development and experimental evaluation of such methods. In its first part, the thesis presents a method based on gamma-ray spectroscopy with germanium detectors that have been used at various power reactors in Europe. The aim with these measurements is to provide information about the thermal power distribution within fuel assemblies in order to validate core physics production codes. The early closure of the Barsebäck 1 BWR offered a unique opportunity to perform such validations before complete depletion of burnable absorbers in Gd-rods had taken place. To facilitate the measurements, a completely submersible measuring system, LOKET, was developed allowing for convenient in-pool measurements to be performed.

In its second part, the thesis describes methods that utilise in-pile measurements. These methods have been used in the Halden test-reactor for determination of fission gas release, pellet-cladding interaction studies and fuel development studies.

Apart from the power measurements, the LOKET device has been used for fission gas release (FGR) measurements on single fuel rods. The significant reduction in fission gas release in the modern fuel designs, in comparison with older designs, has been demonstrated in a series of experiments. A FGR database covering a wide range of burnup, power histories and fuel designs has been compiled and used for fuel performance analysis. The fission gas release has been measured on fuel rods with average burnups well above 60 MWd/kgU. The comparison between core physics calculations (PHOENIX-4/POLCA-7) and the in-pool measurements of thermal power indicates that the nodal power can generally be predicted with an accuracy within 4% and the bundle power with an accuracy better than 2%, expressed as rms errors.

In-pile experiments have successfully simulated the conditions that occur in a fuel rod following a primary debris failure, being secondary fuel degradation. It was concluded that massive hydrogen pick-up takes place during the first few days following the primary failure and that a pre-oxidized layer does not function as a barrier towards hydriding in an environment with a very high partial pressure of hydrogen. Another series of in-pile experiments clearly indicate that increased UO_2 grain size is an effective way of suppressing fission gas release in LWR fuel up to the burnup level covered (55 MWd/kgUO_2).

Keywords: fission gas release, nuclear fuel, core physics, gamma-ray spectroscopy, LOKET, thermal power, burnup, fuel failure, validation, cladding

Ingvar Matsson, Department of Nuclear and Particle Physics, Nuclear Physics, Box 535, Uppsala University, SE-75121 Uppsala, Sweden

ISSN 1651-6214
ISBN 91-554-6582-X
urn:nbn:se:uu:diva-6912 (http://urn.kb.se/resolve?urn=urn:nbn:se:uu:diva-6912)

To my family,
Lena, Karin and Linnea

List of Papers

This thesis is based on the following papers, which are referred to in the text with their roman numerals:

I Matsson, I., Grapengiesser, G., Developments in Gamma Scanning of Irradiated Nuclear Fuel, *Applied Radiation and Isotopes*, 48(10-12), pp. 1289-1298 (1997).

II Matsson, I., Jansson P., Grapengiesser B., Håkansson A., Bäcklin A., Fission Gas Release Determination Using an Anti-Compton Shield Detector, *Nuclear Technology*, 122(3), pp. 276-283 (1998).

III Schrire, D., Matsson, I., Grapengiesser, B., Fission Gas Release in ABB SVEA 10x10 BWR Fuel, *Proceedings from the International Topical Meeting on LWR Fuel Performance*, Portland, Oregon, USA, March 2-5, 1997.

IV Grapengiesser, B., Matsson, I., Schrire, D., Fission Gas Release in ABB SVEA-96/100 Fuel, *Proceedings from the TopFuel '97 Conference*, Manchester, UK, June 9-11, 1997.

V Matsson, I., Grapengiesser, B., The Shut-down of the Barsebäck 1 BWR: a Unique Opportunity to Measure the Power Distribution in Nuclear Fuel Rods, Accepted for publication in *Annals of Nuclear Energy*, April 2006.

VI Matsson, I., Grapengiesser, B. Andersson, B., On-site Gamma-ray Spectroscopic Measurements of Fission Gas Release in Irradiated Nuclear Fuel, Submitted to *Applied Radiation and Isotopes*, April 2006.

VII Matsson, I., Grapengiesser, B. Andersson, B., LOKET- a Gamma-ray Spectroscopy System for In-pool Measurements of Thermal Power Distribution in Nuclear Fuel, Submitted to *Nucl. Instrum. Meth. A*, April 2006.

VIII Matsson, I., Turnbull, J.A., The integral fuel rod behaviour test IFA-597.3: Analysis of the measurements, *OECD Halden Reactor Project Report HWR-543* (1998).

IX Matsson, I., Teshima, H., The effect of fuel micro-structure and burn-up on FGR and PCMI studied in IFA-534.13, *OECD Halden Reactor Project Report HWR-546* (1998).

X Matsson, I., The Effect of Grain Size on FGR and PCMI in High Burnup Fuel (IFA-534.14) (Preliminary Results), *OECD Halden Reactor Project Report HWR-561* (1998).

XI Matsson, I., The Effect of Grain Size on FGR and PCMI in High Burnup Fuel (IFA-534.14), *OECD Halden Reactor Project Report HWR-558* (1999).

XII Broy, Y., Matsson, I., Reaction Kinetics of Oxidation and Hydriding Inside Operating Fuel Rods, *OECD Halden Reactor Project Report HWR-602* (1999).

XIII Limbäck, M., Dahlbäck, M., Hallstadius, L., Dalene, P.M., Devold, H., Vitanza, C., Wiesenack, W., Jenssen, H., Oberländer, B.C., Matsson, I., Andersson, T., Test-Reactor Study of the Phenomena Involved in Secondary Fuel Degradation, *Proceedings of the 2004 International Meeting on LWR Fuel Performance*, Orlando, Florida, September 19-22, 2004.

Reprints were made with permission from the publishers.

Author's Contribution and Comments

Papers I, II, V, VI and VII are based on analyses made by the thesis author and were also written primarily by the thesis author. All experimental work was shared between the thesis author and the co-authors.

Papers III and IV were primarily written by the thesis author whereas the responsibility concerning the conclusions and underlying experimental work was shared with the co-authors.

Papers VIII, IX, X, XI are based on analyses made by the thesis author and were primarily written by the thesis author. The thesis author was also responsible for the experimental setup and monitoring of the experiments in these in-pile measurements.

Paper XII was primarily written by co-author Yvonne Broy. The thesis author contributed with feedback on discussions and conclusions during the

preparation of the paper. The paper is based on a similar methodology as paper XIII.

Paper XIII is based on experimental work for which the thesis author was responsible concerning the in-pile measurements and interpretation of the in-pile data. The paper was not primarily written by the thesis author.

Papers I and II are refereed and published by international journals. Paper V has been accepted for publication in the Elsevier Journal Annals of Nuclear Energy. Papers VI and VI are also planned for publication in international scientific journals and have been submitted.

Papers III, IV and XIII are refereed international conference proceeding papers.

Papers XIII, IX, X, XI and XII are research reports issued by the OECD Halden Reactor Project within the Halden Work Report Series (HWR) and also presented at international conferences.

Contents

1 Introduction 13
1.1 Nuclear power 13
1.2 The nuclear fuel 15
1.3 Gamma scanning 17
1.4 In-pile studies 18

2 Scope of the thesis 19
2.1 Fuel performance studies and code validation 20
2.2 Fuel failure degradation 21

3 Nuclear fuel and its properties 22
3.1 Physical properties of UO_2 23
3.1.1 Properties of UO_2 and PuO_2 23
3.1.2 Fuel swelling and densification 23
3.1.3 Fuel microstructure 25
3.1.4 Thermal properties 25
3.2 Operational properties of nuclear fuel 26
3.2.1 Burnup 26
3.2.2 Volatile element migration 28
3.2.3 Thermal power 29
3.2.4 Fission gas release 31

4 Cladding properties 35
4.1 PCMI 35
4.2 Cladding corrosion and hydriding 36
4.3 Crud deposition 37
4.4 Fuel failures 38

5 Instrumentation and methods: Gamma scanning 41
5.1 Mechanical setup 41
5.1.1 Equipment in Sweden and Finland 41
5.1.2 LOKET 42
5.2 Detectors 46
5.3 Electronics 48
5.4 Computers and software 49
5.5 Fission gas release 50
5.6 Thermal power distribution 53
5.7 Correction for gamma-ray absorption in a fuel assembly 55

6 Instrumentation and methods: In-pile experiments 58
6.1 Fuel performance experiments 61
6.2 Fuel failure experiments 62

7 Results: Fuel performance studies performed by gamma spectroscopy 64
7.1 Paper I: Developments in Gamma Scanning of Irradiated Nuclear Fuel 64
7.2 Paper II: Fission Gas Release Determination Using an Anti-Compton Shield Detector 65
7.3 Paper III: Fission Gas Release in ABB SVEA 10x10 BWR Fuel 66
7.4 Paper IV: Fission Gas release in ABB SVEA-96/100 Fuel 66
7.5 Paper V: The Shut-down of the Barsebäck 1 BWR: a Unique Opportunity to Measure the Power Distribution in Nuclear Fuel Rods ... 67
7.6 Paper VI: On-site Gamma-ray Spectroscopic Measurements of Fission Gas Release in Irradiated Nuclear Fuel 68
7.7 Paper VII: LOKET- a Gamma-ray Spectroscopy System for In-pool Measurements of Thermal Power Distribution in Nuclear Fuel 69
7.8 Crud deposition measurements 71
7.9 Volatile element redistribution 73
7.10 Burnup 76
7.11 Conclusions and remarks 77

8 Results: Fuel performance studies by means of in-pile experiments ... 79
8.1 Paper VIII: The integral fuel rod behaviour test IFA-597.3: Analysis of the measurements 79
8.2 Paper IX: The effect of fuel micro-structure and burn-up on FGR and PCMI studied in IFA-534.13 81
8.3 Paper X and Paper XI: The Effect of Grain Size on FGR and PCMI in High Burnup Fuel (IFA-534.14) 82
8.4 Paper XII: Reaction Kinetics of Oxidation and Hydriding Inside Operating Fuel Rods 83
8.5 Paper XIII: Test-Reactor Study of the Phenomena Involved in Secondary Fuel Degradation 84
8.6 Conclusions and remarks 85

9 Outlook 86

Acknowledgements 89

Summary in Swedish 92
Kärnbränsle 92
Gammaspektroskopi 93
Mätningar i härd 96

References 98

Abbreviations

ADC	Analogue-to-digital converter.
ALHR	Average linear heat rate.
b	Barn, a unit for cross section of nuclear interaction. It could be interpreted as the probability for interaction.
BA	Burnable absorber.
BGO	Bismuth germanate ($Bi_4Ge_3O_{12}$). A scintillation material for gamma quanta detection.
BU	Burnup. The total amount of energy produced in nuclear fuel, i.e. thermal power integrated over time. BU is often expressed in the unit MWd/kgU.
BWR	Boiling water reactor.
CLAB	Swedish interim storage for spent nuclear fuel (Centralt mellanlager för använt kärnbränsle).
Crud	Deposit on the surface of a fuel rod, typically Zn and Fe oxides.
EPMA	Electron probe microanalysis.
FGR	Fission gas release. The fraction of gaseous fission products produced that has managed to escape to the rod free volume.
FWHM	Full width half maximum. Measure of the energy resolution of full energy peaks in a gamma-ray spectrum.
HBWR	Halden Boiling (Heavy) Water Reactor. Test reactor in Halden, Norway, with heavy water as moderator.
HPGe	High purity germanium detector.
HRP	Halden Reactor Project.
IFA	Instrumented fuel assembly.
keV	Kilo electron volt. The unit used for photon energy. 1 keV is equal to the kinetic energy of en electron that has been accelerated over a potential drop of 1 kV.
LHR	Linear heat rate.
LN_2	Liquid nitrogen. Used for cooling the high purity germanium detectors.
LVDT	Linear voltage differential transformer.
LWR	Light water reactor.
MLHR	Maximum linear heat rate.
MOX	Mixed oxide fuel. Reprocessed fuel that is a mixture of

	oxides of uranium and plutonium.
MWd/kgU	Megawatt days of thermal energy produced per kg of uranium that was initially present in the fuel. A unit for burnup (BU).
$MWd/kgUO_2$	Megawatt days of thermal energy produced per kg of uranium dioxide that was initially present in the fuel. An alternative unit for burnup (BU).
NEA	Nuclear Energy Agency.
NIM	Nuclear Instrumentation Module. A standard developed for electronic units used in nuclear data-acquisition systems.
NPP	Nuclear power plant.
OECD	Organization for Economic Co-operation and Development.
PCI	Pellet cladding interaction.
PCMI	Pellet cladding mechanical interaction.
PIE	Post irradiation examination.
ppm	Parts per million.
PWR	Pressurized water reactor.
rms	Root mean square errors.
SKB	Swedish Nuclear Fuel and Waste Management Company. Company jointly owned by the nuclear operators and responsible for the final deposition of spent nuclear fuel in Sweden.
SKI	The Swedish Nuclear Power Inspectorate.
SPECT	Single photon emission computed tomography.
TFDB	Test Fuel Data Bank. Database for experimental data collection, handling and presentation used at the Halden experimental reactor.
TRP	Transistor Reset Preamplifier.
WID	Water ingress device.
XRF	X-ray fluorescence analysis.

1 Introduction

This thesis consists of a comprehensive summary, based on thirteen scientific papers and technical reports. It describes non-destructive measurements, based on high-resolution gamma-ray spectroscopy and in-pile detection technology. Specifically, the thesis describes measurements on nuclear fuel assemblies and fuel rods of the boiling water reactor type and, to some extent, of the pressurized water reactor type. The measurements have been performed during a number of years on nuclear fuel irradiated in commercial reactors in Sweden, Finland, Spain, Switzerland and at the Halden experimental reactor in Norway. For several reasons like safety, efficiency, safeguard and computer code benchmarking, knowledge of the behaviour of nuclear fuel in-pile is needed. The thesis basically compiles the results of a significant number (more than 30) of research reports produced within projects issued by ABB/Westinghouse, the OECD Halden Reactor Project and the Swedish Nuclear Power Inspectorate (SKI).

1.1 Nuclear power

Currently approximately 17% of the world's electric energy is produced by fission in nuclear power plants (NPP). There are more than 430 nuclear reactor units in operation and some 30-40 are under construction, mainly in Asia. In Sweden ten nuclear reactors are operating and serving the grid as in April 2006, producing about half of the electric energy in the country averaged over the year. The utilization of nuclear power has been a political concern in many countries during the last 20-30 years, as a consequence of accidents/severe events like Three Mile Island (TMI or Harrisburg) and Chernobyl as well as the long-term storage problems related to the highly radioactive waste produced in the form of spent fuel. In some countries, e.g. Sweden and Germany there are currently plans to phase out nuclear power. On the other side there are increased global concerns over the emission of carbon dioxide from fossil fuels (oil, coal and natural gas), possibly with global warming as a consequence, as well as the increased needs for electric energy, especially in developing countries, but also in the industrialized countries as it turns out. These latter issues have driven the construction and planning of new nuclear power plants as mentioned especially in Asia, but recently also in Finland (a 1600 MW pressurized water reactor unit). Re-

cently the debate concerning the future role of nuclear power for the worlds energy needs has also been addressed both by the US and EU. This should also be viewed in light of the concerns over the possible near future shortness of oil, assuming that the production of oil is close to its historical peak and that new, real large oil fields are not discovered anymore the so-called peak oil debate [1]. Furthermore, the geopolitical situation concerning the large scale producers of oil and natural gas complicates the situation.

The process that generates the energy is the fission reaction, where a heavy nucleus, such as uranium or plutonium, splits up in fission products after interacting with a slow neutron. The amount of energy released in this process is larger, by more than seven orders of magnitude in comparison to a chemical process like e.g. combustion of coal, oil, natural gas or wood. Typically 2-3 neutrons are emitted in the fission process, which in turn may create new fission reactions and a self-sustained chain reaction can be maintained for continuous and controlled production of thermal energy that in turn can be transformed to electrical energy.

There are a number of different reactor types and concepts in operation worldwide. The most common type is the light water reactor or LWR that include boiling water reactors (BWR) and pressurized water reactors (PWR). In a BWR the water in the core is heated to boiling. The steam is lead through a turbine system that in turn is connected to an electric generator feeding the electric grid. The exhausted steam is condensed back to water and fed back into the core in a closed circuit. In a PWR core boiling is prevented by operating the reactor at a significantly higher pressure as compared with a BWR unit. Steam is instead produced in separate heat exchangers.

The water in a LWR core is used not only for the converting the thermal energy released in the fission process to electrical energy, it is also required for cooling the fuel used for the moderation or thermalization of neutrons. The neutrons initially emitted in the fission process have a too high kinetic energy to efficiently induce new fission reactions. Therefore, their energy has to be decreased (moderated) by repeated collisions with nuclei in a suitable light material e.g. water. Eventually the neutrons reach thermal equilibrium with the surrounding material i.e. they have become thermalized. The moderating property of water is one of the great advantages of LWR cores (in combination with attractive system behaviour from a system control perspective in terms of time constants and feedback mechanisms) and is the main reasons why they have come to dominate the nuclear industry.

There is however a number of other commercial reactor concepts like graphite-moderated cores (like e.g. Chernobyl type of reactors), cores cooled with carbon dioxide (e.g. Magnox reactors in the UK) and heavy water moderated cores (e.g. Canadian CANDU reactors). In addition, a smaller number of more exotic reactor designs have been utilized.

1.2 The nuclear fuel

The nuclear fuel studied in this thesis is mainly of the BWR fuel type. BWR fuel is manufactured by stacking UO_2 pellets in zircaloy tubes of about 4 m length with a diameter of about 10 mm, which then constitutes a fuel rod. Zircaloy is an alloy based on Zirconium (Zr), an element with a low absorption cross section for thermalized neutrons hence it is a very suitable choice for in-core structural materials. The fuel rods are put together in assemblies with about 100 fuel rods in each. A fuel channel is surrounding the fuel rods through which the boiling water is guided. A standard BWR fuel assembly has a total mass of about 200 kg. A modern BWR fuel assembly is illustrated in Figure 1.1. The axial cross section is about 140x140 mm^2 for standard BWR assemblies. Examples of schematic cross sections for two basic designs are illustrated in Figure 1.2. There is an ongoing development of fuel designs in order to improve the in-core performance in various aspects. A more recent example of this is the introduction of part-length rods in the assemblies.

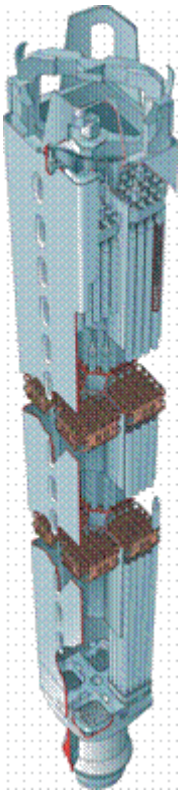

Figure 1.1. Illustration of a fuel assembly for BWRs. Reproduced by courtesy of Westinghouse Electric Sweden AB.

PWR type fuel has a fairly similar appearance, but contains more fuel rods, e.g. 17x17 fuel rods in the assembly cross section. The usage of nuclear fuel could be based on either a so-called once-through fuel cycle strategy or a strategy including reprocessing of the spent fuel. Both strategies start with mining, conversion and enrichment. The latter stage means that the uranium is enriched with respect to its fissile isotope ^{235}U (Table 1.1). Nuclear reactors of the LWR type typically require the fuel to be enriched in fissile ^{235}U to a concentration between 2% and 5%. Fuel of this isotopic composition is denoted as low-enriched nuclear fuel. Cores moderated by heavy water (D_2O) and graphite-moderated reactors could however be operated with uranium of lower enrichments in ^{235}U, even with natural uranium.

After irradiation the spent fuel may be reprocessed in a process where the remaining fissile nuclides (like e.g. ^{239}Pu) in the spent fuel are extracted in a series of complicated chemical and physical steps and used for the manufacturing of new fuel pellets/assemblies (e.g. MOX fuel).

In the once-through cycle the spent fuel is considered as waste and should be disposed off accordingly. The experimental studies in this thesis are concerned with fuel in the once-through cycle, as applied by e.g. Sweden, Switzerland and Finland Experiments have been performed during annual outage or after the in-core irradiation has been finished and the fuel is replaced.

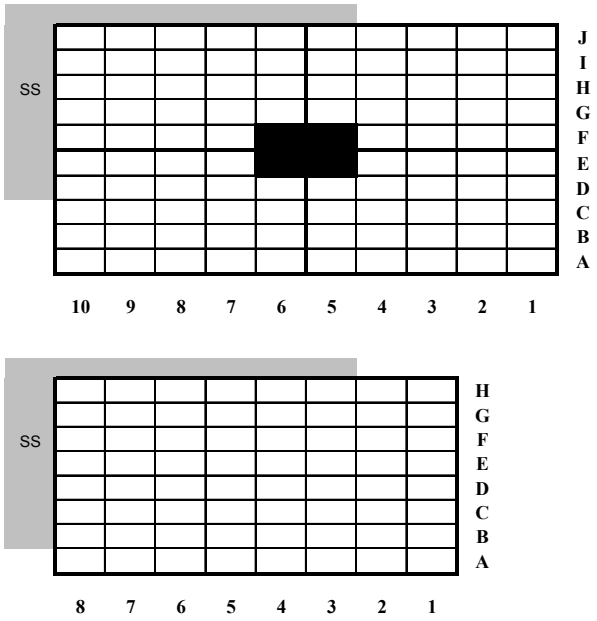

Figure 1.2. The highly schematic cross sections and rod numbering for the modern 10x10 type fuel (upper figure) and the older 8x8 type fuel (lower figure). SS denotes the control rod blade corner and the black cells illustrate the water cross in e.g. SVEA fuel.

Table 1.1: *Isotopic abundance of natural uranium.*

Isotope	Abundance [%]
^{238}U	99.2745
^{235}U	0.72
^{234}U	0.0055

The uranium generally enters the fuel fabrication as uranium hexafluoride (UF_6). During the fuel fabrication stage the enriched uranium is converted to uranium dioxide (UO_2). The UO_2 is sintered to fuel pellets, subsequently stacked in tubes and mounted in assemblies as outlined above. The reason for using UO_2 as fuel material is mainly that it has a very high melting point (2865°C).

Typically LWRs are operated in power cycles of about one year. An irradiation period is followed by a revision shutdown period for a number of weeks when the power plant systems are maintained and a part of the reactor core is exchanged with fresh fuel. A fuel assembly is irradiated for typically five or six such reactor periods, although shorter and longer irradiation might take place. When a fuel assembly has reached its final burnup it is positioned at the power plant storage facility for some time before being moved into some dedicated storage facility (e.g. CLAB in Sweden) awaiting the final storage in a deep geological repository or possibly reprocessing [2].

The fuel studied in this thesis is either irradiated fuel, that is fuel that has been used in power production and is intended to be used again, or spent fuel, that is fuel that will not be used in the reactor core again. Fuel studied in test reactors are either fresh fuel manufactured specifically for the experiment, or commercially irradiated fuel that has been remanufactured/redesigned in order to fit the experimental core.

1.3 Gamma scanning

The measurement techniques described in this thesis are high-resolution gamma-ray spectroscopy (e.g. gamma scanning) and experimental in-pile studies, see Section 1.4. Although denoted by gamma scanning (i.e. the measured object is moved in front of the measurement system), the definition as used in this thesis also applies for a fixed position measurement like for e.g. fission gas release measurements and the wordings gamma scanning and in-pool high-resolution gamma-ray spectroscopy are used interchangeably. In gamma scanning the gamma-ray flux emitted from unstable isotopes, whose production in some way correlates with various physical fuel parameters, is measured using high-resolution gamma-ray spectroscopy. The reason for using high-resolution gamma-ray spectroscopy is the generally very

complex energy spectrum from irradiated fuel. Normally, a high-purity germanium detector (HPGe) has therefore been used.

Gamma scanning has been used for the determination of e.g. burnup, axial power distribution, fuel integrity, and fission gas release as well as for safeguard purposes [3, 4, 5]. It is also an important tool for the verification of computer codes designed to calculate the characteristics of nuclear fuel [6, 7]. Measurements have been applied both on whole fuel assemblies and on single fuel rods (i.e. fuel assemblies are dismantled). The technique has also been applied for studies of crud deposition and migration of certain volatile elements in the fuel matrix (Cs and I). A more recent extension of the gamma scanning technique is emission tomography (SPECT) of nuclear fuel assemblies, where the gamma-ray flux distribution around a fuel assembly is recorded and the interior gamma-ray source distribution in a section of the assembly is reconstructed by computer-aided calculations [8, 9]. In this thesis the (non-tomography) gamma scanning technique has been applied to BWR fuel for determination of fission gas release (FGR), measuring thermal power distribution (e.g. core physics computer code validation), burnup determination, volatile element migration/redistribution in the fuel matrix and studies of crud distribution (indicative results).

1.4 In-pile studies

In-pile studies of nuclear fuel are here defined as experiments where the fuel is irradiated in a test reactor while certain physical properties and conditions are monitored (more or less) continuously. This is achieved by specially designed instrumented fuel assemblies (IFAs), capable of on-line monitoring of e.g. internal gas pressure, neutron flux and fuel temperature. In this thesis experiments have been performed in the Halden Boiling Water Reactor (HBWR) for the study of fission gas release and its dependence on UO_2 grain size and fuel temperature, as well as studies of secondary fuel failure degradation (i.e. in-pile simulations of fuel failures).

The two types of experiments (gamma scanning and in-pile measurements) complement each other and together allowing the determination of a wide spectrum of nuclear fuel performance indicators.

2 Scope of the thesis

It is sometimes argued that nuclear power is a mature technology (even old-fashioned), nevertheless one should keep in mind that it is actually the latest large-scale source of energy discovered (1930s) and utilized (1940s and onwards). New innovative reactor concepts are introduced from time to time where the South African pebble bed reactor project is one recent example as well as the research concerning accelerator-driven systems for transmutation of nuclear waste [10]. The high-level radioactive waste produced has to be thoroughly surveyed and controlled before it is finally deposited in a deep geological repository. Also the remaining fissile material has to be monitored. This is the safeguards aspect of the research within the field. In this thesis the following two areas have been identified where improvements and extensions of experimental nuclear fuel studies will offer continued progress:

- Nuclear fuel is expensive, although the fuel cost actually is a limited part of the total operating costs for a nuclear power plant in comparison to other sources of energy. Therefore the power plant operators want to use the fuel more efficiently and also to limit the amount of nuclear waste generated, which constitutes a significant back-end cost. Extended operating time of the fuel as well as new fuel designs requires increased knowledge of the fuel behaviour in-pile. The benchmarking of computer codes modelling the in-core performance requires high quality experimental data, preferably by non-destructive methods such as gamma scanning or test-reactor in-pile studies.
- Fuel failures, i.e. the damage of fuel rods in-core and the implication of increased activity in the primary cooling system. Such an event could eventually call for unplanned outage and has been identified as a separate issue here due to the immediate economical consequences. In order to understand the mechanism involved in the development of secondary fuel failure degradation, i.e. the possible more severe consequences of a primary failure where water enters the interior of a fuel rod, in-pile studies are required. These studies are, however, typically complemented by post irradiation examinations as well.

Within the scope of this thesis, non-destructive measurements on nuclear fuel have been further developed and performed on objects with highly different characteristics and at different stages in the nuclear fuel cycle. Al-

though it is a matter of definition weather test-reactor studies are considered as non-destructive examinations or not, they are treated as such in this thesis.

2.1 Fuel performance studies and code validation

At a commercial nuclear power plant, different types of measurements are performed in order to follow up on the behaviour of the reactor core. The neutron flux distribution is monitored during operations and during outage various measurements and visual inspections are performed on fuel assemblies removed from the core. Such measurements do not typically include gamma scanning of the fuel, but comprise measurements of parameters such as e.g. cladding oxide thickness (cladding corrosion) by means of electromagnetic methods, visual inspection of fuel assemblies and fuel channel bow measurements.

The operation of the reactor core relies to a large extent on core simulation based on extensive computer code packages. Such computer codes take into account the nuclear processes involved, the geometry of the fuel and the fuel distribution in the core. Together with the thermo-hydraulics of the coolant/moderator, the axial and lateral power distribution can be calculated down to single fuel rods. Such core simulators are often referred to as production codes. Other codes aim at simulating the physical processes within the fuel matrix, cladding and the pellet-cladding gap. Fuel centreline temperature, fission gas release, filling gas pressure and various thermo-mechanical properties are examples of evaluated physical parameters [11]. Events like e.g. excessive fission gas release or fuel swelling could eventually harm the integrity of the fuel and cladding, making non-destructive measurements of such physical behaviour highly valuable for benchmarking computer codes.

The necessity of validating production codes are generally recognized in the community of nuclear operators and among fuel and system suppliers. Since the modeling takes place down to the single fuel rod level, a need for experimental data both on whole fuel assemblies and single fuel rods are recognized. The introduction of new fuel designs as well as more flexible reactor operation cycles and power up-rating of reactor systems have even further increased the need for experimental data within the field.

In this thesis, measurements (gamma scanning and in-pile experiments/measurements) have been performed on BWR and PWR fuel of highly varying burnup and irradiation history with the purpose to investigate a number of fuel performance parameters (e.g. linear heat rate distribution, fission gas release, burnup, fuel pellet thermal properties and pellet cladding interaction) and how they relate to the history/usage of the fuel. This part is covered in Papers I-XI.

2.2 Fuel failure degradation

Improved quality control and design upgrading as well as improved control of the core operation have all contributed towards reducing the occurrence of in-pile fuel rod failures. However, a limited number of failures still occur in LWRs, primarily due to cladding fretting, hydriding or pellet cladding interaction [12]. When fuel rod cladding fails, coolant water enters into the fuel rod interior to equalize the pressure difference between the reactor vessel and the rod free space. The entrained water/steam reacts with both fuel pellets and the inner wall of the cladding to liberate hydrogen.

Efforts are being made in order to understand the mechanisms involved in the secondary fuel degradation subsequent to the primary failure. Massive local cladding hydriding is believed to be the main cause of such degradation and eventually a circumferential break in the cladding. Understanding the degradation process is extremely important to avoid large radioactivity levels in the plant circuits and costly unscheduled shutdowns for removing the leaking assembly.

In-pile experiments have been designed and performed in the Halden experimental reactor in order to study the dynamics of the phenomena involved in secondary fuel degradation after simulating a primary failure in a test loop. The experiment was performed using fuel rods of different design, pre-oxidized and with normal liner cladding. This part of the thesis work is accounted for in Papers XII and XIII. We will use the terminology secondary fuel degradation and secondary fuel failure degradation interchangeable in the thesis.

3 Nuclear fuel and its properties

In this chapter some basic parameters of the nuclear fuel are defined and discussed. The description is limited to the parameters covered in the work constituting this thesis and is not an attempt to fully cover the rather complex physics and chemistry involved.

When the nuclear fuel is irradiated in the reactor core, typically in a neutron flux density of about 10^{14} $cm^{-2}s^{-1}$, a wide variety of nuclear reactions and related physical processes occur. As a consequence the composition and the physical and chemical properties of the fuel (and also of the cladding) are altered with time. Fission products are created with half-lives ranging from fractions of a second to several decades. Neutron capture and decay of fission products and heavy nuclei also change the composition of the nuclear fuel during irradiation.

Other mechanisms contribute as well e.g. interaction takes place between the fuel pellets and the cladding, so called pellet-cladding mechanical interaction (PCMI) or pellet-cladding interaction (PCI). Fission gas release alters not only the physical properties of the fuel matrix through e.g. increased porosity, but also the composition of the gas in the free rod volume which affects its thermal resistance.

Thus, with time, the physical and chemical properties of nuclear fuel change quite dramatically. In fresh fuel the vast majority of the fissions are due to ^{235}U. The remaining part occurs in the much more abundant ^{238}U due to the fast neutron flux [13, 14]. During the irradiation ^{235}U is thus depleted, while other fissile nuclei are created, such as ^{239}Pu and ^{241}Pu through neutron capture in ^{238}U and successive beta decays. Towards the end of the irradiation, say after five reactor cycles or so, these new fissile nuclides normally contribute to the major part of the fission rate (about 80%) while the contribution from ^{235}U is only some 10% [13]. The altered elemental composition of the fuel inevitably leads to changed physical properties such as e.g. thermal conductivity degradation and changes in the fuel matrix microstructure and density.

3.1 Physical properties of UO_2

3.1.1 Basic properties of UO_2 and PuO_2

Uranium dioxide (UO_2) is a ceramic with the advantages of high-temperature stability and an adequate resistance to radiation. The melting point is very high (2865 °C), and it is chemically inert to attack by hot water. The most important physical properties of UO_2 are summarized in Table 3.1.

Table 3.1: *Some basic physical properties of uranium dioxide.*

Property	**Value**
Melting point	2865±15 °C
Crystal structure	Face-centered cubic
Lattice parameter	0.5465 nm
Theoretical density[a)]	10.96 g/cm^3
Thermal conductivity	~8.4 Wm^{-1}K^{-1} (20 °C)
Thermal expansion coefficient	~10^{-5} (0 to 1500 °C)
Specific heat	63.6 Jmol^{-1}K^{-1} (25 °C)
Fracture strength	~110 MPa
Modulus of elasticity	2.0 (at 20 °C)

[a)] A theoretical density without any porosity present in the material.

The main disadvantage of uranium dioxide as a fuel material is its low thermal conductivity [15]. However this drawback is partially offset by the fact that very high operating temperatures are possible in the centre of the fuel rod due to the high melting point [16].

The melting point and thermal conductivity for PuO_2 are somewhat lower than for UO_2. As a reactor fuel, plutonium dioxide (PuO_2) is not used alone, but together with UO_2 as a so-called mixed oxide fuel or MOX. UO_2 and PuO_2 form a solid solution into MOX during sintering. Since the main part of MOX fuel is uranium dioxide (some 90%), the characteristics and behaviour of MOX fuel are considered to be very similar to UO_2 fuel.

3.1.2 Fuel swelling and densification

During irradiation the volume of UO_2 fuel changes continuously with burnup. Initially, at the start of irradiation, there is a contraction in volume as pores remaining from the sintering process continue to shrink. This process is most pronounced in low-density fuel and especially if the pores are small, typically less than 1 μm in diameter. The pellet-cladding gap thus increases at the beginning of the irradiation due to the fuel densification, giving higher fuel temperatures [17, 18].

The process of fuel densification quickly saturates and is followed by a monotonic increase in volume as more and more fission products replace the fissionable uranium. Fuel swelling can give rise strain in the cladding at high

burnup. This can result in both radial expansion and elongation of the fuel rod cladding and can in severe cases during high power transients ultimately result in fuel failure. This swelling is caused by a number of mechanisms:

- solid fission products
- fission gas as individual atoms
- fission gas precipitated into intra-granular bubbles
- fission gas as grain boundary bubbles (inter-granular)

The first two are referred to as inexorable swelling since the volume change they cause is only dependent on burnup. More often they are referred to as solid fission product fuel swelling since they are hard to separate experimentally. Swelling caused by the formation of gas bubbles only occurs at temperatures sufficiently high to permit atomic migration (see Section 3.2.4 on fission gas release mechanism below). The largest single contribution to fuel swelling originates from inter-granular fission gas bubbles. Microscopy on cross sections of fuel rods operated at high temperatures reveals the presence of cigar shaped pores at the grain boundaries. Examination of fractured surfaces of irradiated fuel show gas bubbles on grain surfaces and also along grain edges. Measurement of the change in volume after isothermal irradiation of both restrained and unrestrained UO_2 samples shows that the swelling rate is strongly dependent on fuel temperature [19]. The swelling properties of fuel doped with e.g. niobium and lanthanum oxide shows no significant dependent on the choice of dopant [20, 21].It is clear that the processes involved in fission gas release and fuel swelling are strongly interconnected [22, 23].

The solid fission products causing swelling can be divided into three groups, soluble fission products (Nb, Y, Zr), metallic inclusions (Mo, Ru, Te, Rh, Pd) and others (Cs, Rb, I, Ba, Sr). When isolated in the UO_2-lattice, the rare gases Xe and Kr should be added, when evaluating the contributions to the solid swelling. The theoretically predicted total solid volume swelling is around 0.84% per 10 MWd/kgU. This is in very good agreement with various experimental results (0.8 to 1.0 % per 10 MWd/kgU) [24].

In summary the fuel matrix swelling consist of fission gas bubble swelling (which is strongly temperature dependent) and solid fission product swelling (that is essentially temperature independent) [25]. The net change in fuel volume is the sum of the densification and swelling. The changes in the fuel density affect the pellet-cladding gap (and thus the gap conductance and fuel temperature) as well as diametric and axial strain of the cladding. Furthermore the fuel pellet column length will change during irradiation as a consequence of the density changes.

3.1.3 Fuel microstructure

The radial variation in the fuel pellet microstructure (pores and gas bubble size, grain size and fission product disposition) is a good indicator of the status and in-pile behavior of the fuel and has a bearing on the potential for fission product release during a transient. At high burnup, especially the rim region of the pellet undergoes significant micro-structural changes associated with the enhanced local burnup caused by resonance neutron capture in ^{238}U and the resulting plutonium buildup and fission [26, 27]. Above a local burnup threshold (~70 MWd/kgU) significant microstructural changes are observed like lower dislocation density and lower density of intragranular bubbles.

3.1.4 Thermal properties

Reliable thermo-physical data are required to predict the nuclear fuel behaviour under both normal conditions and under anticipated accident situations [28]. The thermal analysis in a fuel rod is governed by the basic heat conduction equation:

$$c\rho\frac{\partial T}{\partial t} = \nabla \cdot \lambda \nabla T + q'''$$

From this equation it can be seen that the local temperature T depends on local material properties like thermal conductivity (λ), specific heat (c), density (ρ) and the local power density (q’’’). It also depends on time-dependent boundary conditions and heat transfer coefficients (coolant-to-fuel rod and pellet-cladding gap conductance). Under steady-state normal operating conditions the gap conductance and the thermal conductivity generally dictates the thermal behaviour. The heat capacity is important under transient conditions.

The thermal conductivity of LWR fuel has been extensively investigated both theoretically and experimentally, see e.g. [29, 30, 31]. Three contributions to the thermal conductivity are generally identified: conduction through lattice vibrations (the phononic term), conduction through free electrons and a small contribution due to radiation. At lower temperatures the phononic term is supposed to dominate. At higher temperatures the electronic contribution is of relevance. Together, both contributions lead to a minimum of the thermal conductivity at temperatures around 2000 K for UO_2. Experimental data above 2000 K are scarce and quite uncertain. The thermal conductivity of molten UO_2 (as needed in accidental core safety analysis) is even more uncertain.

Besides the dependence on temperature, the thermal conductivity of uranium dioxide depends on the stoichiometry, the porosity and the burnup. In a ceramic material the thermal conductivity decreases with the porosity. The geometry (e.g. size and shape) and the physical properties (e.g. gas trapped inside) of the pores are of importance. In general models a 100% dense material is considered when the effect of porosity is taken into account. Hypo- and hyper-stoichoimetric fuel has a lower thermal conductivity than stoichiometric fuel. This is because the introduction of point defects that increase phonon scattering. The thermal conductivity of UO_2 decreases with burnup [32, 33]. This is mainly due to the formation of solid fission products and fission gas bubbles. An observed permanent decrease in the phonon scattering component (the major part of the thermal conductivity in the temperature regime of interest) is thought to be mainly due to the impurity effect of the fission products [34]. Porosity gives an additional reduction (degradation) in the thermal conductivity, this is especially important at the rim of high burnup fuel. Considering that the heat flux density is highest at the pellet surface, this rim effect would further increase the fuel temperature. Experimental results indicate that the thermal conductivity in the rim zone is considerably lower than in the remaining fuel matrix. Such an additional reduction in the fuel thermal conductivity leads to higher fuel temperatures for a given linear heat rate (LHR).

The fuel centreline temperature is a function of the coolant temperature, the LHR and the total thermal resistance from the coolant to the pellet centre. The largest resistances (and thus temperature differences) are found across the fuel-cladding gap and along the fuel pellet radius. At higher burnup the pellet-cladding gap is essentially closed resulting in smaller temperature differences across the gap, so that the centreline temperature mainly depends on the pellet thermal conductivity integral. A good understanding on the fuel centreline temperature is thus essential for fuel performance code benchmarking since many important fuel phenomena and parameters are temperature dependent.

3.2 Operational properties of nuclear fuel

3.2.1 Burnup

Burnup (BU or β) is a measure of the amount of thermal energy produced in the fuel. Burnup is either expressed as the number of fissions per 100 heavy nuclides (i.e. mass number ≥232) initially present in the fuel and is expressed in percent, or the integrated energy released from fission of initially present heavy nuclides, usually expressed in MWd/kgU. The two definitions are related through a conversion factor that is the energy released per fission,

which is approximately 200 MeV. The first definition is often used for dissolved irradiated fuel (i.e. destructive post irradiation examination or PIE) and is based on the concentration of one or more neodymium isotopes measured by a chemical separation and isotopic dilution mass spectrometry procedure [35]. Usually the ratio of ^{148}Nd to U+Pu is determined and the resulting burnup is expressed as FIMA (fissions per initial metal atom).

Non-destructive burnup measurements are based on the detection of the ^{137}Cs activity in the fuel using a high-resolution gamma-ray detector. The ^{137}Cs activity is to a very good approximation linearly dependent on the burnup [3, 8, 36]. The production pathways and decay scheme for ^{137}Cs are shown in Figure 3.1. The production of ^{137}Cs is dominated by direct fission leading to mass chain 137 in combination with repeated beta decay. An alternative production path is neutron capture in the stable isotope ^{136}Xe, however with a small cross section of 0.26b. Furthermore the loss of ^{137}Cs through neutron capture is almost equally large (0.25b), the two processes more or less balancing each other.

Burnup can also be experimentally determined non-destructively using detection of neutrons emitted by the fuel, like e.g. utilized by the FORK measurement system, equipped with a fission chamber, that have been used for safeguard purposes [37]. Both active and passive neutron measurements can be used for neutron assays. In passive assay spontaneous fission neutrons emitted by the fuel are measured.

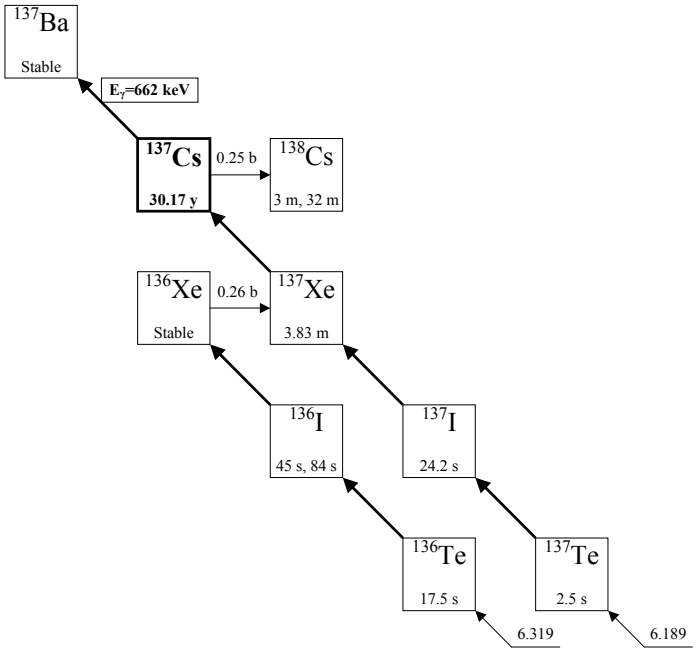

Figure 3.1. Production and decay pathways of ^{137}Cs. Beta decay is illustrated with diagonal arrows and neutron capture with horizontal arrows. Half-lives and cross sections are taken from ref. [38]. Cumulative chain yields in percent per fission for each mass chain are presented for fission induced by thermal neutrons in ^{235}U as given in ref. [39].

Burnup is an important parameter as it basically defines the operating life-time (or age of the fuel) of the nuclear fuel. Modern BWR fuel is irradiated up to an average fuel rod burnup of 60-70 MWd/kgU and there has been a steady increase in this target burnup over time. Not very surprisingly, several characteristics of nuclear fuel will be dependent on burnup as we shall see later.

3.2.2 Volatile element migration

Volatile elements are particularly sensitive to migration, i.e. relocation of elements in the fuel matrix due to high temperatures. Xenon, cesium, and iodine are examples of volatile elements encountered in the nuclear fuel matrix. For a discussion of xenon (and other fission gases) behaviour, see section 3.2.4 on fission gas release.

The low boiling point of cesium (670°C) as well as the low dissociation temperature of its oxides (<600°C) dictates that its migration has to be taken into account in nuclear fuel performance studies [40]. The migration and

accumulation of cesium and iodine at pellet interfaces can be studied using gamma scanning with high axial resolution. The short half-life of ^{131}I (8.05 days) is however a challenge in this context, since the memory of the migration will vanish and the fuel to be measured must be accessed shortly after reactor shut-down [41]. The radial distribution in a fuel pellet could be studied using gamma scanning or XRF (X-ray fluorescence analysis) and EPMA (electron probe microanalysis).

The axial redistribution of cesium is enhanced during a power transient followed by elevated fuel temperatures. Intensity peaks in cesium specific gamma radiation could then be observed at pellet interfaces where cesium has condensed. At temperatures above 1200°C cesium follows approximately the same release paths as xenon [40]. However, at the rim of high burnup fuel, where the microstructure has transformed, the cesium appears to be retained completely, although a high percentage of fission gas is released from such regions of the fuel.

3.2.3 Thermal power

The linear heat generation rate (LHGR or LHR), or linear thermal power, is usually expressed in kW/m and is basically proportional to the fission rate in the fuel. The fission rate can be expressed as (highly simplified model assuming neutrons with just one velocity):

$$R=\Phi\Sigma$$

Where Φ is the neutron flux density and Σ is the macroscopic cross section for fission. Considering reactor cooling, it is often of interest to estimate the maximum heat generation rate at a given point in a given fuel channel rather than for the whole reactor core. The correct description of local power is thus a general requirement and needs to be both modelled adequately and measured with good precision. Fuel development, burnup increase, more complex enrichment designs (different reactivity), plant power up-ratings and new licensing requirements have led to a greatly increased complexity in core designs. This is particularly evident for high power density BWR cores.

The thermal power distribution can be obtained by theoretical calculations using reactor physics codes which model the neutron flux distribution and hence the power distribution. Uncertainties in the calculations and the need for independent verification of these codes due to e.g. regulatory demands calls for the need of experimental methods allowing such verification with acceptable precision. The 1596 keV gamma radiation from the fission product ^{140}La, decay controlled by the parent ^{140}Ba with a half-life of 12.75 days, may be used to study the thermal power distribution in fuel assemblies (see also Section 5.6). The main production paths of ^{140}Ba are presented in Figure 3.2. The production of ^{140}Ba is dominated by direct fission in mass chain 140

in combination with repeated beta decay. An alternative production path is through neutron capture in ^{139}Ba. This production could however be neglected due to the short half-life of ^{139}Ba of 83 minutes and the small neutron cross section (5 b). A small loss of ^{140}Ba takes place through neutron capture (cross section 1.6 b), noticeable at high neutron flux i.e. high thermal power.

Because ^{140}La is also produced by neutron capture in the stable ^{139}La (cross section 9b), it is important from an experimental point of view to wait until the ratio ^{140}La/^{140}Ba reaches equilibrium to avoid a time dependent component (preferably 10-20 days after reactor shutdown).

In order to avoid using the control rods for reducing the surplus reactivity, or so to say even out the thermal power distribution over the reactor cycles, some fuel rods in the fuel assemblies are typically so-called burnable absorber rods, or BA-rods. Such rods contain gadolinium (Gd in oxide form, Gd_2O_3) in special fuel pellets. The gadolinium are efficiently absorbing neutrons due to its high absorption cross section until it is depleted in the fuel. In this way an automatic control of the reactivity is achieved in comparison with the case using the control rods. The Gd content is typically around 3-4 weight-%. The usage of burnable absorbers thus allows the thermal power to be reduced in the beginning of the reactor cycles.

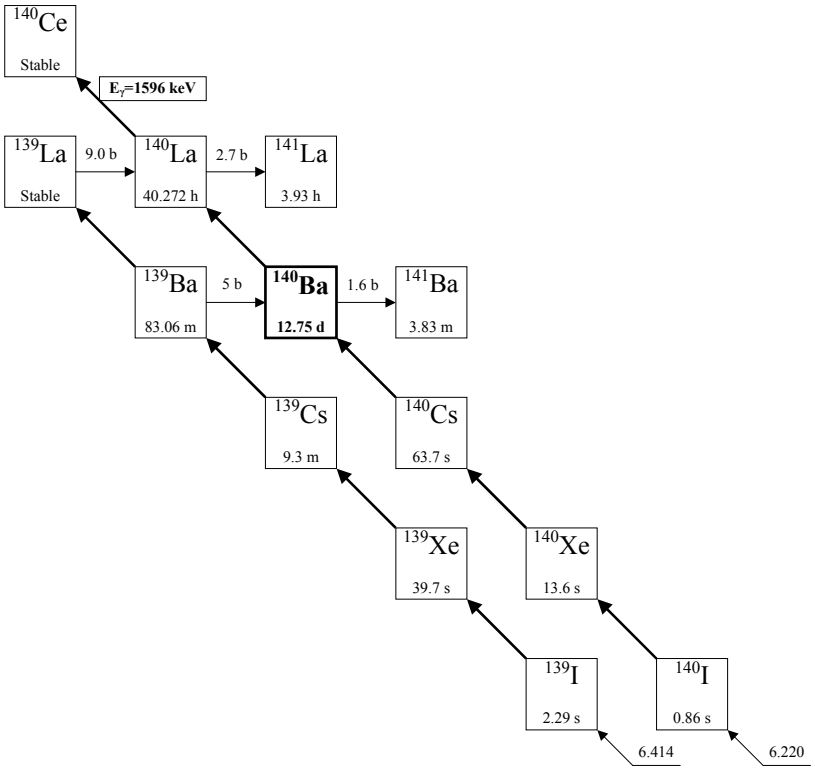

Figure 3.2.. Production and decay pathways of ^{140}Ba. Beta decay is illustrated with diagonal arrows and neutron capture with horizontal arrows. Half-lives and cross sections for thermal neutron capture are taken from ref. [38]. Cumulative chain yields in percent per fission for each mass chain are presented for fission induced by thermal neutrons in ^{235}U, as given in ref. [39].

3.2.4 Fission gas release

The two maxima (peaks) in the doublet distribution of mass numbers of the fission products in the fission process occur in the regions A=90-100 and around A=140. This fact implies that high yields are obtained for the rare gas species xenon and krypton as well as of the volatiles iodine and cesium. Because both krypton and xenon have lower thermal conductivities than helium (the common filler gas from manufacturing), the release of these gases to the pellet-cladding gap causes a decrease in the gap conductance and hence increased fuel temperatures. The increased internal pressure, possibly internal rod overpressure, can induce cladding lift-off and gap re-openings at high burnup, i.e. radial expansion of the cladding.

Fission gas release is defined as the ratio of the number of krypton and xenon gas atoms present in the plenum and the pellet-cladding gap (i.e. in the rod free volume) expressed as a percentage of the total inventory of Kr and Xe produced:

$$FGR=N_{Released}/N_{Total}\cdot 100$$

Two main processes are involved in fission gas release (FGR). The first is the basically temperature independent athermal release and the second is thermal release through a diffusion mechanism which gives rise to a temperature dependency.

In athermal release two distinct mechanisms are involved. Direct recoil release is possible if a fission event is taken place close enough (~8 μm) to a free surface. Due to its high kinetic energy, in the range of 60-100 MeV, the fission product will escape the fuel. Usually these atoms are trapped in the cladding but some will be stopped in the gap through interaction with the filling gas. When a fission product travels through the uranium dioxide, it losses its energy at a rate of ~1 keV/Å, leading to a high local heat pulse along its path. When the fission product leaves or enters a free fuel surface, the heated local zone will evaporate, or sputter. Virtually all the volatile fission products available in this volume are released in the gap. This second mechanism is also sometimes referred to as knockout. Both the direct recoil release rate and knockout release rate are proportional to the fission rate and the range of fission fragments. Furthermore, they both depend on the fuel specific surface, i.e. the surface to volume ratio of the fuel (S/V).

Usually the athermal release is treated as a linear function of burnup. A standard empirical correlation is the ANS-5.4 model:

$$FGR_{Athermal}=8.5\cdot 10^{-5}\cdot BU$$

where BU is the burnup in MWd/kgU. The correlation is valid for burnups up to around 40 MWd/kgU [42, 43]. At higher burnup (>60 MWd/kgU) the athermal release is no longer a simple linear function of burnup, due to plutonium production in the rim zone and the increase in fission product generation rate there. Sine this zone is close to the free fuel surface this will theoretically lead to an enhanced athermal release. However, there is currently no general consensus on how the enhanced fission gas release from the high-burnup rim structure occurs.

Thermal fission gas release is a temperature dependent release mechanism with onset above ~700 °C [42]. It includes lattice diffusion of gas atoms to grain boundaries, trapping of gas atoms by crystal defects or gas bubbles, fission induced re-solution of grain boundary bubbles and saturation of grain boundaries with gas bubbles leading to macroscopic release. When the temperature is high enough, bubbles will nucleate, grow and interlink leading

gas to escape to the rod free volume. The most basic theoretical models for thermal fission gas release assume diffusion in spherical grains of UO_2 in which a uniform generation rate of fission products is imposed. The boundary conditions imply that spherical symmetry prevails and that the outer boundary is a perfect sink for gas atoms, i.e. maintaining a concentration of zero. The fractional fission gas release from a spherical fuel grain of radius r can thus be expressed as:

$$FGR = 4\sqrt{\frac{Dt}{\pi r^2}} - \frac{3Dt}{2r^2}$$

where D is the diffusion coefficient of fission gas atoms in UO_2 and t is time. This is the Booth short time solution where the grain boundary is treated as a perfect sink for fission gas atoms [44]. The gas atoms arriving to the grain boundaries do not get released instantly; rather they precipitate into intergranular bubbles. Fission fragments can collide with these bubbles and gas atoms to be resolved back into the grain matrix, i.e. a re-solution process. In this way the gradual accumulation of gas atoms on the grain boundaries is opposed by the irradiation induced flux of atoms back into the grains. The period from the start of the irradiation to the point at which the boundaries are saturated are referred to as the incubation period.

When the grain boundaries are saturated with gas bubbles the resultant porosity can extend across many grains and provide a route along which gases and volatile fission products can escape to the pellet-cladding gap and the plenum. This process is usually referred to as the interlinkage. Based on Halden reactor experiments, a burnup dependent threshold for the onset of thermal fission gas release has been established, the Vitanza, or Halden, empirical threshold [45]. This threshold basically reflects the competition of the diffusion and re-solution processes discussed above.

Fission gas release can be measured in-pile in a test reactor using instrumented fuel assemblies, by poolside gamma-ray spectroscopy using the activity of ^{85}Kr (Figure 3.3) in the plenum or by rod puncturing in a hot cell laboratory measuring the amount of gas in the free rod volume. Such studies also allows the analysis of the isotopic composition of the fission gas, see e.g. Paper III.

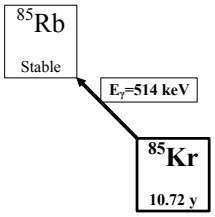

Figure 3.3. The simple decay pathway of ^{85}Kr (a fission product). The beta decay is illustrated with the diagonal arrow. The gamma emission takes place in only about 0.4% of all disintegrations. The production of ^{85}Kr by neutron capture in stable ^{84}Kr is omitted in the figure since it is insignificant considering the applications. The fission yield for ^{85}Kr is about 1.3 for fission in ^{235}U and about 0.6 for fission in ^{239}Pu.

Figure 3.4 shows an example of poolside measurements using gamma-ray spectroscopy of fission gas release for high burnup commercial BWR fuel (see Chapter 7).

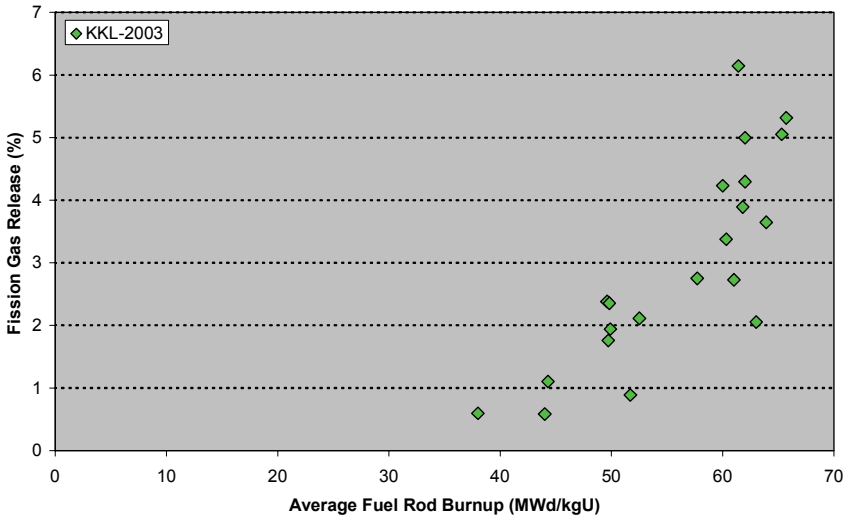

Figure 3.4. Fission gas release measured poolside by gamma-ray spectroscopy, plotted versus rod average burnup.

4 Cladding properties

The metal zirconium has a small capture cross section for thermal neutrons and is resistant to corrosion by water at the operating temperatures of water-cooled reactors. Consequently, various zirconium alloys (zircaloy) has found extensive use as material in the fuel cladding for LWRs. This chapter gives a short overview on pellet cladding mechanical interaction (PCMI), cladding corrosion and hydriding, fuel failure mechanisms and crud deposition on the cladding surface.

4.1 PCMI

Swelling (thermal swelling and swelling due to fission products) and cracking of UO_2 fuel pellets can result in pressure on the inner cladding surface. In an ideal wide gap fuel rod, the cladding extends longitudinally during a power ramp solely by the thermal expansion until the pellet-cladding gap is closed and the expansion is driven by the expansion of the fuel stack instead due to pellet-cladding physical contact/interaction. Theoretically, the point of interaction is sharply defined, but experiments have shown that this is generally not the case. The point of interaction is evident but the behaviour is usually a smooth transition between the two regimes.

Experiments have confirmed the expectations that the power necessary for the onset of PCMI increases with increasing gap size but decreases with burnup as the gap is closed due to fuel swelling. The degree of axial elongation due to PCMI, also increases slightly with pellet length. In absolute measures, the interaction is greater in long rods than in shorter rods and the interaction is generally larger in high-density fuel. The behaviour of MOX fuel is not significantly different from that of standard UO_2 fuel in this respect. The degree of PCMI also depends on the detailed pellet geometry. The pellet-cladding contact also induces diametrical strain in the cladding, both elastic and plastic. Greater permanent strain is induced during rapid power ramps as compared to slow ramps.

Fuel rod geometry changes are caused by creep and irradiation growth of the zircaloy cladding as well as corrosion [46]. The creep rate is dependent on the applied stress, the fast neutron flux and the temperature. The irradiation-induced growth is primarily due to fast neutron flux. The cladding initially creeps down (i.e. the rod diameter decreases) due to the difference

between the external coolant pressure and the rod internal pressure. The creep may be permanently reversed at high burnup if hard contact is established with swelling fuel pellets or if the internal rod pressure exceeds the coolant pressure. Temporary creep-out may occur due to PCMI caused by a local, temporary power increase (see above).

The rod cladding length may increase due to the following circumstances: irradiation growth, creep-down (negligible), fuel pellet swelling (fuel cladding bonding or friction) or volumetric changes caused by corrosion. The latter two effects are only observed at high burnup.

4.2 Cladding corrosion and hydriding

Corrosion of the cladding in the reactor water leads to the build-up of an oxide layer and the absorption of hydrogen. Waterside corrosion of the cladding tube is a key issue for nuclear fuel performance at high burnup and accurate models for cladding corrosion are therefore important tools [47]. The oxide layer formed on the cladding surface has negligible tensile strength, so the oxidation results in a reduction in the effective wall thickness. The oxide layer has a far lower thermal conductivity than the cladding metal, so an increase in the oxide layer thickness leads to increased fuel temperatures. The cladding corrosion rate depends on the type of material, the fabrication procedure, the reactor water chemistry, the local void fraction, the neutron flux and surface heat flux, oxide thickness, hydriding and proximity to spacer grids (which causes a local increase in the cladding corrosion rate).

Hydrogen is picked up by the zircaloy in connection with the corrosion process. Hydrogen in excess of the solubility limit (approximately 50 ppm at the operating temperature) forms brittle zirconium hydride platelets in metal, potentially leading to a reduction in the ductility and fracture stress at sufficiently high hydride phase volume fractions [48]. The cladding hydrogen pickup apparently depends on the material fabrication, reactor water chemistry, local void fraction and neutron and surface heat flux. Hydrogen in zirconium alloys migrates along temperature- and stress gradients. The former effect leads to a pronounced increase in the hydrogen concentration locally at cooler locations in the cladding, like e.g. at areas in contact with fuel pellets. The hydriding of the cladding is also one of the causes of fuel failures (see also Section 4.4 below).

Oxide thickness measurements can be performed (non-destructively on-site) using electromagnetic methods like e.g. the Eddy Current (EC) lift-off method. It has been observed that EC lift-off measurements can give erroneous oxide thickness values if e.g. Zn is injected into the reactor water. During the 1995 shutdown at the Leibstadt nuclear power plant (KKL) in Switzerland, routine oxide thickness measurements indicated values up to 300

μm at the lower part of some fuel rods [49]. Such thick oxide layers, if real, would mean a drastic reduction of the cladding material stability and significantly increased fuel temperatures. Fuel rods were examined by PIE that revealed a perfectly normal behaviour without an extremely thick oxide layer. Before that, on-site gamma scanning of the fuel rods for migration of ^{131}I and Cs did not indicate any elevated fuel temperatures [41]. It was subsequently concluded that the erroneous oxide thickness measurements was attributed to the magnetic properties of the inner crud layer (see Section 4.3 below) which had high Zn content with a composition comparable to a $ZnFe_2O_4$ spinel in the zone where the EC lift-off signal was disturbed. A new method (Magnacrox) has since then been developed by Westinghouse with the capacity to separate the crud deposit from the oxide thickness in Zn doped reactors. The method utilizes a data inversion algorithm in order to separate the oxide signal from the crud signal [50].

Enhanced spacer shadow corrosion (ESSC) is a phenomenon where corrosion rates appear significantly higher in the vicinity of spacers. Analyses show a strong correlation between ESSC and iron deficient water chemistry in the reactor [51]. Quantitatively, the number of years and the extent of the iron deficiency are exhibited in the degree of ESSC in the plants affected.

4.3 Crud deposition

Crud is impurities in the reactor water that deposit on hot cladding surfaces. These impurities mainly originate from corrosion of the construction materials in the primary system. Corrosion products, which are not removed by the condensate demineralizers or are the result of the corrosion of material downstream of the demineralizers may be introduced into the reactor core. Iron oxide is normally the primary corrosion product constituent. It is found in the form of hematite (Fe_2O_3) with traces of magnetite (Fe_3O_4) and iron hydroxides. Zinc will be a main constituent in the crud if Zn injection is utilized in the reactor system (see also Section 4.2 above). Other constituents are nickel, chromium, manganese, cobalt and copper. At high crud deposition values, crud can have a significant impact on the fuel performance through:

- Crud deposits increase core or local channel pressure drop.
- Crud buildup can lead to increases in the extent of local boiling and can initiate boiling transition.
- The higher neutron absorption cross section of crud compared to zircaloy causes reactivity losses.
- Crud deposits on the fuel contribute to the buildup of radiation fields outside the core, since crud constituents activated by neutrons are released back into the coolant.

- Crud deposits containing significant amounts of copper may increase the cladding corrosion rate.

Of the activated crud deposit products the most problematic one is ^{60}Co with a half-life of about 5.3 years, produced through the neutron activation of stable ^{59}Co (Figure 4.1). Typical crud thickness is in the range of 10-30 μm for moderate burnup BWR fuel. Crud deposits can be measured by modern non-destructive electromagnetic methods [52], by on-site scraping and collecting the crud layer down to the much harder oxide layer followed by profilometry measurements, or by destructive PIE.

Gamma scanning of fuel rods utilizing the 1173 and 1333 keV full energy peak from the decay of ^{60}Co (Figure 4.1) can be used to indicate the axial distribution of cobalt in fuel matrix, cladding and crud, and is typically expected to be highly dominating in the crud activity. Measured profiles are in good agreement with PIE and on site crud scraping studies with a peak in cobalt activity (~crud thickness indicative) at the lower part of the fuel rods [53].

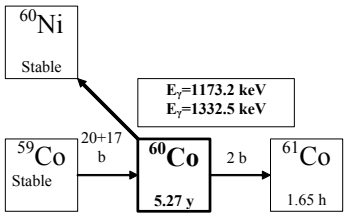

Figure 4.1. The predominant production and decay pathways of ^{60}Co. Beta decay is illustrated with diagonal arrows and neutron capture with horizontal arrows. Half-lives and cross sections for thermal neutron capture are taken from ref. [38].

4.4 Fuel failures

Debris fretting failures and possible manufacturing defects are considered to be the major remaining causes of primary fuel failures. Improved fuel assembly designs and manufacturing as well as operational constraints during service have considerably reduced the frequency of fuel failures. Liner fuel was developed to mitigate the effect of pellet-cladding interaction (PCI), which may lead to fuel failure [12]. The liner refers to a layer of un-alloyed or low-alloyed zirconium which is metallurgically bonded to the outer zircaloy component of the cladding tube. The Zr-liner by virtue of its softness and different chemical composition, compared to zircaloy, inhibits the initiation and propagation of PCI cracks. Liner fuel was introduced in the early 1980s in commercial BWRs and rapidly decreased failure rates.

The primary fuel failures still being observed (predominantly debris fretting) may cause a secondary defect (secondary failure) away from the location of the primary failure. The un-alloyed liner then corrodes rapidly in steam under defect fuel rod conditions and may promote the development of long axial secondary cracks, with extensive activity and fuel release [54, 55]. Consequently several types of alloyed liners have been developed to improve the post-primary failure corrosion resistance of the clad inner surface (like e.g. the ZrSn liner) [56]. If a primary failure progresses, the consequence can be a large activity release and that the plant must be temporarily shut down and the degraded rod removed. This has significant economical consequences, in addition to aggravating the plant dose burden. In order to prevent the propagation of a primary failure into a large secondary failure a number of procedures have been developed. The general rule is to localize the core region of the primary failure and then reduce the power locally by control rod insertion.

Experience with LWR fuel shows that a primary failure may remain in a stable condition for long times or it can produce extensive secondary failures. The secondary failure generally takes place at quite some distance from the primary rod defect. Typically, the secondary failure, when it occurs, develops in a time frame of a few weeks or months after the primary failure. The most important mechanism associated with failure degradation is massive hydriding of the cladding. Steam ingress promotes oxidation of both the fuel matrix and the cladding with generation of hydrogen as a consequence. The reaction between the zircaloy cladding and the coolant water (steam) can be written as:

$$Zr+2H_2O \rightarrow ZrO_2+2H_2$$

The hydrogen generated is picked up by the cladding, which becomes brittle [57]. The secondary failure is thus usually caused by extensive hydriding in presence of cladding stress. Experimental work has shown that a critical amount of hydrogen must be present in the hydrogen/steam mixture in order to promote cladding hydriding [58]. This is due to the fact that a sufficient amount of oxidant can produce a protective layer at the cladding inner surface. Small primary defects are thus potentially more dangerous than larger defects. Larger primary defects may provide enough steam (i.e. oxidant) to prevent massive hydriding by the creation of an oxide layer on the cladding inside. The defect size is however not the only geometrical factor. The residual pellet-cladding gap size is another critical parameter; a very small or even closed gap may produce steam starvation conditions along the fuel column and thus more favourable conditions for hydriding of the cladding.

This makes secondary failures strongly affected by the operating power. Another source of hydrogen in the rod interior is the radiolytic decomposition of steam, producing molecular hydrogen and hydrogen peroxide. Hy-

drogen peroxide is highly reactive and enhances the UO_2 oxidation. In this fuel failure degradation model, the steam entering the primary defect diffuses along the pellet-cladding gap and is gradually enriched in hydrogen while the water molecules are consumed in the oxidation process. Hydrogen can enter the cladding at sites where the protective oxide layer is damaged or through diffusion to the zircaloy during the cladding oxidation process. Heavily hydrided cladding may undergo extensive failure in the presence of cladding stress. The stress may arise from pellet-cladding interaction since UO_2 swells due to oxidation. Other possible sources of cladding stress are changes in gap chemistry causing increased fuel temperatures (higher thermal resistance) or anisotropic expansion of the cladding due to local hydriding.

Basically all primary failures lead to some type of secondary degradation, e.g. locally reduced mechanical strength of the cladding due to the hydriding. Secondary degradation causes however no actual problem until a secondary crack is formed, a process that may result in fuel washout. Even if the probability for the development of a long axial crack is very low for modern fuel with ZrSn-liner (close to zero from a practical perspective), secondary failure in the form of circumferential breaks has occurred with a higher frequency. Circumferential breaks are generally not as severe as long axial cracks, since the fuel washout resulting from a circumferential break is typically much lower than the washout from a long axial crack. Further insight into the phenomena involved in the formation of circumferential breaks (or failure of the guillotine type as they are sometimes referred to) is needed to improve the post-primary failure behaviour of the nuclear fuel through e.g. in-pile studies of simulated primary fuel failures [59, 60].

Chapters 3 and 4 have introduced a number of important issues regarding the fuel pellets as well as the cladding and their interactions. In Chapters 5 and 6 we will now introduce the experimental methods that could be used for studying these parameters, in-pile, in-pool and on-site.

5 Instrumentation and methods: Gamma scanning

The energy and intensity distribution of the intensive gamma-ray flux from irradiated nuclear fuel can be utilized to gain information of the various parameters of the fuel. The measurement technique is generally called gamma scanning, although in our definition it does not have to include a steady movement of the fuel during measurements. For the fuel parameters studied in this work, a gamma-radiation detection system offering high energy resolution and ability to handle high counting rates is required. Furthermore proper shielding of the detector has to be achieved.

5.1 Mechanical setup

Depending on the site of the gamma scanning, two different mechanical setups have been used. For measurements at BWR facilities in Sweden and Finland a collimator through the fuel storage pool wall allows for mounting the detector, electronics and data acquisition computers in a dry environment in the corridor outside the wall. For measurements elsewhere (like e.g. in Switzerland or Spain) a submergible detector and collimator housing has been developed, the so-called LOKET concept.

5.1.1 Equipment in Sweden and Finland

A pre-manufactured hole in the pool wall allows for the instalment of collimators with different sizes and slit heights. A specially designed elevator (the “gamma wagon”) is used to move the fuel assembly in front of the collimator. Also single fuel rods can be moved with a similar device. The control unit for movements of the fuel is located near the pool-rim so that the operator can visually check the movements and observe any deviation from normal behaviour [61]. The elevator system has an adjustable speed control which is used to optimize the scanning velocity with respect to fuel length, general time planning, the need of counting statistics and cooling time. The axial positioning is indicated by a tachometer connected to the chain driving wheel for assembly or rod elevation. The readout of the tachometer is performed by using a digital instrument. The tachometer signal is calibrated

against a precision meter ruler. During measurements the position signals are then registered simultaneously with detector data output by the data acquisition system. Typically the speed during scans is constant within 1%. In the fixture in the gamma wagon the fuel assembly can be rotated round its axis 360°.

When mounted in the fixture the distance between the centre of the fuel and the pool wall (collimator front) is approximately 50 cm. The collimator arrangement consists of two massive (200 mm in diameter) steel half-cylinders. Between the two half-cylinders is a thin steel plate and the collimator height is defined by a horizontal slit routed in the steel plate. The width of the collimator slit increases towards the fuel assembly enabling the detector to view the full diagonal width of an assembly. Both the slit height and width can be changed and optimized for a specific application. The total weight of the collimator system is about 200 kg and the length is about 120 cm. Figure 5.1 shows the principal components of the full experimental arrangement.

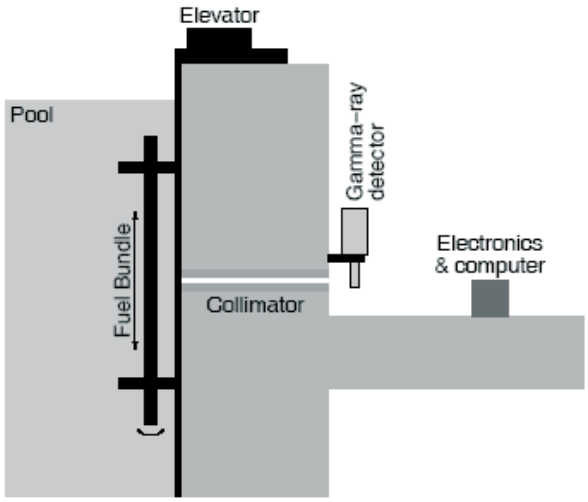

Figure 5.1. The principal setup for gamma spectroscopy experiments using the through-wall collimator option.

5.1.2 LOKET

For gamma scanning at sites lacking the through wall collimator option a special submersible detector and collimator housing has been developed called LOKET (actually not an acronym, the chosen name is due to the fact that the equipment resembles an old-fashioned steam locomotive!). In the housing the detector resides under dry conditions and normal pressure below

about 7 m of water in the fuel storage pool, see e.g. ref. [62]. Concerning the gamma wagon the set up is basically the same as described in Section 5.1.1. Figure 5.2 shows the basic design of LOKET with the internal positioning of e.g. the detector and dewar for liquid nitrogen.

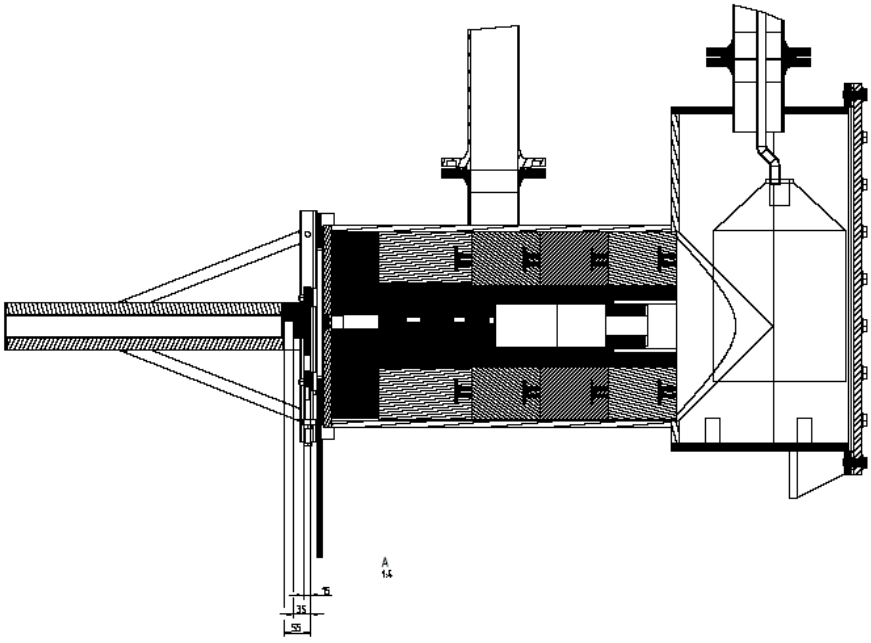

Figure 5.2. A schematic illustration of the submersible detector housing (LOKET). The dewar for liquid nitrogen is to the right in the figure, the collimator system is in the mid part and the air-filled part is to the left in the figure.

The total weight of the system is about 1500 kg, which includes the collimators and the length and height is about 2 m and 1.5 m, respectively. The housing is connected to the pool surface by a pipe of about 7 m length where data transmission cables and power supply cables are located. This means that the data acquisition system can be set up near the pool rim giving operators a good overview over the fuel handling and communication with personnel handling the fuel transport and management in the pool. Figure 5.3 gives a general overview over LOKET when submerged in the fuel storage pool for gamma measurements. Figure 5.4 shows LOKET from a top view perspective in the fuel storage pool and Figure 5.5 shows a photography of LOKET with the detector and its dewar for liquid nitrogen from behind.

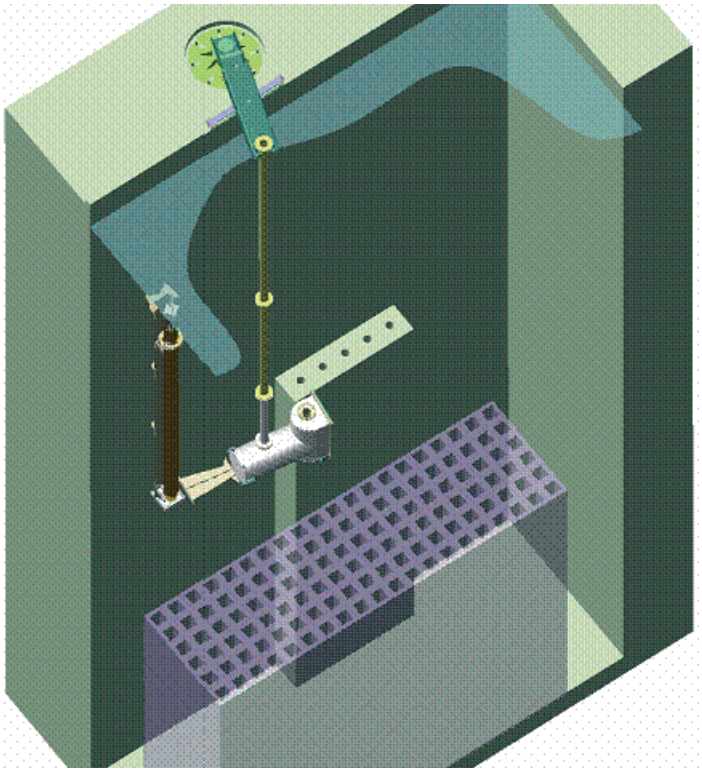

Figure 5.3. LOKET when submerged into the fuel storage pool for gamma scanning. The object to the left is the fuel assembly to be measured.

Similar to the through wall collimator system, the collimator and attenuators of LOKET can be changed and optimized according to the type of measurements to be performed. The detector shielding is made from tungsten, since a very efficient attenuator is needed in order to shield both against other assemblies or single fuel rods handled in the vicinity as well as to fulfil requirements from different types of measurements (like e.g. fission gas release and thermal power) as the system is designed for multiple applications.

If whole fuel assemblies are to be measured the collimator part closest to the fuel (see Figures 5.2, 5.3 and 5.4) is an air-filled steel box in order to utilize the shielding effect of the surrounding water. In addition, the increased source to detector distance of about 1 m obtained with this arrangement is experimentally beneficial since a full size fuel assembly is a very strong gamma source after about 20 days from reactor shutdown (typical time planning for measurements of thermal power distribution in nuclear fuel). No beam is defined in this air-filled part of the collimator system.

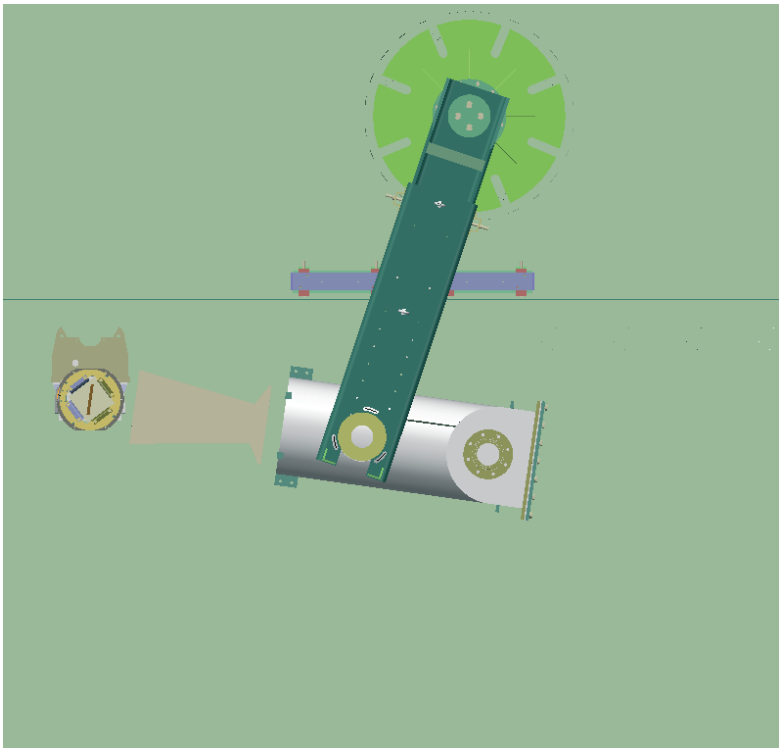

Figure 5.4. LOKET when positioned in the fuel storage pool, top view. The nuclear fuel assembly to be measured is the object to the left in the picture.

The need for liquid nitrogen (LN_2) for cooling the semiconductor detector while submerged in the fuel storage pool put some restraints on the construction. An open connection with the atmosphere is secured through the 7 m long pipe. In this way the buildup of internal overpressure in the detector housing is prevented. LOKET is mechanically stabilized by a pair of suction feet attached to the pool wall.

Figure 5.5. LOKET from behind showing the detector's dewar (filled with LN_2) as well as the signal cables when mounted inside the housing.

5.2 Detectors

For the nuclear fuel studies performed in this thesis, a high energy resolution is generally required, which calls for the usage of semiconductor detectors like e.g. high-purity germanium detectors (HPGe). In such detectors the energy deposited by gamma quanta excites electrons from the valence band to the conduction band leaving holes behind. The pairs of electrons and holes are collected through an electric field applied and a detectable electric signal is obtained. The amplitude of the generated pulse is proportional to the energy deposited by the quanta in the detector. By using suitable electronics and software, an energy spectrum can be generated and displayed where the various peaks identifies the measured isotopes uniquely. Figure 5.6 shows a typical gamma spectrum of LWR nuclear fuel a few weeks after irradiation in the core, when the activity is dominated by the Ba/La decay series.

At present germanium detectors offer the highest energy resolution available for gamma-ray energies in the range from a few keV up to some 10 MeV. Typical energy resolution for germanium detectors is in the order of 0.1% at 1.33 MeV gamma energy. This may be compared to the considerably cheaper scintillator type detectors such as e.g. NaI where the energy

resolution is about 10%. However, for some applications, like e.g. migration of volatile elements like Cs in the fuel matrix, scintillation detectors like NaI or BGO can be used since a high energy resolution is not required here. The ratio of the full energy peak to the corresponding Compton scattering background (peak to Compton ratio) is larger for a germanium detector for a given volume than for e.g. NaI or BGO detectors. For a general overview on germanium detectors, see e.g. refs. [63, 64].

The p-type HPGe detectors used in this work are cooled with liquid nitrogen through a cryostat equipped with a 13 liter dewar, which allows for about 5 days of measurements without refilling. The main detector has an energy resolution of about 2 keV at 1.33 MeV and a relative efficiency of 25%. The detector is operated at +2.5 kV. For some specific experiments, e.g. fission gas release measurements, a Compton suppression system of BGO detectors has been used in order to enhance the peak-to-Compton ratio in cases where the full energy peak (in these cases gammas from the decay of ^{85}Kr) is expected to be weak due to low fission gas release levels. Detailed performance studies of Compton suppression systems are given in e.g. refs. [65, 66].

Using the Compton suppression system, the improvement factor of the peak-to-Compton ratio in the energy interval of interest was about a factor of four in our study as presented in Paper II [67].

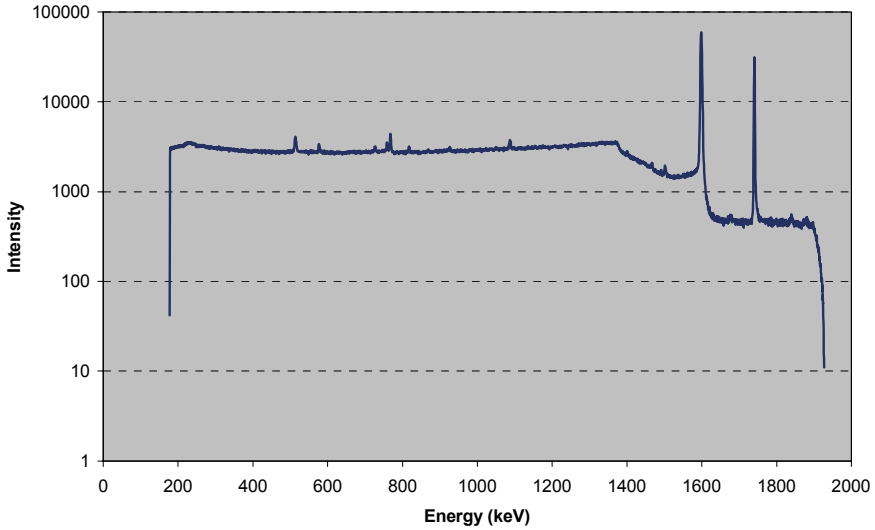

Figure 5.6. Gamma-ray spectrum of a fuel column a few weeks after the in-core irradiation is ended. Such a gamma-ray spectrum is dominated by gamma activity from Ba/La (left large peak). The right large peak is the pulse generator signal used for system dead time correction.

5.3 Electronics

Concerning the properties and performance of the electronics the most critical issues are:

- The system should be portable or at least easy to transport. Nuclear facilities always have certain restrictions concerning transporting items in and out of controlled zones.
- Ability to handle high count rates is important due to the usually limited time available for performing measurements.

The electronics used in the experiments here is based on the Nuclear Instrumentation Module (NIM) standard, see e.g. [68]. In this standard the basic electronic devices (like e.g. amplifiers and discriminators) are fitted in mechanical modules that fit into standardized bins that supply the modules with appropriate levels of power voltage. In this way a specific electronic system for a given application can easily be assembled by collecting the necessary modules, installing them in a bin and connecting them accordingly. For the studies in this thesis a switch between fast and standard amplifiers is a typical example when the NIM standard is very useful and versatile.

The detector pulses are first amplified in a pre-amplifier (Transistor Reset Preamplifier or TRP) capable of handling high counting rates with a retained good energy resolution. The pre-amplifier is integrated with the detector and mounted in the cryostat. The TRP is followed by a gated integrator amplifier (in applications where high counting rates are inevitable) type Ortec 973U. For applications like e.g. fission gas release measurements a standard Gaussian shaping amplifier was used due to its somewhat better performance regarding energy resolution. Analogue to digital conversion was done using a fixed conversion time ADC (e.g. Ortec ADC 914).

A pulser signal with an accurately known and stable frequency is fed continuously into the signal chain directly after the detector (i.e. through the pre-amplifier circuit) in order to allow for dead time correction. In such a way an artificial peak is obtained in the spectrum. Keeping the pulser frequency much below the measuring count rate it can be assumed that the artificial pulse is subject to the same dead time as the gamma-ray induced detector pulses. The proportional loss of pulses in the pulser peak is then used to correct the number of pulses in the gamma energy peaks in the spectrum. This gives adequate correction for losses from the combined effect of dead time and pulse pile-up.

It should be kept in mind though that pulses generated by commonly used NIM-compatible pulse generators are typically not Poisson distributed. In addition the peak shape of such artificial pulses may differ slightly from true events with a difference in dead time as a consequence due to varying modes

of processing in the amplifier electronics. However, these effects are negligible concerning the applications presented in this thesis.

The amplitude of the pulser signals are adjusted to position the peak in an energy region where the spectrum is virtually free from other gamma peaks, allowing for a high accuracy in determining the pulser peak area. The sampling time for each single spectrum recorded during scanning is short (about 0.5 s for thermal power measurements) making it necessary to use a rather high pulser frequency (typically 1-2 kHz was used generated by e.g. a Tennelec TC 814). The uncertainty in dead time corrections using the pulser method has been shown to be as low as 0.1% [69].

The output from the ADC connects to the computer via an interface (PC-card) capable of storing spectra into the computer memory at count rates exceeding 100 kcps with an energy resolution of about 3 keV (FWHM) of the ^{137}Cs peak at 662 keV. The interface was a FIFO GDM PC 16BIV2 [70]. Figure 5.7 shows the principal block scheme of the electronics as used in the gamma scanning presented in this thesis.

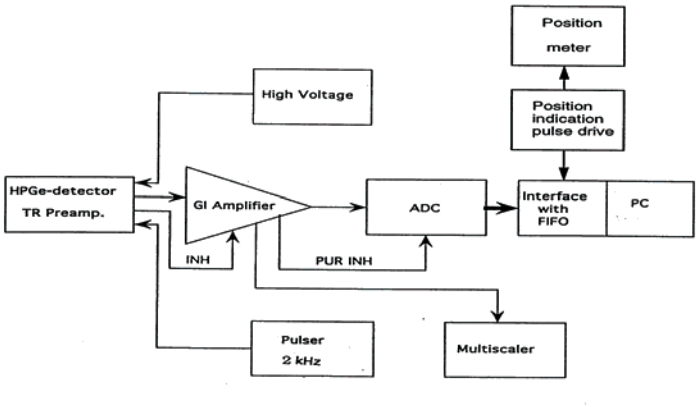

Figure 5.7. Schematic block scheme of electronics.

5.4 Computers and software

A dedicated IBM compatible PC is used for the data acquisition and storage and visual observation of gamma spectra, histograms of specific peaks or energy intervals and general data quality control. The computer operates with a basic DOS operating system installed in order not to interfere with the data collection software. The software used is SEDAS (latest version 3.71), a computer code for non-interrupt measurements of sequential spectra, dead time correction, peak evaluation and data storage [61]. The data acquisition module essentially performs multi spectrum scaling, i.e. it continuously

stores data from the ADC while switching the data area with regular time intervals. This switching is performed within a very small time frame of less than 1 μs so that virtually no data loss occurs [5]. Some modifications to the original SEDAS code have been implemented due to special needs identified in certain experiments performed [70]. Special software has also been developed in order to facilitate the comparison of measured and calculated data (e.g. GASCE, see also sections below on specific measurement techniques).

5.5 Fission gas release

For the non-destructive experimental determination of fission gas release (FGR), the gamma activity originating from ^{85}Kr, a direct fission product, is measured in the plenum volume of the fuel rod after 1-2 years of storage, allowing short-lived nuclides to decay [71, 72, 73, 74]. ^{85}Kr is the only inert fission-gas product with a half-life long enough (about 10.7 years) to let the large number of short-lived nuclides decay before measurement of the weak 85Kr activity is possible. The decay of ^{85}Kr is accompanied by the emission of a 514 keV photon in about 0.4% of the disintegrations (see Figure 3.3). Furthermore, the fission yield for ^{85}Kr itself is also low.

Cobalt impurities in the plenum springs give rise to a strong ^{60}Co gamma source, whose Compton distribution tends to overshadow the weak 514 keV gamma peak from ^{85}Kr (see also Section 5.2). However, the main challenge is the separation of the 514 keV peak from the 511 keV peak, emanating from annihilation radiation and from 512 keV photons due to the decay of ^{106}Rh. The half-life of ^{106}Rh is only 29.8 s, but its decay is controlled by the half-life of the parent ^{106}Ru (372.6 days).

A typical plenum gamma spectrum is shown in Figure 5.8 (for a fuel rod with high FGR) and the details of the peak triplet in the energy region 510-515 keV is illustrated in Figure 5.9. Thus the ^{85}Kr peak at 514 keV is one component of an unresolved peak triplet. The spectrum is analyzed using a dedicated computer code (LADAKH). The code evaluates the area of the ^{85}Kr 514 keV peak by means of least square fitting of Gaussians to the unresolved structure. The area of the ^{106}Rh peak (512 keV) is determined using the 622 keV and 1050 keV peaks due to the same nuclide. The background is determined by linear regression analysis.

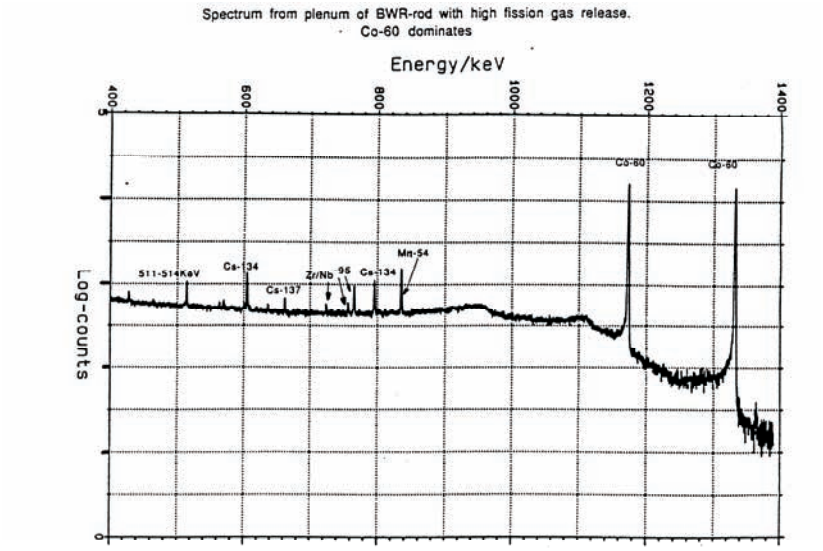

Figure 5.8. Gamma-ray spectrum of the fuel plenum. Main peaks are indicated.

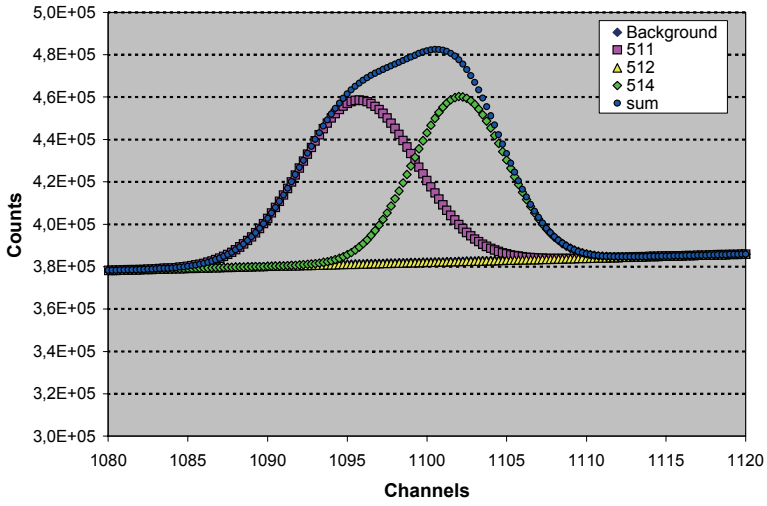

Figure 5.9. Plenum spectrum around the gamma-ray energy region 510-515 keV (actually LADAKH fit to channel counts).

The uncertainty of the intensity of the 514 keV peak is assessed by means of a Monte-Carlo like method. Each channel content of the spectrum is randomized in accordance with its standard deviation (square-roots of counts for a Poisson distribution), and the complete evaluation is re-performed a number of times. The standard deviation of the resulting values is taken as a measure of the uncertainty.

In order to evaluate the macroscopic fission gas release other inputs are needed as well such as fission yields, half-lives, branching ratios, attenuation factors and geometrical factors. Since it is (currently) not possible to obtain the absolute detection efficiency for ^{85}Kr, a reference measurement of the 662 keV gamma radiation from ^{137}Cs in the fuel pellet column is performed with an identical detector arrangement and experimental geometry except for a calibrated absorber that attenuates the considerably more intense radiation from the fuel column. The ^{137}Cs measurements determine the burnup and thus the produced amount of ^{85}Kr.

The analysis is incorporated in the LADAKH computer code and valid inputs are supplied through a standardized input file. The underlying equation used for the FGR evaluation in LADAKH is shown in Figure 5.10. Apart from measured intensities and well-known physical parameters such as yield, emission, decay corrections and attenuation factors, the formula utilizes a few geometrical factors that are defined for the specific fuel design to be measured and partly dependent on the burnup of the object (such as plenum length and pellet stack length) as well as the detector efficiency curve. Consequently, the uncertainty in these factors introduces an additional uncertainty in the finally determined fission gas release of approximately the same magnitude as the statistical error in peak areas. These error sources (systematic or stochastic) can be divided into two categories, those with impact on individual rods only and those in common for the whole set of rods. The first category relative error is estimated to be <±5% while the second is estimated to be <±10% [75]. This could be compared to a typical relative statistical counting error of 2-15% depending on measuring time and absolute level of fission gas release.

$$FGR = 100 \cdot \frac{A_5^* \cdot \tau_7}{A_7 \cdot \tau_5} \cdot F_n(z) \cdot \frac{l \cdot k_k}{L} \cdot \frac{Y_7 \cdot \varepsilon_7}{Y_5 \cdot \varepsilon_5} \cdot \frac{(1-e^{-\lambda_7 t_B})e^{-\lambda_7 t_D}}{(1-e^{-\lambda_5 t_B})e^{-\lambda_5 t_D}} \cdot \frac{\alpha_\mu(662)}{\alpha_\mu(514)} \cdot P_\mu \cdot Q_\mu \cdot \frac{\eta(662)}{\eta(514)} \cdot K_e$$

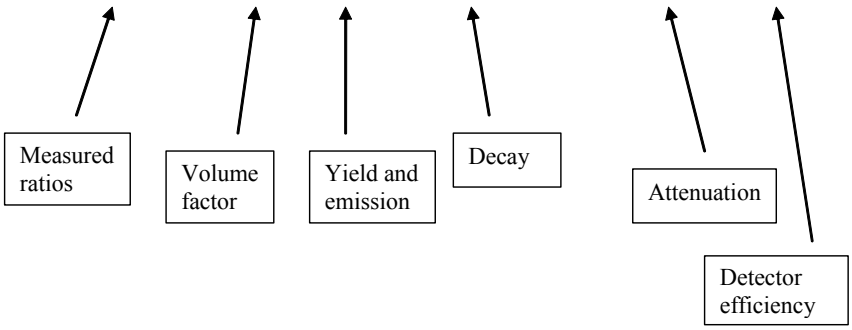

Figure 5.10. The formula (in the LADAKH computer code) used to evaluate the fission gas release from the activity of ^{85}Kr in the plenum.

Typically a plenum measurement takes 20-40 minutes in order to gain sufficient counting statistics while the fuel pellet column reference measurement takes about five minutes. Calibration of the method with destructive post-irradiation examinations for fission gas release has indicated a good correlation [71]. However, the calibrations have so far only been performed on 8x8 fuel designs and not on the more modern fuel designs (10x10). For these designs only fuel rods from the same assemblies, that is fuel rods with identical power histories as poolside measured rods, have been examined in hot-cell laboratories.

5.6 Thermal power distribution

The axial thermal power distribution in single fuel rods or fuel assemblies is measured using the 1596 keV radiation from ^{140}La (see Section 3.2.3). The measurements have to be performed after the ratio ^{140}La/^{140}Ba has reached equilibrium, but before the barium activity is too low for accurate measurements. This implies that the optimal time for measurements is 3-4 weeks after reactor shutdown. For earlier work on the measurement of power distribution in BWR fuel assemblies and fuel rods see e.g. refs. [13, 76, 77, 78].

The fuel column is scanned using a division in typically 500-700 axial (spectrum) channels or sections. If measurements are performed on fuel assemblies the corner of the assembly faces the detector and the measurements are repeated for each corner. The results are in turn transformed into a 25 nodes representation to allow a direct comparison with core physics codes, such as e.g. PHOENIX-4/POLCA-7 [6]. This code has the capacity of explicitly tracking the ^{140}Ba concentration at fuel rod level, enabling a direct comparison with these types of measurements. For assembly measurements the count rates of the four corners are added in order to characterize the result for the full assembly. Example of a gamma spectrum is given in Figure 5.6. Figure 5.11 shows the 1596 keV La peak and the background definition used in order to evaluate the full peak intensity (there are however a number of other options for background evaluation available in SEDAS).

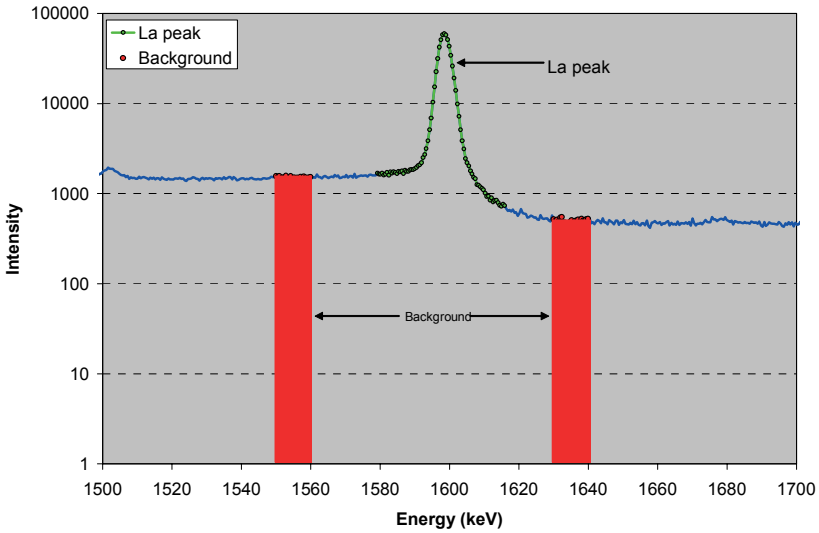

Figure 5.11. Close view of the ^{140}La peak and the background definition used in order to evaluate the number of events. The background is defined as a straight line fitted to the points in the shaded regions.

The condensation of the raw data is performed by a computer code (GASCE) that inspects raw data for noise (electric disturbances affecting the signal from the position indicator), evaluates the fuel column length using fuel column end points, allocates 25 nodes, integrates the intensity level of each node, calculates mean values, corrects for decay, integrates the four separate corners (if assemblies are measured) and generates and stores the final data in a suitable format for subsequent comparison with core physics data.

The long-term stability of the experimental set-up is checked by recurrent measurements on a reference fuel assembly or rod. Since a linearity check of the measurement system by the two-source method is not easily arranged for fuel assemblies (only applicable for single rod measurements), measurements using different well-defined absorbers are used instead [62]. Ratios between the strengths of the two sources i.e. measurements at different axial levels should come out equal independently of absorber thickness (Figure 5.12). The deviation from linearity has been proven to be within 1% in the intensity regions encountered in most of our experiments.

Figure 5.12. Result from a linearity test using the absorber method when measuring fuel assemblies. The figure shows the maximum deviation in detector response between low and high intensity between different absorbers at different intensity (i.e. axial) levels.

Other possible sources of errors are e.g. varying pool water temperatures, which may give rise to thermal deformation of the collimator, pulser stability (dead time correction), rotational asymmetry or mechanical instabilities. The estimated total error (1-σ level) for an average assembly node measurement is estimated to be within ±2%.

5.7 Correction for gamma-ray absorption in a fuel assembly

A point-kernel based adjustment for the relative pin contribution to the measuring efficiency is evaluated by a Monte-Carlo simulation technique [79, 80]. The main reason for this type of correction is if fuel designs with different cross section geometry are included in the same experiment [62]. To be able to directly compare the measured barium distribution between the different fuel geometries and subsequently with the calculated barium distribution the relative pin contribution is needed. Figure 5.13 shows the pin contributions for the GE14 fuel assembly geometry at a certain axial level, summed over the four corners and normalized to an average pin value of unity. Corresponding simulations are performed for all fuel types measured during an experiment and for all the relevant axial levels in order to include part length rods.

The angular position of the fuel assembly in the experimental rig may involve a certain uncertainty. An estimate of change in measured count rate due to this uncertainty has been obtained by simulating various angular offsets of the fuel assembly using the same Monte-Carlo technique. The change in average pin contribution is estimated below 0.7% for an angular offset of 2° [80].

	A	B	C	D	E	F	G	H	I	J
1	1.606	1.436	1.368	1.306	1.269	1.267	1.294	1.349	1.443	1.631
2	1.436	1.042	0.936	0.914	0.877	0.858	0.881	0.946	1.084	1.443
3	1.368	0.936	0.686	0.632	0.654	0.631	0.650	0.756	0.946	1.349
4	1.306	0.914	0.632	0.468	0.452	0	0	0.650	0.881	1.294
5	1.269	0.877	0.654	0.452	0.403	0	0	0.631	0.858	1.267
6	1.267	0.858	0.631	0	0	0.403	0.452	0.654	0.877	1.269
7	1.294	0.881	0.650	0	0	0.452	0.468	0.632	0.914	1.306
8	1.349	0.946	0.756	0.650	0.631	0.654	0.632	0.686	0.936	1.368
9	1.443	1.084	0.946	0.881	0.858	0.877	0.914	0.936	1.042	1.436
10	1.631	1.443	1.349	1.294	1.267	1.269	1.306	1.368	1.436	1.606

Figure 5.13. Pin contributions for the GE14 fuel type assembly cross section geometry at an axial level of 2133.6 mm above the reference level, summed over the four corners and normalized to an average pin value of unity.

Another reason for performing the pin contribution calculations is the burnup dependent cross sectional redistribution of rod power in a fuel assembly. In turn this is due to the fact that the cumulative yield of ^{140}Ba is different for fission in different mother nuclei (see Table 5.1). Since fission occurs more frequently in ^{239}Pu and ^{241}Pu with increasing burnup, the yield of ^{140}Ba will decrease with burnup and the development in burnup looks different for fuel rods depending on their location in the assembly matrix and the corresponding neutron flux density (as evaluated by the core physics codes). Since the gamma measurements are integrated over the whole assembly cross section (i.e. measurements are the average of intensities measured by the detector in four directions) this effect would have to be taken into account before comparing with calculated barium distributions and is actually applied to the calculated pin power distribution. This effect is estimated at below 0.5% (on the 1-σ level) and is generally ignored in the comparison between measured and calculated Ba concentrations (since it also can be said to introduce a certain circular-argument in the comparison between measured and calculated Ba concentrations).

Table 5.1: The cumulative yield of ^{140}Ba in thermal fission of typical fissile nuclei present during BWR operations. For ^{238}U the yield relates to fission induced by fast neutrons. Table taken from ref. [9].

Fission target	**Cumulative yield of ^{140}Ba (nuclei per 100 fissions)**
^{235}U	6.21
^{239}Pu	5.35
^{241}Pu	5.77
^{238}U	5.82

6 Instrumentation and methods: In-pile experiments

The in-pile fuel performance experiments described in this thesis have been performed in the Halden reactor (HBWR). This research reactor was originally constructed for commercial reasons since its purpose was to generate process steam for a neighbouring paper mill plant back in the late 1950s. It is a heavy water boiling reactor with natural circulation and a maximum thermal output of about 25 MW. The reactor is located in a rock cavity (tunnel) just outside the city of Halden in southernmost Norway. The OECD Halden Reactor Project (HRP) is a joint undertaking of national organizations in 19 countries sponsoring the research program under the auspices of the OECD Nuclear Energy Agency (NEA). In addition there are collaborations with several East-European countries. The research areas cover not only fuel physics but also fields as man-machine systems, accident management, core surveillance and control room engineering. HRP forms a part of The Institute for Energy Technology with research activities also in e.g. oil and gas technology, materials science, medical technology and isotope irradiation technology (located in Kjeller just outside Oslo). Furthermore, post irradiation hot cell studies can be performed in Kjeller.

The first instrumented fuel assembly (or IFA) was installed in the HBWR back in 1963 in support of core dynamics studies. Others were soon followed and the assemblies gradually grew in number and complexity, allowing the instrumentation of individual fuel rods, thus allowing studies of more fuel parameters. The first instruments were gas pressure sensors and fuel centre thermocouples together with instruments for determination of the power produced in the test rig. In 1965 the first differential transformer extensometer was successfully applied for measurements of fuel rod dimensional change. Figure 6.1 shows a top view of the Halden core configuration. Figure 6.2 shows the basic design of a Halden experimental test rig.

The reactor water temperature is 240°C, corresponding to an operating pressure of 33.3 bar. The maximum thermal neutron flux is about $5 \cdot 10^{12}$ $n \cdot cm^{-2} \cdot s^{-1}$. The reactor system contains about 14 tons of heavy water (D_2O). A heavy water reactor has a much larger core volume than a light water reactor of equivalent power (due to longer neutron thermalisation length in heavy water). This leaves correspondingly more room for experimental equipment. The flat reactor lid has individual penetrations for fuel assemblies, control

stations and experimental equipment. The core consists of about 110-120 fuel assemblies, including the experimental fuel assemblies in an open hexagonal lattice with a lattice pitch of 130 mm. 30 lattice positions are occupied by control stations. The maximum height of the fuel section is 1710 mm, and the core is surrounded by a reflector of heavy water. Each driver fuel assembly consists of eight or nine fuel rods with 6 % fuel enrichment and standard fuel pellet diameter. The driver fuel assemblies maintain the neutron flux density in the core. The active core has a height of 80 cm. There are normally 2-3 main shutdowns per year, dictated primarily by the various experimental programmes, and typically a few additional cooling downs or scrams for special tests as well.

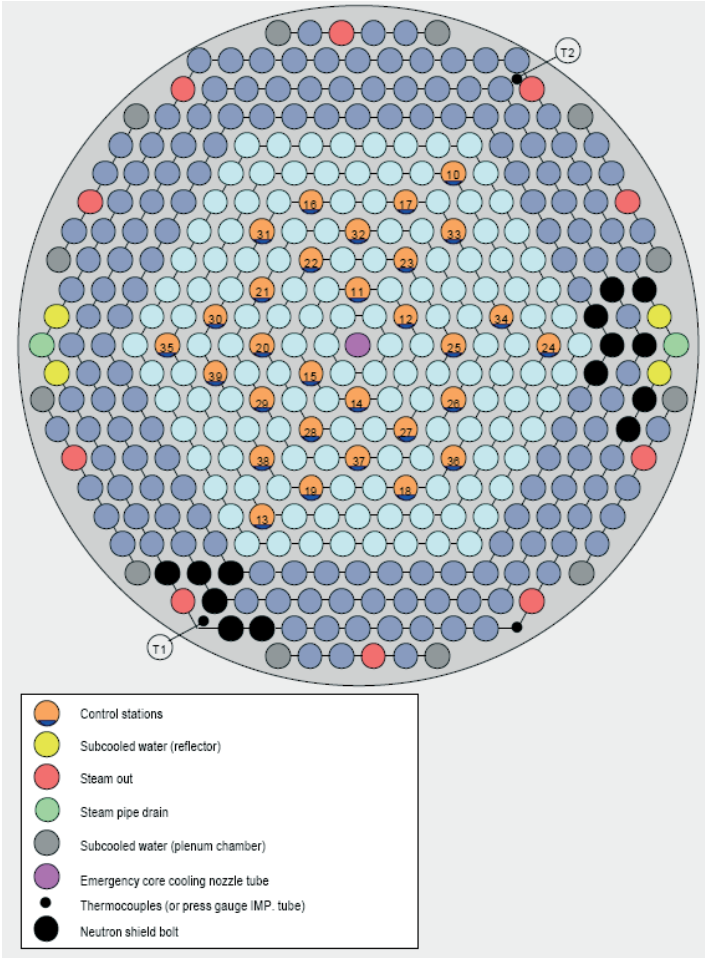

Figure 6.1. Top view of the core layout in the Halden test reactor. Reproduced by courtesy of the OECD Halden Reactor Project.

Currently some 30 test rigs are installed in the reactor core providing suitable conditions for measurements/experiments on e.g. fuel thermal properties, PCMI, fission gas release, fuel failure degradation, material corrosion testing and water chemistry investigations performed in experimental loops with prototypical coolant conditions. Experiments can be performed both under BWR and PWR conditions in the individuals test rigs. An extensive real-time data collection system and databases (the Halden Project's data acquisition and management system-TFDB) also forms part of the facility infrastructure [81]. The analogue signals are sent to the mainframe computer via fast multiplexers. More than 1000 signals from the instrumented test rigs are logged at regular intervals and sent to an on-line conversion system and stored in a circular buffer. Every 15 minutes all signals are entered into the TFDB system for permanent storage and analysis. More frequent data sampling are sometimes required by special experiments and the system allows for sampling intervals down to 10 ms.

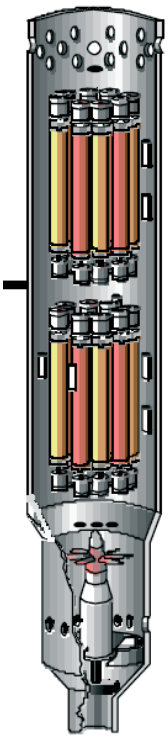

Figure 6.2. A Halden experimental fuel assembly (experimental rig- IFA) showing two clusters of test rods. Reproduced by courtesy of the OECD Halden Reactor Project

6.1 Fuel performance experiments

The instrumentation consists of devices in the rig, e.g. inlet and outlet thermocouples, neutron detectors or flow meters, and fuel rod instrumentation, e.g. fuel centre thermocouples, pressure transducers or cladding elongation sensors. To meet the extreme in-core environmental conditions the instruments are manufactured from materials which are highly resistant to irradiation, elevated temperatures and corrosion. This leaves only special metals and ceramics as a choice.

After design of the experiment and decision of the fuel parameters to be measured (and thus the necessary instrumentation) the instrumented fuel assembly (IFA) is loaded into the Halden core. In order to be able to follow the burnup of the experimental rods, the linear heat rate has to be evaluated. In the power calibration, typically carried out in the beginning of the experiment, the assembly power is determined by thermo-hydraulic measurements using the inlet and outlet thermocouples, and a factor is determined that relates the measured thermal power to the neutron detector signals [82]. Also fuel depletion functions are determined for the individual fuel rods. These functions describe the change of the relationship between the rig thermal power and the neutron detector signals as a function of burnup [83]. Neutron detectors (typically self powered with vanadium absorber) are located at several axial levels in the experimental rig.

Fuel centre thermocouples can be inserted in hollow pellets (central holes are 2-2.5 mm in diameter) in the upper and/or lower end of the fuel pellet column, typically 100-150 mm from the end point. Depending on the temperature regime, different types of sheaths are used, however in the experiments described in this thesis type I thermocouples (W3%Re/W25%Re) with beryllium insulation in tungsten/25% rhenium sheath of 1.6 mm outer diameter was used. The thermocouples could be used for fuel centre temperature measurements up to 2000°C, occasionally 2500°C. A special gas tight seal is arranged inside the fuel rod end plug to prevent fission gases to diffuse into the cable insulation. The thermocouple temperature measured in a fuel pin is a function, not only of the current power level, but also of the recent power history [84]. The time constants (the function $F(\tau)$ describing the relationship between the temperature now and the power τ seconds ago) are studied by noise analysis performed during power ramps. The irradiation induced de-calibration of thermocouples is compensated for in the data handling system (TFDB). So-called normalized fuel temperatures i.e. temperatures at a constant linear heat rate, are also evaluated in the TFDB system (the data conversion routine).

Pressure bellows transducers are used to measure the internal rod pressure and (indirectly) the fission gas release. A bellow is mounted inside the fuel rod. A ferritic armature is mechanically connected to the bellows. A differential transformer (see below) outside the fuel cladding senses the position

of the armature and thus the deflection of the bellows. The measuring range is up to 120 atm with an accuracy of about 1% of full scale. The transformation from rod pressure measurements to FGR is performed in the TFDB system through the data conversion routine. Irradiation induced creep of the bellows might introduce a drift in the instrument signal. This effect is compensated for using the pf-drift computer code developed in Halden [85].

The linear voltage differential transformer (LVDT) is used as fuel cladding extensometer, fuel stack end pellet position sensor and as part of bellows based pressure sensor. The design is a single primary coil and a secondary coil in two halves electrically balanced. A coaxial ferritic core controls the balance of the secondary voltage and causes a signal proportional to the core offset from central neutral position. The instrument has a full scale of about 200 mV at 50 mA (400 Hz excitation). A number of linear ranges are available. The accuracy is better than ±1%.

6.2 Fuel failure experiments

Fuel failures due to fretting on the cladding resulting in a primary failure and eventually a secondary failure with significant activity releases are costly for a nuclear facility. In order to simulate a primary failure of the fuel cladding and study the fuel degradation and eventually the development of a secondary fuel failure, the fuel rods were equipped with a water ingress device (WID) at the upper end plug. When the valve in the WID opens the water is allowed to pass through a 110 mm long tubing before entering the rod free volume (plenum) at the upper end plug. In addition the test rods must be equipped with instrumentation that provides information on the fuel rod performance during the degradation process. In the secondary fuel failure experiment described in this thesis (IFA-631.1) the fuel rods were equipped with thermocouples both at the upper and lower ends. Earlier experiments also used so called hydrogen detectors [59, 86]. The fill gas (2.9 bar at 20°C) was chosen as a composition of He and Ar giving a thermal conductivity distinctly higher than that of steam and markedly lower than that of hydrogen. This choice allows tracking of the development in the gas mixture due to the liberation of hydrogen and the entrance of steam/water in the rod free volume.

The experimental condition in the HBWR rig was BWR (286°C and 70 bar) and the loop was operated under normal BWR water chemistry conditions. The axial power profile was peaked towards the lower end of the test rods. This was done in order to simulate the type of axial power profile that is obtained in a commercial BWR at the beginning of a reactor cycle. The maximum linear heat rate (MLHR) during the base irradiation was about 30 kW/m. This limitation was mainly set for preventing thermal fission gas release and poisoning of the pellet-cladding gap with fission gas (Xe and Kr)

and thus altered thermal conductivity conditions. The active fuel length was 120 cm.

Prior to simulation of the primary failure the test rods were irradiated under steady-state conditions for 144 days to a burnup of 5.3 MWd/kgUO_2. After opening the valves of the WID the in-pile experiment continued for another 118 days with the valves open under stable heat rate. Following the water ingress water sample from the loop was taken regularly. At the end of the in-pile experimental period the burnup was about 9 MWd/kgUO_2. Simultaneously both the test rods and the rigs central cable tube were used for the study of enhanced spacer shadow corrosion (ESSC), see Section 4.2. This was done by using a significant number of specimens threaded onto the fuel rods and cable tube. Following the in-pile phase of the experiment the four fuel rods and specimens were sent to post irradiation examinations (PIE) at Kjeller hot cell laboratory. These examinations included neutron radiography, hydrogen analysis and metallography. In addition, dimensional measurements were performed on three fuel rods (the fourth one was observed to have a part-circumferential crack after core unloading).

By inserting a known amount of water in an experimental fuel rod the reaction kinetics of hydriding and oxidation can be studied in-pile by monitoring the rod internal pressure. For the experiment (IFA-634) described in this thesis the amount of water was 300-400 mg which was sufficient to fill the rod free volume with steam during operations. The test rods were equipped with pressure bellows transducers (pre-pressurized to 15.5 bar) at the lower end. The IFA-634 experiment was also performed under BWR conditions.

7 Results: Fuel performance studies performed by gamma spectroscopy

The poolside (and in-pool) gamma spectroscopy (scanning) technique offers means to obtain information concerning the performance of the fuel rod or fuel assembly without requiring expensive, and from a risk perspective unwanted, transports and complex handling procedures. The technique is therefore considered suitable for the studies of fuel rods or assemblies that are to be reloaded in the core again, or fuel that is to be temporarily stored awaiting a final storage, like e.g. in a geological repository.

The applicability has been investigated in a more general manner in paper I, specifically for fission gas release in Papers II-IV and Paper VI and specifically for thermal power determinations in Papers V and VII. Studies of crud deposition are presented briefly in Section 7.8 and studies of volatile element redistribution are presented briefly in Section 7.9. Burnup determinations are shortly commented upon in Section 7.10.

7.1 Paper I: Developments in Gamma Scanning of Irradiated Nuclear Fuel

Existing methods based on gamma-ray spectroscopy have been further developed for on-site determination of fission gas release, axial thermal power distribution, burnup profiles and the redistribution of cesium in the fuel matrix [5]. The determinations of fission gas release (FGR) shows a good correlation with post-irradiation examinations using mass spectrometry for 8x8 fuel types. The FGR results indicate a thermal component of the measured release in 8x8 type fuel in that fuel rods with higher burnup within a given fuel assembly show significantly higher release levels. Since these rods are the ones that have been operated with the highest linear heat rates in order to reach their high burnup (i.e. identical power histories within the assembly) they have also experienced the highest maximum fuel (centre) temperatures.

The relative axial power distributions are determined with a precision (reproducibility) of about ±1% (on the 1-σ level) for a single rod node measurement and are thus fully useful for the benchmarking/validation of production codes. Furthermore, the experience shows that the possibility of feed-

back to the reactor operators is of importance when the fuel is to be reloaded in the core.

The results obtained in several poolside measurement programmes/experiments (often in close co-operation with reactor operators) show that high-resolution gamma scanning is a versatile method for the determination of several fuel performance indicators such as fission gas release, cesium migration and thermal power distribution, see e.g. refs. [53, 62].

7.2 Paper II: Fission Gas Release Determination Using an Anti-Compton Shield Detector

Fission gas release can be measured by studying the 514 keV gamma-ray in high-resolution gamma-ray spectrometry with HPGe detectors, see Sections 3.2.4 and 5.5. In order to enhance the sensitivity of high-resolution gamma-ray spectroscopy for measurements of fission gas release in 10x10 fuel irradiated in the TVO2 reactor (BWR) in Finland the germanium detector was provided with an anti-Compton shield of BGO detectors. The reason was mainly that the expected low fission gas release in the fuel to be measured and thus the suspicion that the Compton distribution could possibly obscure the weak ^{85}Kr peak at 514 keV.

The system was first characterized in a laboratory environment using a ^{60}Co source. A Compton suppression shield of BGO detectors instead of NaI detectors can be more compact in size [87].

The laboratory investigations showed that the maximum peak-to-Compton ration (p/c) was improved substantially using the anti-coincidence technique. A comparison is given in Table 7.1, including the poolside measurements.

Table 7.1: *Peak-to-Compton ratio (p/c) with and without the BGO shield active. The peak is the 1332 keV gamma line of ^{60}Co.*

Energy range of Compton background (keV)	p/c with BGO shield active	p/c with BGO shield inactive	Improvement factor (laboratory)	Improvement factor (poolside)
515-522	~420	~70	6.0	4.2
1040-1096	~200	~70	2.9	3.2

In the poolside measurements larger amounts of scattered gamma radiation is present, originating from the surrounding materials. This affects the p/c ratio, explaining the smaller improvement in p/c ratio in comparison with the laboratory tests. The relative errors (1-σ level) in the FGR determinations were significantly smaller (by approximately a factor of 2) for measurements using the anti-Compton shield for equal acquisition times.

As both the level of the fission gas release and the measuring times are typical for a majority of realistic cases, the use of the shielding detector system means a substantial improvement in practice.

7.3 Paper III: Fission Gas Release in ABB SVEA 10x10 BWR Fuel

The introduction of the 10x10 fuel design (such as ABB SVEA 10x10) has proven highly successful in limiting the fission gas release in BWR fuel under normal (commercial) operating conditions. The design has permitted a considerably higher fuel assembly thermal power with a generally reduced rod average linear heat rating (ALHR) and surface heat flux, compared to older 8x8 and 9x9 lattices. Also the SVEA water-cross concept has enabled the individual fuel rod heat ratings to be more closely matched. This reduction in both the absolute level and relative spread in LHR within a given assembly has implied a significant reduction of the maximum FGR levels in the fuel. The release fractions in the SVEA 10x10 fuel are generally far lower than in 8x8 fuel despite higher assembly powers, and also show less variation between rods within an assembly. This has made it possible to avoid unacceptably high rod internal pressures and fuel temperatures when operating the reactors at extended burnup levels. The fractional fission gas release, as measured by non-destructive gamma-ray spectroscopy for the plenum content of ^{85}Kr, was found to increase generally with burnup, reaching a maximum value of about 5% at rod average burnups of 50 MWd/kgU.

Based on analyses of the release gas isotopic composition, as determined by mass spectrometry [88], it is concluded that also in SVEA 10x10 fuel the FGR is primarily governed by thermal processes. The results also indicate that the fission gas release in the 10x10 lattice fuel generally occurs later in life than in the 8x8 fuel. The released gas isotopic composition, based on the ^{134}Xe/^{86}Kr-ratio, does not support an athermal enhanced pellet rim release model.

7.4 Paper IV: Fission Gas release in ABB SVEA-96/100 Fuel

As stated in paper III, the SVEA 10x10 fuel designs have proven very successful in limiting the fission gas release in BWR fuel. Non-destructive measurements of FGR based on the plenum content of ^{85}Kr as determined by high-resolution gamma-ray spectroscopy has generated a valuable database both for older 8x8 lattice type fuel and for SVEA 10x10 fuel.

BWR fuel rods are often subject to relatively complicated power histories, including quite rapid and large local power changes due to control rod blade maneuvering. Large differences in the axial power profile during a fuel rod's history may lead to a high local power and resulting FGR. The effect on FGR from control blade movements that have been established for 8x8 fuel are not significant for SVEA 10x10 fuel. The control blade corner rod (J10 in the lattice) shows no significant tendency to have a higher FGR compared to other rods in the assembly. By comparison, in 8x8 type fuel, the FGR values are significantly higher for the H8 corner rods compared to other rods in the fuel lattice.

It has been proposed that the increased FGR in the H8 corner rod may have been at least partly due to an increased oxygen/uranium (O/U) ratio in the fuel as a result of the far higher proportion of plutonium nuclide fissions in the low-enrichment corner rod, compared to in other, higher enrichment, rods [89]. The corner rods in the SVEA 10x10 fuel assembly designs also have a lower initial enrichment than the interior fuel rods. However, the effect does not appear to have had a detectable impact on FGR, probably due to the generally lower heat ratings and fuel temperatures in 10x10 type fuel.

From the FGR measurements it is concluded that FGR also in the SVEA 10x10 lattice type fuel is still largely temperature dependent, and is consequently dependent on both the LHR and the burnup.

7.5 Paper V: The Shut-down of the Barsebäck 1 BWR: a Unique Opportunity to Measure the Power Distribution in Nuclear Fuel Rods

Reactor poolside measurements of gamma radiation specific for the fission product ^{140}La (1596 keV) have been used for an experimental determination of the axial power distribution in 55 nuclear fuel rods irradiated in the Barsebäck 1 BWR nuclear power plant. The measurements took advantage of the unique situation of a very short last reactor cycle of only three months due to the out-phasing of the reactor unit at November 30 1999. ^{140}La, whose decay is controlled by the mother nuclide ^{140}Ba with the half-life 12.75 days, reflects the average power distribution, representative for the latest weeks of core operation (in this case basically during November 1999). The measured intensities have been transformed into a 25 nodal representations to allow a precise and direct comparison with the corresponding calculated power distributions. The 55 rods were selected from two different fuel assemblies with average burn-ups of 1.9 and 9.7 MWd/kgU, respectively (that is one fresh bundle and one slightly more than one cycle bundle). The stability and the linearity of the measurement system were evaluated. The linearity was checked using the two-source method. The stability was checked by recur-

rent measurements on a reference fuel rod. The results have been used in the validation of the pin power reconstruction model of Westinghouse 3-D core simulator POLCA-7. The deviation between the measured and the calculated ^{140}Ba concentrations (expressed as rms radial errors) is typically a few percent on the rod level. The results indicate that also Gd-rods are properly modelled over a broad range of conditions. It is indicated that predictions for fuel rods in their first month of operation are less accurate than for the rest of the fuel rods. Figure 7.1 shows measured and calculated Ba concentration profiles for a selection of fuel rods measured during the experiment.

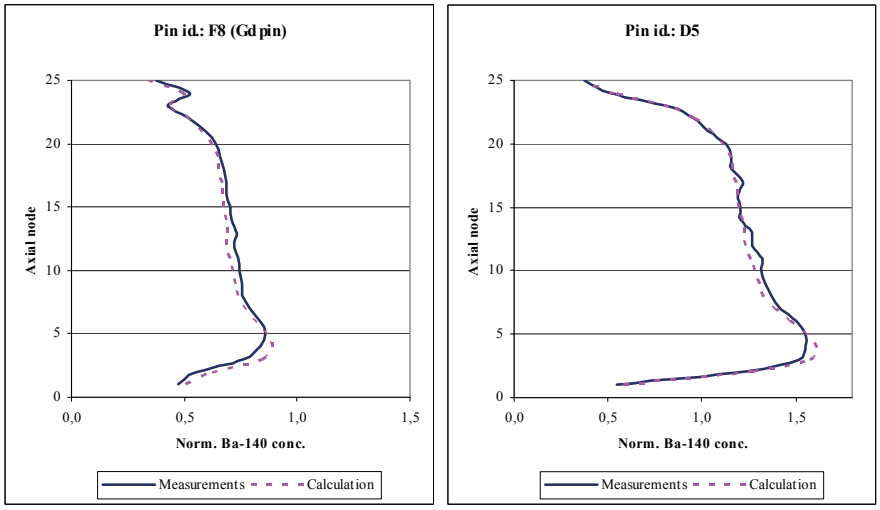

Figure 7.1. Measured and calculated Ba concentration profiles at nodal level (normalised over all nodes) for selected fuel rods in FA 23199 (fresh bundle). Rod F8 is a burnable absorber (Gd) rod.

7.6 Paper VI: On-site Gamma-ray Spectroscopic Measurements of Fission Gas Release in Irradiated Nuclear Fuel

The gases xenon and krypton, produced during fission of uranium and plutonium, have low solubility in UO_2. Therefore, after a relatively short irradiation period a large number of fission gas filled bubbles are generated within the fuel grain. The fission gas affects the performance of the nuclear fuel in a number of ways. An experimental, non-destructive in-pool, method for measuring fission gas release (FGR) in irradiated nuclear fuel has been developed. Using the method, a significant number of experiments have been performed in-pool at several nuclear power plants of the BWR type. The method utilises the 514 keV gamma radiation from the gaseous fission prod-

uct ^{85}Kr captured in the fuel rod plenum volume. A submergible measuring device (LOKET) consisting of an HPGe-detector and a collimator system was utilized allowing for single rod measurements on virtually all types of BWR fuel. A FGR database covering a wide range of burnups (up to average rod burnup well above 60 MWd/kgU), irradiation history, fuel rod position in cross section and fuel designs has been compiled and used for computer code benchmarking, fuel performance analysis and feedback to reactor operators. Measurements clearly indicate the low fission gas release in more modern fuel designs in comparison to older fuel types (see also paper III and paper IV). Figure 7.2 illustrates recurrent measurements, separated by several years and using different measurement geometry, of fission gas release using the method on a specific fuel rod.

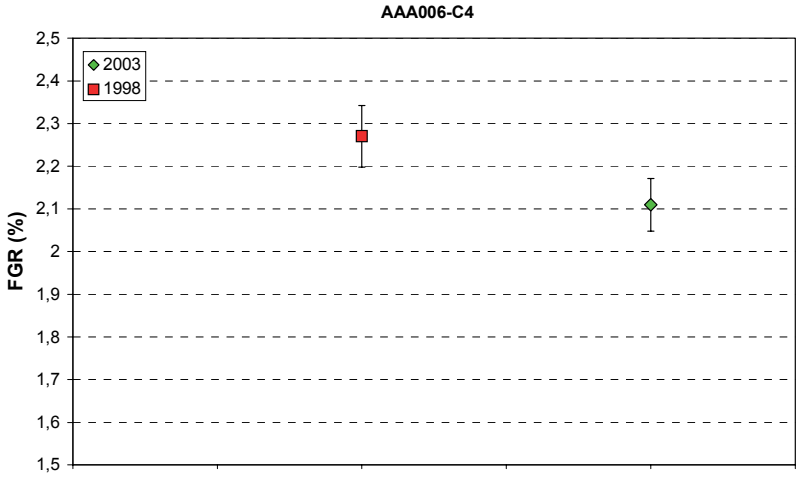

Figure 7.2. Recurrent measurements of FGR of the same fuel rod (rod C4 in the fuel assembly denoted AAA006) measured in 1998 and re-measured in 2003. These measurements were performed at the Leibstadt nuclear power plant (KKL) in Switzerland.

7.7 Paper VII: LOKET- a Gamma-ray Spectroscopy System for In-pool Measurements of Thermal Power Distribution in Nuclear Fuel

An important issue in the operations of nuclear power plants is the independent validation of core physics codes like e.g. Westinghouse PHOENIX-4/POLCA-7. Such codes are used to predict the thermal power distribution down to single node level in the core. In this paper, a dedicated measurement system (LOKET) has been developed and is described and experimental

results are discussed. The system is based on a submergible housing, containing a high-resolution germanium detector, allowing for measurements in-pool. The system can be transported to virtually any nuclear power plant's fuel storage pool for measurements in-pool during outage. The methodology utilizes gamma radiation specific for ^{140}La, whose decay in turn is governed by the parent ^{140}Ba, reflecting a weighted average power distribution, representative for the last weeks of operation of the core.

Good agreements between measured power distribution and core physics calculations (Ba distribution) have been obtained during a series of experiments at Leibstadt NPP in Switzerland and Cofrentes NPP in Spain (BWRs) for both fuel assemblies and single fuel rods. The system has proven as a very useful tool for the experimental validation of core calculations also for the most complex fuel designs and challenging core configurations. Experimental errors (on the 1-σ level), has been demonstrated below ±2% on nodal level for assembly measurements. Figure 7.3 illustrates the deviation between experimentally determined Ba concentration and Ba concentration as evaluated by core physics calculations on the assembly level. Figure 7.4 show examples of the deviation on nodal level.

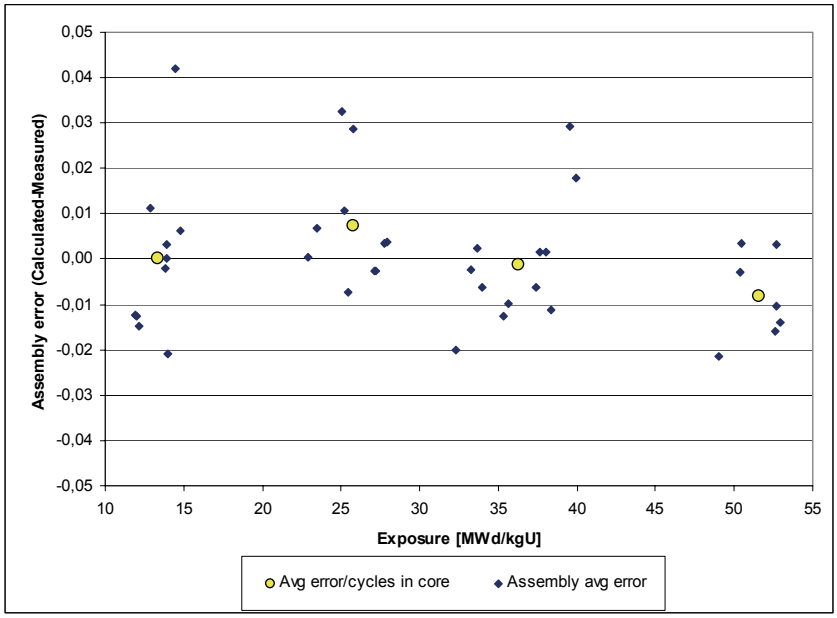

Figure 7.3. The deviation between experimentally determined thermal power and core physics evaluations (expressed as radial rms errors at bundle level) as a function of exposure during measurements at Leibstadt NPP (KKL) in 2003.

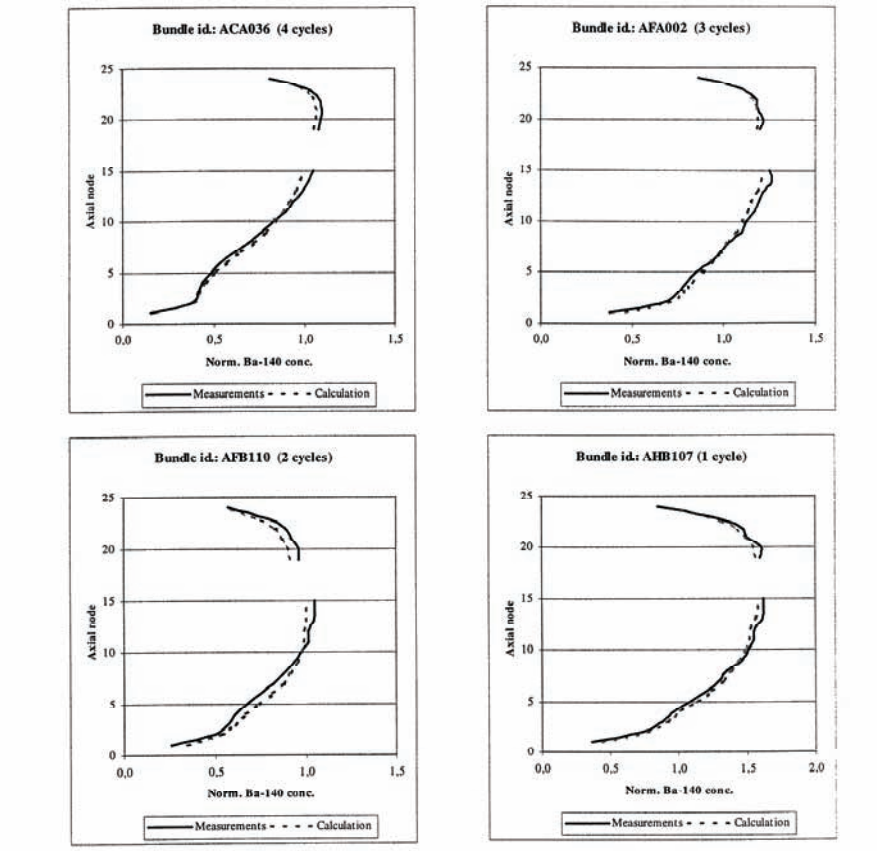

Figure 7.4. Nodal comparisons between measured and calculated Ba concentrations after KKL cycle 15 measurements, using LOKET. Nodes 16-18 have been excluded from the comparison due to interfering structural materials close to the gamma scanning equipment.

The overall comparison between core physics codes (PHOENIX-4/POLCA-7) indicates that the nodal power can generally be predicted with an accuracy of 4% (rms error over all nodes). Bundle power can be predicted with an accuracy of better than 2% (rms error of the comparison at the bundle level).

7.8 Crud deposition measurements

Crud is impurities in the reactor water which deposits on the hot cladding surfaces. At high crud deposition values, crud can have a significant impact on the fuel performance (see Section 4.3). Axial gamma scanning specific for ^{60}Co gives a strong response for the plenum spring but also a weaker profile over the fuel column dominated by cobalt in the crud layer. Such

measurements could well be performed in conjunction with ^{85}Kr measurements, allowing for short-lived nuclides to decay (the half life for ^{60}Co is about 5.3 y). Additional sources of ^{60}Co are cobalt impurities in the fuel matrix and the cladding material. Since the fuel mass is much larger than the mass of the crud for a given part of the fuel rod, as viewed by the detector, the cobalt content of the fuel is a critical parameter in interpreting the data. The cladding is ignored in comparison with the fuel due to its significantly smaller mass (about 20% per unit length). However, based on manufacturing specifications and production pathways these two concentrations are believed to be negligible in comparison with the crud related signal.

Experiments performed at the Leibstadt BWR showed downward peaked ^{60}Co profiles, i.e. in the lower part of the fuel rods, where the cobalt intensities were about a factor of four larger than in the upper part for high burnup fuel rods (Figure 7.5). The difference showed an increase with exposure time as well [53, 90]. These results are well in line with post irradiation examinations on fuel rods of similar burnup and core history as the ones being gamma scanned, showing thicker crud deposits in the lower parts of the fuel rods [49]. The results are only indicative however. The more precise relation between measured ^{60}Co intensity, activation on different axial levels and amount/thickness of the crud layer is not yet thoroughly evaluated. However, the results look promising.

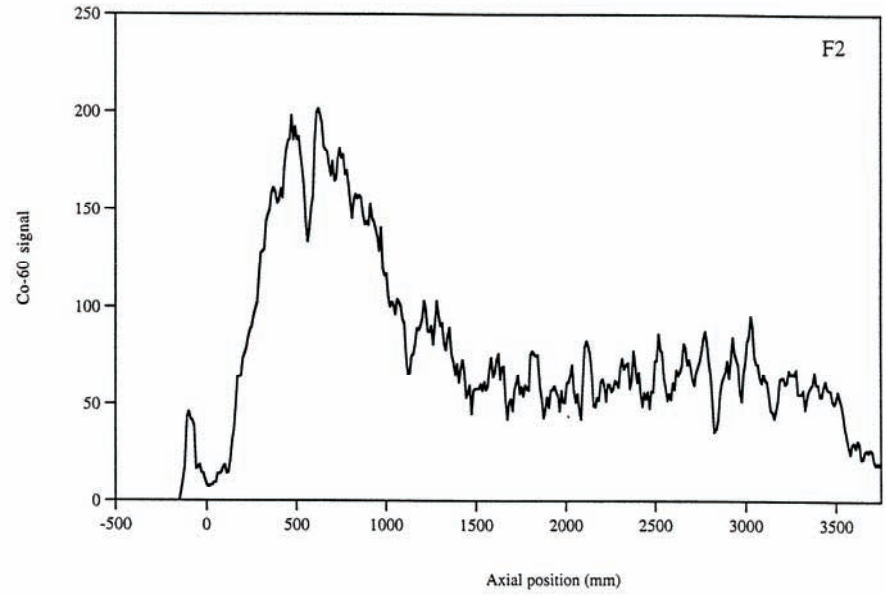

Figure 7.5. Profile of the ^{60}Co gamma-ray intensity (the 1332 keV peak) over fuel rod F2 from fuel assembly ACC 117 (KKL). The interpretation is thicker crud deposits in the lower part of the fuel rod.

In order to reduce the man-doses in LWRs, a method has been developed at Westinghouse Electric Sweden AB for the decontamination of irradiated fuel assemblies, ICEDEC^{TM}. The method uses a slurry of small ice particles mixed in water that are guided through the fuel assembly flow channel. The water containing the detached particles (which is basically crud) is then filtrated in a special filter unit (FILDEC^{TM}), with the same dimensions as a fuel assembly box. Real fuel decontamination was performed in the Ringhals 1 BWR unit in Sweden in order to test the system on-site. Two burned-out fuel assemblies were cleaned using the (test) decontamination facility. The result was that the fuel integrity was maintained and that 60-80% of the loose crud was removed and collected in the filters. The fuel assemblies were gamma scanned for ^{60}Co before and after the decontamination process, an experiment that supported the degree of decontamination, i.e. ^{60}Co count rates were reduced to 20-40% after finishing the decontamination. The activity circulating in the decontamination loop was also monitored using NaI detectors at specific points in order to be able to track the decontamination process dynamically.

7.9 Volatile element redistribution

The axial migration of volatile elements (with Cs being the most prominent example) in fuel rods can be measured by high axial resolution gamma scanning. Extensive migration of volatiles indicates elevated fuel temperatures, possibly beyond safety margins or leading to non-adequate in-pile performance of the fuel. Such measurements have been performed either by using an energy window dominated by the cesium activity and measured by NaI detectors or single peak events measured by high resolution germanium detectors. Significant volatile element migration (to e.g. pellet interfaces where condensation would take place) in the fuel rod is a clear indication of elevated fuel temperatures during operation and would probably also correlate with increased fission gas release.

A series of measurements performed at the Leibstadt nuclear power plant (BWR) showed low degrees of cesium migration [53, 90]. Table 7.2 illustrates the low degree of volatile element migration as evaluated by the computer code RUNE and the low to moderate fission gas release as determined by gamma ray spectroscopy . An energy window between 250 and 850 keV strongly dominated by cesium was defined and the (dimensionless) degree of cesium migration to pellet interfaces was quantified for each fuel rod (Figure 7.6). The degree of cesium migration is basically expressed as a relation between (average) signal strengths over a portion of the fuel rod including several fuel pellets and the signal strength over pellet interfaces [91]. A low degree of cesium migration as measured using the methodology would be indicated by pronounced dips in signal strength over pellet interfaces (Figure

7.6). A full length scanning using the cesium dominated energy window is shown in Figure 7.7, still with dips in signal strength at pellet interfaces clearly visible.

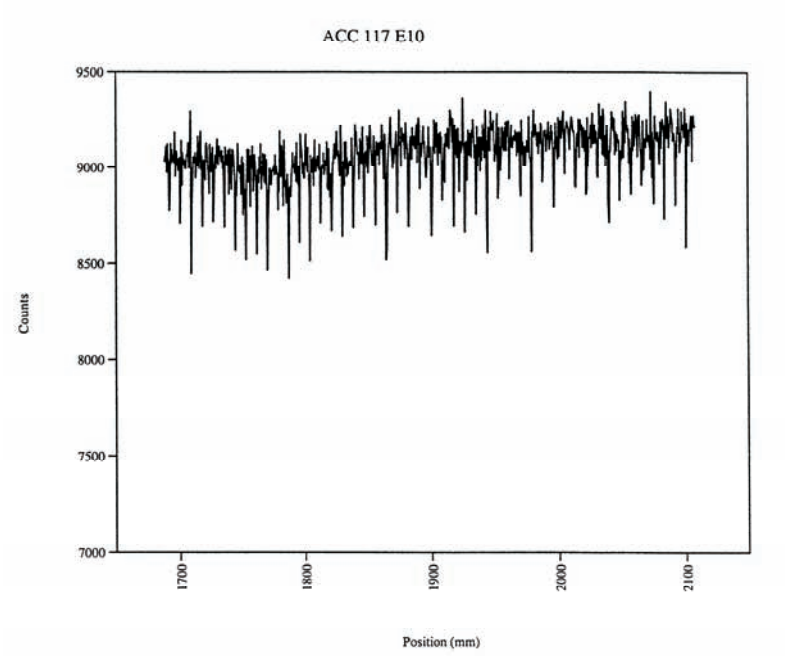

Figure 7.6. Selected part of axial profile measuring cesium migration in the fuel matrix. The dips in count rate are fuel pellet interfaces indicating low degree of migration of volatiles in this case.

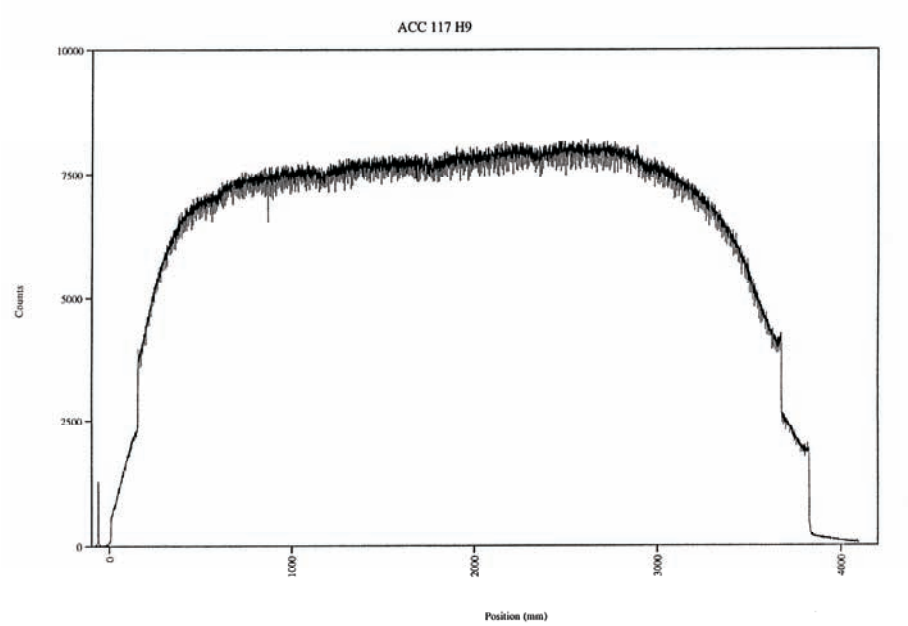

Figure 7.7. Axial profile measured with high axial resolution using a gamma-ray energy window dominated by cesium activity. Dips in the activity at pellet interfaces are clearly indicated.

Table 7.2: *Cesium migration results and fission gas release results for measurements performed at the Leibstadt BWR.*

Assembly	Rod	Cs migration	FGR (%)
ACC 119	F2	0.8	4.8
ACC 119	F9	0.8	3.6
ACC 119	G8	0.8	3.5
ACC 119	H10	0.7	4.0
ACC 119	J3	0.8	4.4
AAA 006	E2	1.0	5.3
AAA 006	F9	1.2	3.7
AAA 006	I5	1.1	5.5
AAA 006	I6	0.8	4.0
AAA 006	J10	0.7	4.6
ACC 117	B6	0.7	0.4
ACC 117	E10	0.5	0.4
ACC 117	F9	0.5	0.4
ACC 117	H9 (BA rod)	0.6	0.2
ACC 117	H10	0.6	0.6
ACC 117	I10	0.6	0.4

Also at the Leibstadt BWR measurements of the axial distribution of the highly volatile iodine was performed. The intensity distribution of the 364.5 keV line of ^{131}I was used for the detection of migration of iodine in the fuel matrix of rod F8 in assembly AAA 023 with an average burnup of 41.7 MWd/kgU. The short half life (8.05 days) of ^{131}I was a challenge at these measurements and they were therefore performed just five days after the reactor shutdown. The background for performing the experiment was the measurements of remarkably thick oxide layers (sometimes as high as 290 μm) on fuel rods by means of poolside eddy current techniques. Such thick layers raised strong concerns over the fuel performance since possible overheating due to the thermal resistance in such a thick oxide layer could be expected.

It was later confirmed (by PIE) that the high oxide thickness measurements was erratic and that the standard eddy current method (the lift-off signal) was influenced by the crud layer due to the Zn injection in the coolant at Leibstadt [49, 50]. However, even before that, it was concluded from the in-pool gamma scanning of the iodine and cesium distribution that the fuel matrix had not been exposed to any abnormal temperatures during operations [41].

7.10 Burnup

Non-destructive burnup determinations based on the ^{137}Cs activity from the fuel column (see Section 3.2.1) have been performed in conjunction with fission gas release experiments, or rather as a by-product of these experiments since the ^{137}Cs intensity is needed for the FGR evaluation [53, 90]. Both full axial scans and measurements at a fixed axial level were performed and measurements were compared to core physics calculations of burnup [53, 90]. Figure 7.8 shows calculated burnup versus ^{137}Cs count rate [75]. Due to three basic causes BA-rod results must be adjusted:

- The density of 3.5 weight-% BA fuel is about 1.2% lower then for standard fuel.
- Only 96.5 % of the fuel material is UO_2.
- The self attenuation in the BA-fuel for 662 keV gamma radiation is reduced somewhat.

Altogether a correction on ^{137}Cs intensities of about +4.0 % for 3.5 weight-% BA-rods should be used in order to use the results as burnup measures for the two kinds of rods mixed.

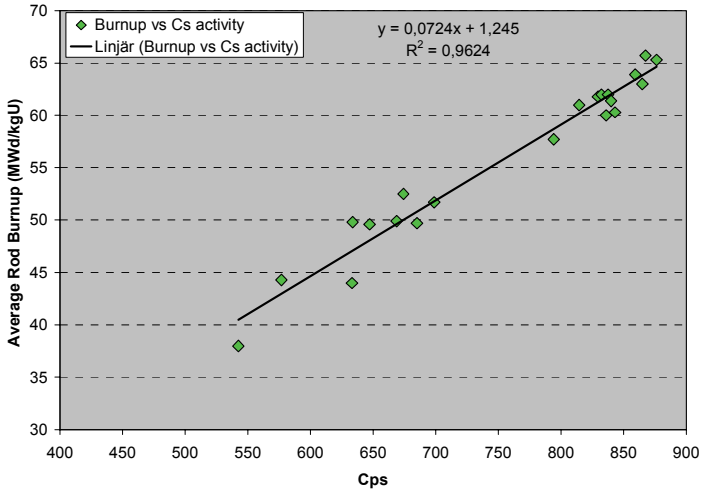

Figure 7.8. Calculated rod burnup versus ^{137}Cs cps with a linear fit.

7.11 Conclusions and remarks

Non-destructive pool-side and in-pool measurements in which the gamma radiation from various nuclides is utilized has been proven successful for the determination of fuel performance indicators and code benchmarking. Measurements have been able to track the significant improvements in fission gas release characteristics from improved fuel designs (e.g. from a 8x8 fuel lattice to a 10x10 lattice and also part length rod designs and SVEA or water cross designs). The non-destructive ^{85}Kr method has generated a valuable data bank covering a wide spectrum of reactors, fuel designs, burnup values and power histories, showing that also in the modern fuel designs the thermal fission gas mechanism appears to be in operation. Based on PIE of the isotopic composition of fission gases also the timing of the release and fuel matrix origin (rim or central parts) has been indicated and compared between older fuel designs and more modern fuel designs.

The increased complexity of modern nuclear fuel designs is the response to challenging demands imposed by the economical demands on commercial nuclear power generation of today and calls for the independent evidence of the reliability of computer codes. The poolside experimental determination of the axial distribution of the Ba/La concentration (thermal power distribution) has provided an extensive dataset for validation of core physics codes like the PHOENIX-4/POLCA-7 package, for several fuel designs, both on fuel bundle level and fuel rod level at various stages of burnup. The high precision of the measurements allows for high quality validation of core physics code packages. For the series of experiments performed on assembly

level at the Leibstadt BWR (KKL), the comparison indicates that the nodal power can be predicted with about 4% uncertainty and the bundle power with an uncertainty of less than 2%. Similar prediction power was demonstrated at other experiments both on single fuel rod level and bundle level [6].

Measurements utilizing radiation from cobalt (^{60}Co) have demonstrated that the thickness/amount of activated crud deposits on the fuel rod surfaces can be determined in relative terms along the axial profile. This method has also been used for an independent verification of a recently developed fuel decontamination method [92].

The migration of volatile elements (basically Cs and I) in the fuel matrix has been measured by means of high axial resolution gamma scanning. The potential of such experiments has been demonstrated under conditions in which the thermal performance of the fuel was questioned during annual outage due to exceptionally thick oxides measured by standard EC methods. Measurements indicated, as confirmed by subsequent PIE, that the fuel had behaved perfectly normal during operations and that the thick oxide layers indicated was an artifact due to choice of reactor water chemistry.

8 Results: Fuel performance studies by means of in-pile experiments

In-pile experiments in test reactors offer real-time information of fuel performance key indicators under highly controlled operational conditions. However, the fuel to be tested has to be specifically designed or remanufactured to fit in the test reactor core and to allow the fuel rig to be properly equipped with sensors. Thus full scale commercial fuel can seldom be studied and the method does consequently not allow for the reloading of fuel in a commercial facility post-experiment. This is in contrast to the pool-side gamma scanning technique, where performance of the fuel can be studied non-destructively and the fuel reloaded after completion of the measurements. The two methods thus complement each other in a most useful way.

Studies of FGR, fuel temperatures and PCMI are addressed in Papers VIII-XI while secondary fuel failure degradation experiments are presented in Papers XII and XIII.

8.1 Paper VIII: The integral fuel rod behaviour test IFA-597.3: Analysis of the measurements

The objective of the IFA-597.3 experiment was to study fission gas release, thermal behavior and pellet-cladding mechanical interaction in high burnup commercial fuel. Two remanufactured fuel rods have been further irradiated from 59 MWd/kgUO_2 to 61.5 MWd/kgUO_2. One fuel rod was instrumented with a fuel centerline thermocouple and a bellows pressure transducer. The other fuel rod was instrumented with a cladding elongation transducer.

The percentage of fission gas release has been evaluated from the pressure readings. An FGR of about 10% is reached at a burnup of 60.3 MWd/kgUO_2. The fission gas release appears to obey a diffusion controlled dependence on time. Fission gas release is only detected by the pressure transducer following a power decrease when the pellet-cladding gap reopens allowing escape ways for the fission gases to the rod free volume (i.e. the phenomenon of delayed fission gas release). The pellet-cladding gap was shown to be tightly closed at nominal power levels.

The fuel centerline temperature is above the Halden threshold for 1% fission gas release during the whole irradiation period of the experiment [45].

In the beginning of the experiment, the peak fuel centreline temperatures are close to 1350°C. Fuel centreline temperatures normalized to a constant linear heat rate showed an increase with burnup that was higher than fuel temperature model codes predictions based on fission gas release poisoning of the pellet-cladding gap and thermal conductivity degradation of the UO_2. The extra increase in the observed fuel centreline temperature may be due to the thermal resistance created by the additional grain boundary fission gas porosity and a radial redistribution of the power generation within the pellet due to the softer neutron spectrum of the HBWR in comparison with the significantly harder neutron spectrum of a LWR. This interpretation is also supported by fuel temperature model codes [93, 94]. Figure 8.1 shows the measured fuel centreline temperature, the average linear heat rate and the moderator temperature for rod 8 during irradiation in the Halden in-pile experiment IFA-597.3.

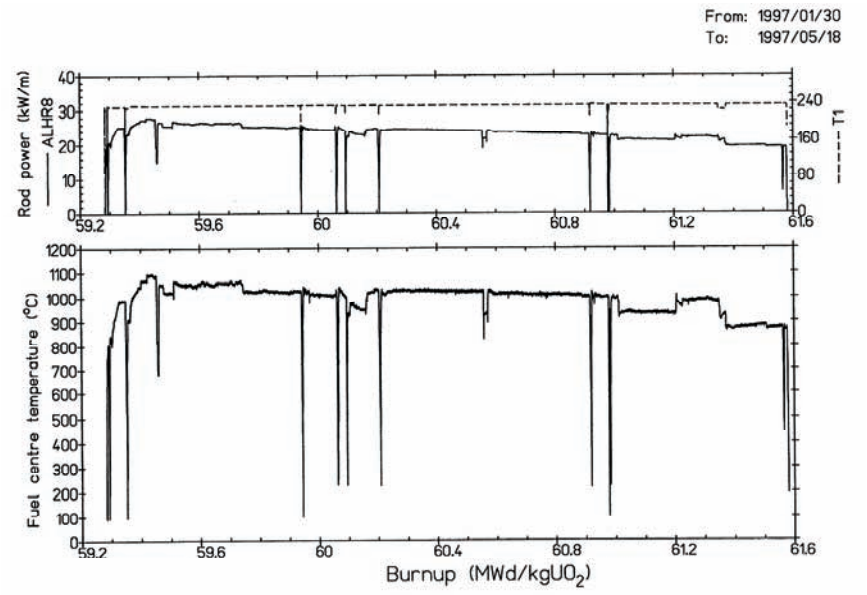

Figure 8.1. Measured fuel centre temperature, average linear heat rate (ALHR8) and moderator temperature (T1) for fuel rod 8 in the experiment IFA-597.3.

The measured cladding elongation has been divided into thermal expansion, permanent elongation and plastic and elastic elongation due to pellet-cladding mechanical interaction. The high degree of PCMI decreases during the first part of the irradiation, showing relaxation of cladding axial stress and strain probably as a consequence of pellet-cladding slip and fuel densification or creep. Following this period there is an increase in normalized

PCMI induced elongation (elongation at a constant LHR) at a rate similar to that expected from solid fission product fuel matrix swelling.

A significant increase in fuel temperature time constants, evaluated at four reactor scrams during the irradiation period, could be observed. The increase with burnup is due to the general thermal degradation of the fuel matrix.

8.2 Paper IX: The effect of fuel micro-structure and burn-up on FGR and PCMI studied in IFA-534.13

Fission gas release and cladding elongation in-pile data have been collected for four high burnup PWR fuel rods with two different grain size (8.5 and 22.1 μm) in the IFA-534.13 experiment. The theoretical expectation is that the larger grains size should have a positive impact on fission gas release (i.e. a lower observed release), mainly as a consequence of the distance the gas atoms have to diffuse before reaching a grain boundary and subsequently reaching the rod free volume [95, 96]. The fission gas release is low for both fuel types. During the first part of the irradiation period there is no significant difference between the normal grain size fuel (8.5 μm) and the large grain size fuel (22.1 μm).

During the second half of the irradiation period the FGR was slightly higher in the large grain size fuel. The fission gas release at end-of-life in the large grain size fuel is about 2.1% while it is about 1.5% in the normal grain size fuel. The reason for this result is unknown although the possibility of an irregular behavior of the pressure transducer in the normal grain size fuel is a possibility (although no clear indication of this was observed during the experiment). It was basically concluded that it was necessary to await the next experiment in the series (IFA-534.14, see Section 8.3) due to these uncertainties.

The degree of pellet-cladding mechanical interaction was higher in the large grain size fuel during the first part of the in-pile experiment. During the second period the difference between the two grain sizes were insignificant. The point of onset of PCMI had shifted to lower power between the beginning and end of the irradiation period, with a similar behavior of both fuel types. No clear indication of relaxation was observed for either fuel type, an observation possibly connected to the very weak rim structure in these rods.

8.3 Paper X and Paper XI: The Effect of Grain Size on FGR and PCMI in High Burnup Fuel (IFA-534.14)

Fission gas release and cladding elongation data of four high burnup PWR fuel rods with three different grain sizes (8.5, 22.1 and 38.0 μm, respectively) have been analyzed and compared in the IFA-534.14 in-pile experiment. The fission gas release measurements shows that rod 19, with the smaller grain size of 8.5 μm, has experienced a higher degree of fission gas diffusion to grain boundaries than rod 18 with the larger grains size of 22.1 μm, and that this fission gas is subsequently released to the free volume of the rods during the power ramps (i.e. the phenomenon of delayed fission gas release is observed). At the end of the experiment (at a burnup of 55.1 MWd/kgUO_2) the fission gas release is about 3% in rod 18 and about 9% in rod 19.

The conclusion reached from the comparison of experimental data and computer code predictions is that the characteristics of the fission gas release reflect the difference in rod design, which was grain size in this experimental setup. The fit between measured and predicted fission gas release is very good at the end of the experiment, see Figure 8.2 [97].

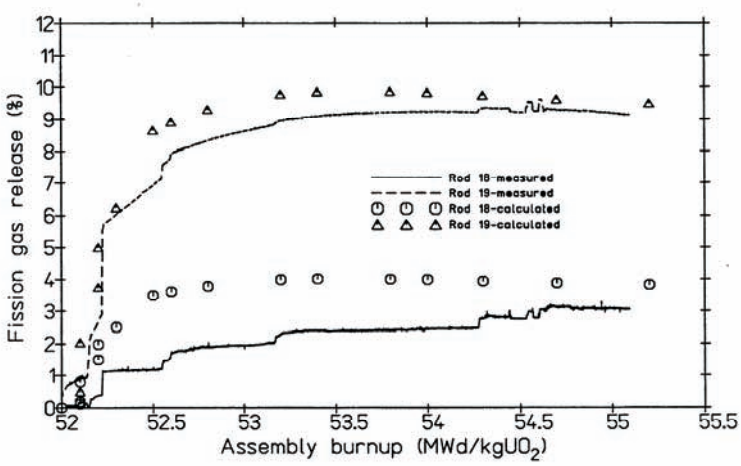

Figure 8.2. Measured and predicted fission gas release in the IFA-534.14 Halden in-pile experiment.

The increase in cladding elongation for rods 20 (grain size 22.1 μm) and 21 (grain size 38.0 μm) is similar to that expected from a solid fission product fuel swelling rate of 0.75% $\Delta V/V$ per 10 MWd/kgUO_2. Some relaxation takes place during the first part of the irradiation period. An observed permanent elongation of 0.20-0.30 mm at the end of the experiment is believed to be due to cladding creep and/or plastic deformation to accommodate the solid fission product fuel swelling, with some small contribution from irra-

diation induced cladding growth. There is no significant difference between the two fuel rods in terms of cladding elongation behavior (PCMI).

The IFA-534.14 experiment clearly indicates that increased UO_2 grain size is an effective way of suppressing fission gas release in LWR fuel to the burnup level covered by this experimental investigation.

8.4 Paper XII: Reaction Kinetics of Oxidation and Hydriding Inside Operating Fuel Rods

The fuel degradation test series in IFA-634 were carried out to study the reaction kinetics of oxidation and hydriding of fuel and cladding after a rod primary failure. In order to simulate such conditions the fuel rods were filled with a known amount of water and irradiated under BWR conditions in the HBWR. Four loadings of totally seven fuel rods with different pellet-cladding gap, initial water amount and cladding material, have been irradiated during one Halden reactor cycle and target power levels ranging from 13 to 30 kW/m. The rods were equipped with pressure transducers to measure the rod internal pressure changes with time.

In the beginning of the experiment all rods showed a similar development in pressure. The rod pressure increased and reached a peak value. At this stage the differences in rod pressures are caused by the different linear heat rates. After reaching the peak pressure a decrease could be observed. For fuel rods with a pure zirconium liner cladding the pressure decrease apparently occurred when the same calculated inner cladding oxide thickness was reached for these rods. The calculation of the thickness of the oxide layer was according to ref. [98]. Subsequently the pressure fell at different rates depending on the pellet-cladding gap, the initial amount of water and the cladding type as well as the linear heat rate.

The rate of pressure decrease with time was higher for rods with a higher average linear heat rate and for rods with a lower amount of water present. Since the time-dependent pressure changes should reflect the reaction kinetics in the rods, a clear difference in the corrosion behavior can be expected between rods with pure zirconium liner and rods with a Fe-enhanced liner. An improvement in the corrosion resistance leads to a thinner oxide thickness as well as less hydrogen uptake. Such a behavior was also observed in the experiment.

8.5 Paper XIII: Test-Reactor Study of the Phenomena Involved in Secondary Fuel Degradation

The test rig IFA-631, holding four instrumented test rods, was loaded in a BWR loop in the Halden test reactor to study the phenomena involved in secondary fuel degradation after simulating a primary failure. Liner claddings with an outer zircaloy-2 component and an inner ZrSn-liner were used. Two out of the four claddings were pre-oxidized to enable evaluation of a thin zirconia layer as a potential barrier towards hydrogen pick-up thereby also being a possible remedy against secondary fuel failure degradation (Table 8.1). Primary failure was simulated at power after a base irradiation period of 144 days and the rods were subsequently irradiated under primary failure conditions for another 118 days. The primary failure was simulated by opening the valves of a so-called water ingress device (WID) in the upper part of the fuel rods and coolant water entered the test rods at power.

The data from the in-pile measurements clearly show the evolution of so-called oxygen- or steam starvation immediately after the simulation of the primary failures. The upper part of the rods (close to the simulated primary failure) is dominated by steam, while the lower part of the rods is characterized by a gas mixture with a very high hydrogen partial pressure. The upper parts of the rods were filled with steam from the point in time where the primary failure was simulated until the end of the in-pile experiment. The environment in the lower end of the fuel rods changed within a few days after simulating the primary failure showing that steam after a certain period reached all parts of the fuel rods.

Table 8.1: *The main features of the test rods in the IFA-631.1 secondary fuel degradation experiment.*

Parameter/Rod	**631-1**	**631-2**	**631-3**	**631-4**
Pellet-cladding gap (μm)	85	55	85	55
Pre-oxidized inner cladding surface	No	No	Yes	Yes

The post-irradiation examination showed heavily hydrided areas in regions of the cladding near the lower end of the fuel stack in all four rods. In these regions the measured hydrogen concentration was in the range from 400 to above 5500 ppm, while 100-160 ppm of hydrogen was measured in the upper and middle sections of the claddings.

It is concluded that the experimental set-up enabled simulation of the conditions that occur following a primary debris failure in the top end of a fuel rod in a commercial reactor. It is further concluded that excessive hydrogen pick-up takes place during the first few days after the occurrence of a

primary failure and that a pre-oxidized layer does not function as a barrier towards hydrogen pick-up under exposure in an environment with a very high partial pressure of hydrogen.

8.6 Conclusions and remarks

In-pile experiments have been performed with the aim to study the impact on fission gas release from various grain size distributions of the UO_2 matrix. The results are well in accordance with computer code simulations, showing the positive effect (lower fission gas release levels that is) on macroscopic fission gas release from larger grain size.

The in-pile secondary fuel failure degradation experiments clearly demonstrated the development inside an operating fuel rod with a simulated primary failure in its upper part. The experimental set-up was able to track the change in gas composition in the fuel pellet cladding gap following the primary failure and ingress of water/steam and that steam starvation conditions prevailed in the lower part of the operating fuel rods (i.e. a very high partial pressure of hydrogen). Subsequent PIE also demonstrated massive hydriding in the lower parts of the cladding. It was also concluded that a pre-oxidized inner surface of the liner does not act as a very efficient remedy against the development of secondary fuel failures under steam starvation conditions. However, our conclusion is that a second in-pile experiment with a somewhat modified experimental set-up (like e.g. different pellet-cladding gap and geometry of the simulated primary failure) would be highly beneficial.

9 Outlook

The very high demands on modern commercial nuclear fuel, originating from a combination of a more competitive economic environment (both concerning price for electricity, competition from other modes of producing electricity and spent fuel management costs) and the generally high focus on safety within the nuclear industry in comparison with most other industry sectors, call for methods for the non-destructive determination of various fuel performance indicators. The non-destructive nature of measurements keeps the possibility of feedback to reactor operators and regulators open. The collected data bank is typically used for the benchmarking of core- and fuel physics computer codes. This application also calls for the ability to create a data set covering a wide spectrum of operating characteristics and objects (fuel types).

The evolution of on-site gamma ray spectroscopic methods applicable to nuclear fuel performance studies could be briefly summarized as below:

- Measurements at a number of fixed axial positions for e.g. burnup and thermal power axial distributions (late 1970s).
- Continous scanning of the intact assembly or single fuel rod for e.g. burnup and thermal power (1990s).
- Submergible detector housing and collimator system for in-pool measurements (LOKET in the late 1990s).
- On-site tomographic techniques (PLUTO in the early 2000s).
- Next generation of tomographic techniques (KARON as a concept).

The two last points are still under development and the tomographic techniques have not yet been used to collect any volumes of experimental data. The submergible detector and collimator housing system has been developed and used for the collection, in parallel with measurements utilizing the through-wall collimator, of an extensive dataset concerning fission gas release, axial thermal power distribution, volatile element migration and burnup. The dataset covers a wide spectrum of fuel types, reactor units, burnup and power histories. The experiments performed reflects the developments in fuel designs, from 8x8 type fuel to advanced water cross and part length rods fuel assemblies. The potential of the poolside gamma scanning method has been demonstrated also for measuring the level of crud deposition on irradiated fuel rods.

The following areas/tasks are identified for further usage and development of the gamma-ray spectroscopy method as presented in this thesis:

- Benchmarking and validation of the crud measuring technique versus poolside electromagnetic measurements (i.e. Magnacrox) and/or PIE, relating the measured cobalt activity to the actual amount of crud present. In this way a very versatile method for non-destructive crud measurements will emerge.
- The method is suggested to be used as a benchmarking tool for the tomographic measurements. It is suggested that an experiment/campaign is performed in which data are collected from a fuel assembly using both the tomographic technique and gamma scanning of a more limited number of fuel rods from the assembly.
- The method should be used to collect data at even higher burnups since the core- and fuel physics codes should be evaluated for the most modern fuel designs now starting to reach very high burnup levels, where specific high burnup phenomena might be encountered, e.g. rim effects in fission gas release.

The in-pile secondary fuel failure degradation experiments have been able to simulate the conditions in an operating fuel rod experiencing a primary (debris) failure. It is concluded that excessive hydrogen pick-up takes place during the first few days of the occurrence of the primary failure and that a pre-oxidized layer does not function as an efficient barrier when the partial hydrogen pressure is very high. It is suggested that a second secondary fuel failure degradation in-pile experiment is performed in order to reach a better understanding of the dependence on hydrogen partial pressure for the development during irradiation.

In the in-pile fission gas release experiments the positive effect from increased grain size of UO_2 was demonstrated. The ongoing developments in fuel composition for increasing the fuel performance in various respects, like e.g. fuel additives such as Al_2O_3 and Cr_2O_3, should preferably be experimentally verified in a test reactor.

In view of the intensive discussions going on regarding the effects on the global climate from increasing emission of greenhouse gases in combination with currently high demands for oil and gas and finite supply concerns, a renaissance of nuclear power is not only thinkable but maybe also necessary. Clear signs of such a change in standpoint are e.g. the new reactor (PWR) under construction in Finland and the extensive nuclear plans in China (one of the really large and fast growing consumers of energy resources). Also the ongoing research efforts within the field of transmutation could very well put extra confidence in the nuclear technology, potentially providing a way of at least reducing the problems related to the long term storage of spent fuel. Taking such a perspective a possible scenario could be the initiation of new

nuclear programs in various parts of the world, the development of new reactor concepts (like the pebble bed reactor) and the successive replacement of older reactors on a global basis. Such a development will demand accurate methods for the determination of fuel and fuel material performance, fuel safety, computer code benchmarking and safeguard systems.

The non-destructive gamma-ray based methods presented and used for measurements in this thesis may well serve as a starting point for the development of new methods, techniques and applications.

Acknowledgements

Not very surprising, there are a lot of people who have helped me and supported me during the work with this thesis throughout the years (and quite a number of years have accumulated since the start to be honest). The work presented in this thesis has been performed within a number of institutions, namely Westinghouse Electric Sweden AB (formerly ABB Atom AB), the Department of Nuclear and Particle Physics (IKP), formerly Department of Radiation Sciences at Uppsala University and the OECD Halden Reactor Project (HRP) in Halden, Norway. Following my Licentiate degree, the work has also been performed within the framework of the Graduate School for Advanced Instrumentation and Measurements (AIM) at Uppsala University.

First and foremost, I would like to thank my three supervisors Prof. Anders Bäcklin and Ass. Prof. Ane Håkansson at Department of Nuclear and Particle Physics and Dr. Björn Grapengiesser, Senior Specialist at Westinghouse Electric Sweden AB. The integrated knowledge and experience of these three guys is truly astounding, furthermore they possess a sense of humor I certainly appreciate. A special thank to Björn for the interesting kind of guidance during the always chaotic (but in the end successful) on-site experiments. Here, the humor was many times unintentional. Björn is not only a supervisor and former colleague he is also a good friend and excellent travel companion. I would also like to thank my examiner Prof. Bo Höistad, as well as Prof. Sven Kullander, both at Department of Nuclear and Particle Physics.

Concerning the part of the thesis work performed at the Halden research reactor I would like to send my special thanks to Erik Kolstad, Dr. Carlo Vitanza, Dr. Wolfgang Wiesenack, Hideyuki Teshima, Yvonne Broy and Dr. James Turnbull. The two years I spent as a secondee (or guest scientist) in Halden was both stimulating from a scientific and educational perspective and also very nice from a social perspective. I hereby thank all personnel and secondees at the Halden facility for a good time and new friends from all parts of the world.

I spent more than five years at Westinghouse and the major part of the work resulting in this thesis was performed there. I would like to thank all my former co-workers there for making working hours to something more than just hours at the office. A special thank to Tommy Bard, Pascal Jourdain, Dr. Kurt-Åke Magnusson, Dr. Lars Hallstadius (who also employed me), Mats Dahlbäck, Björn Andersson, Dr. Lembit Sihver, David Schrire

(co-author), Magnus Limbäck, Maciej Kosinski, Karin Backman, Dr. Per Tägtström, Lennart von der Burg, Juan Casal, Dr. Ali Massih and Ann-Kristine Timmonen. I also want to specifically recognise all the people at the Service Division that I work with during the on-site measurements, as well as the core physicists at Westinghouse for very good cooperation. I received financial support from Westinghouse during the spring 2005 (note, several years after leaving the company) helping me finalising the thesis. This unselfish act is something that in my mind indicate the very deep interest Westinghouse people have in their field, so ones again thank you all.

At Department of Nuclear and Particle Physics I send my thanks to the other, current and former, members of the Applied Nuclear Physics Group, Dr. Staffan Jacobsson Svärd, Christofer Willman, Otasowie Osifo, Dr. Peter Jansson and Tobias Lundqvist. Staffan, Peter and I started our thesis work at about the same time (give and take a year or so) and they have always been helpful in every respect. Both Staffan and Peter should also be recognised for contributing to the content in my thesis. I also like to recognise the diploma workers active in the group, securing the future of this interesting and important field of science and technology. Although I spent rather limited time at the Department, I certainly needed access to the computer system when I was there and I would like to thank Ib Koersner for helping me out with this issue. The valuable assistance and advice of the administrative personnel at IKP, particularly Inger Ericson, is hereby also recognised.

The measurement campaigns at various nuclear facilities would not have come out as good as they did without the strong engagement and smoothness of their personnel. I hereby collectively thank all the personnel that I interact with at Leibstadt NPP in Switzerland, Cofrentes NPP in Spain, Barsebäck and Ringhals in Sweden and TVO in Finland. A special thank to Dr. Hans-Urs Zwicky at Leibstadt (at the time).

The AIM graduate school partly introduced a new view on licentiate and doctoral programs with a profile targeting professional careers in research and research leadership in industry. I tried to be a good disciple, and maybe I was even a little bit too dedicated to the ideas behind AIM, after all, it is not necessary start working at a bank just because you are a part of the AIM graduate school. A warm thanks to AIM directors Erkki Brändas and Bo Thidé as well as all the graduate students engaged in AIM during the years. A special thank to Mattias Lantz for the extra efforts in arranging AIM activities, coming to think of it, I owe you a AIM seminar concerning my work at the bank.

Speaking about banks, I spent the last five years, first as a financial analyst and currently as a senior risk analyst, at Skandinaviska Enskilda Banken or SEB in Stockholm. Although it stretched the time planning for my thesis significantly (to say the least) I never regret starting off in this new direction. A thank to all my former co-workers at the Credit Analysis (Industry and Corporate Analysis) Department, and especially my team there, and my cur-

rent colleagues at Group Risk Control (GRC). A special thank to Egil Aarrestad, Kristian Andersson and Philip Winckle for the opportunity to finalising the thesis on a part time basis. Furthermore, I would like to thank Lidia Pixell, Erik Fröjd, Philip and Michael Ahlberg at GRC for very interesting discussions concerning credit risk models (and yes, credit risk models are interesting, at least to some people).

I want to express my deepest gratitude towards my parents Folke and Ann-Marie, as well as my little brothers Erik and Per-Olof (it felt good to refer to the former weight-lifter Erik as little by the way). My father's unlimited supply of so called Fermi problems is hereby recognised, as well as the fact that he basically inspired my interest in science when I was a young boy. To the other caring members of my own family and my wife's, thank you all. A special thanks to my dear friend Kurt, especially for all these discussions concerning our actual, but more often only pure speculations on the potential (and usually also highly unrealistic), performances in various sports. I would like to thank my cousin Bengt for inspiration. Bengt was a brilliant physicist who is sadly enough no longer with us.

Last, but to me a very important part, I thank my wife Lena and my two daughters Karin and Linnea for their love, support and understanding. Lena has shown a tremendous patience with me and my projects throughout the years, she has encouraged me in my work, and she shows me basically every day that it is true as it is written: *"Kärleken är tålmodig och god"*.

Summary in Swedish

Direkt översatt till svenska blir denna avhandlings lite omständliga titel **Studier av kärnbränsles egenskaper med hjälp av gammaspektroskopi vid pool och mätningar i härd**. Avhandlingen sammanfattar innehållet i, och utvecklingsarbetet knutet till, ett antal rapporter inom industriell forskning, publikationer i internationella tidskrifter och presentationer vid internationella konferenser. Två delområden avhandlas, dels oförstörande studier av bestrålat kärnbränsle på kärnkraftverk med hjälp av gammaspektroskopi, dels mätningar på kärnbränsle under bestrålning i testreaktorer med instrumentförsedda bränsleelement. Med oförstörande studier förstås att experimenten kan utföras utan att bränslets integritet påverkas. Arbetet syftar till att generellt öka förståelsen för de processer som äger rum i kärnbränsle under drift såsom t.ex. fissionsgasavgivning (FGR) och fördelningen av den termiska effekten i bränslet. Speciellt har effekterna på olika parametrar då nya bränsledesigner introducerats studerats. En annan målsättning har varit att generera ett dataunderlag för validering av härdfysikaliska och bränslefysikaliska beräkningsprogram.

Skador som uppstår på bränslet under drift kan orsaka utsläpp av radioaktivitet i kärnkraftverkets primära system och leda till stora kostnader. Därför har förloppet när en skada uppstått på bränslets kapsling studerats under kontrollerade former i en experimentreaktor. Med ökad förståelse för dessa processer kan bränslet utnyttjas bättre ur ett rent ekonomiskt perspektiv med bibehållna säkerhetsmarginaler. I förlängningen kan man även därigenom minska den totala mängden producerat kärnavfall.

Kärnbränsle

Den grundläggande process som genererar energin i en kärnreaktor är klyvning, eller fission, av tunga atomkärnor som uran och plutonium. Till skillnad från en kärnvapenexplosion så kontrolleras fissionsprocessen i en kärnreaktor så att en stabil kedjereaktion upprätthålls. I så kallade lättvattenreaktorer (LWR), och kärnbränslet som studerats i denna avhandling är avsett för denna typ av reaktorer, så anrikar man bränslet på den klyvbara uranisotopen U-235 upp till ungefär 5 % av det totala innehållet av tunga atomkärnor. Ett antal olika bränsledesigner för lättvattenreaktorer av så kallad kokarvattentyp (BWR) finns, alla har dock det gemensamt att de består av kutsar av

urandioxid som staplas på varandra i kapslingsrör, bestående av en zirkoniumlegering, av cirka 4 m längd och cirka 10 mm i diameter. Här sker emellertid en ständig utveckling för att öka bränslets prestanda och säkerhetsmarginaler. Exempel är bränsleelement med så kallade dellånga stavar, fler bränslestavar i tvärsnittet och speciella vattenkanaler i tvärsnittet. Tidigare bränsletyper hade ofta 8x8 bränslestavar i ett tvärsnitt, medan de moderna har 10x10 eller fler. Bränslet till tryckvattenreaktorer (PWR) består av fler stavar i varje element (t.ex. 17x17 stavar) men har i övrigt en likartad teknisk uppbyggnad.

Normalt drivs reaktorerna i cykler om omkring ett år, varefter man byter ut delar av bränslet i härden och går igenom anläggningens olika system. Efter 4-6 sådana cykler är bränslet slututbränt och förvaras i väntan på geologisk slutförvaring, vilket är det vanligaste alternativet hos de länder som har kärnkraftprogram, eller annan behandling i from av upparbetning för att återvinna klyvbara isotoper, detta tillämpas av vissa länder helt eller delvis. I en framtid hägrar möjligen även så kallad transmutation, ett sätt att på teknisk väg behandla det utbrända kärnbränslet så att långlivade radioaktiva kärnor omvandlas till stabila eller kortlivade kärnor.

Innan kärnbränslet har bestrålats i en reaktor avges endast en mycket begränsad mängd strålning från de naturligt förekommande uranisotoperna. Detta förändras emellertid snabbt efter påbörjad bestrålning i en reaktorhärd. Ett nyligen uttaget bränsleelement är en mycket kraftig strålkälla, främst på grund av alla de fissionsprodukter som byggts upp under driften. Samtidigt innebär naturligtvis detta att materialets egenskaper, både fysikaliska och kemiska, förändras radikalt. Den starka joniserande strålningen från fissionsprodukterna och nuklider bildade genom så kallad neutroninfångning, kan emellertid användas för att dra slutsatser om bränslets egenskaper genom att mäta energispecifikt och/eller med hög rumslig (axiell) upplösning. Detta för oss in på gammaspektroskopiska metoder.

Gammaspektroskopi

Mätmetoden bygger på användandet av germaniumdetektorer, HPGe, som tillåter hög energimässig upplösning och därmed nuklidspecifik information. Mätningar har antingen utförts bakom bränslebassängens vägg i torrt utrymme eller med mätsystem nedsänkt i bränslebassängen. Den första optionen har dock bara varit möjlig vid vissa kärnkraftverk som har haft en förberedd kollimator i poolväggen. Kollimatorn definierar upp en lämplig strålgång mellan bränslet och detektorn. För mätningar på andra kärnkraftsanläggningar har ett speciellt mätsystem, kallat LOKET, utvecklats. LOKET består av en vattentät enhet i vilken en germaniumdetektor kan placeras tillsammans med sin kylning av flytande kväve. Ett kollimatorpaket finns inbyggd i det cirka 1.5 ton tunga mätsystemet. Vid mätning sänks LOKET ner

i bränslebassängen till cirka 7 m djup och kärnbränslet hanteras i en speciell fixtur. Figur 1 visar LOKET under slutmontering vid bränslebassängen. Namnet kommer sig av att mätsystemet till det yttre liknar ett gammeldags ånglok och inte på grund av fysikers ökända fascination för långsökta akronymer.

Två egenskaper har särskilt studerats hos kärnbränslet i denna avhandling, fissionsgasavgivning (FGR) och fördelningen av termisk effekt över bränsle och härd. En betydande del av klyvningsprodukterna är gasformiga såsom xenon och krypton, och har därmed sin speciella påverkan på kärnbränslets egenskaper. Gaser lösta i matrisen, eller ansamlade i form av bubblor i eller mellan mineralkornen, påverkar bland annat bränslets termiska egenskaper på ett genomgripande sätt. Den andel av gaserna som slipper ut ur bränslematrisen och samlas i gapet mellan kutsarna och kapslingen samt i bränslets så kallade plenum, påverkar dessutom de termiska egenskaperna hos gasblandningen där. I båda fallen är påverkan av det negativa slaget, med ökat termiskt motstånd som konsekvens och därmed högre temperaturer vid en given effektutveckling. Detta kan resultera i en positiv återkoppling där högre bränsletemperaturer leder till högre fissionsgasavgivning, vilket i sin tur resulterar i högre bränsletemperatur och så vidare. Fissionsgasavgivningen kan mätas med hjälp av gammastrålning specifik för Kr-85, en ädelgas med en halveringstid på omkring 10 år. Aktiviteten från Kr-85 i bränslestavens plenum (ett gasfyllt utrymme i stavarnas övre del), ett mått på den mängd fissionsgas som avgivits, relateras till producerad mängd i staven för att beräkna avgiven fraktion i procent. Denna typ av mätmetod har påvisat, bland annat, den betydligt lägre fissionsgasavgivningen i moderna bränsletyper jämfört med äldre typer. Den stora fördelen med denna mätmetod är dess oförstörande natur vilket tillåter att en omfångsrik databas har kunnat byggas upp för olika bränsletyper.

Figur 1. LOKET under montering innan nedsänkning i bränslebassängen. Detektorn med sitt flytande kväve placeras i bildens vänstra del (”hytten”) medan kollimatorpaketet finns i bildens högra del (”ångpannan”). Genom röret (”skorstenen”) leds signalkablarna upp till elektronikenheter och mätdatorer.

Den termiska effektens fördelning i bränslet och över härden beräknas med hjälp av storskaliga beräkningsprogram, som exempelvis Westinghouse PHOENIX-4/POLCA-7. Beräkningarna sker ner till enskilda så kallade noder, 25 stucken fördelade längs en stav eller patron. Dessa beräkningskoder behöver valideras experimentellt och här erbjuder gammaspektroskopin möjligheten att mäta fördelningen av Ba-140 över enskilda bränslestavar eller över hela bränslepatroner. Intensitetsfördelningen av Ba-140 är ett bra mått på den termiska effekten som bränslet har genererat under de sista 3-4 veckorna i härden. LOKET har använts vid ett stort antal sådana experiment vid reaktorer av BWR-typ i Schweiz och Spanien. Resultaten visar att överensstämmelsen mellan beräkningar och mätningar, uttryckt som rms fel, är bättre än 2% för effekten över en hel patron och bättre än 4% för en enskild nod hos patron. För mätningar på enskilda stavar är överensstämmelsen ytterligare cirka en faktor två bättre.

Utöver dessa två tillämpningar har den gammaspektroskopiska metoden använts för att påvisa en eventuell omfördelning av volatila element som exempelvis jod och cesium i kutsarna. En mer omfattande sådan omfördelning skulle indikera onormalt höga bränsletemperaturer under driften med sämre säkerhetsmarginaler som konsekvens. Sådana experiment har utförts genom att skanna bränslestavarna med hög axiell upplösning för energiområden som domineras av aktivitet från sönderfallet av t.ex. cesium. Den axi-

ella fördelningen av Co-60 har även studerats som en indikation på mängden crud på bränslestavarna. Crud är benämningen på en mer eller mindre lös beläggning på bränslets kapsling bestående av aktiverade korrosionsprodukter. Crud är mycket aktivt och bidrar till att dosbelasta kärnkraftverket.

Mätningar i härd

I experimentreaktorn i Halden, Norge, eller OECD Halden Reactor Project som detta internationella forskningssamarbete kallas, har fissionsgasavgivning, interaktionen mellan kutsar och kapsling samt hur dynamiken i en bränsleskada utvecklas under drift studerats i denna avhandling. Detta har skett med hjälp av speciellt instrumenterade bränslestavar samlade i grupper. Dessa kallas IFA, Instrumented Fuel Assembly. Fördelen med denna experimentella metodik är att parametrarna kan studeras i realtid och under realistiska driftförhållanden. Fissionsgasavgivningen mäts med hjälp av trycksensorer och kapslingens och bränslets interaktion med hjälp av olika typer av extensometrar. Höga krav ställs här på den experimentella utrustningen som skall klara de kraftiga strålningsfält som uppstår under reaktordriften utan att degenerera för snabbt. Fissionsgasavgivningen i bränslen med olika kornstorlek hos urandioxiden har speciellt studerats. Större korn begränsar fissionsgasavgivningen enligt teoretiska modeller, detta bekräftades också genom de experimentella resultaten (se Tabell 1).

Tabell 1. *Fissionsgasavgivningen uppmätt i experimentreaktorn i Halden i bränslen (urandioxid) med olika kornstorlek.*

Stav	**Kornstorlek**	**Fissionsgasavgivning**
19	8.5 μm	3%
18	22 μm	9%

Skador på bränslekapslingen kan resultera i aktivitetsutsläpp i primärsystemet och därmed en ökad dosbelastning på anläggningen. Degenererar en bränsleskada ytterligare kan man tvingas till en oplanerad avställning för att byta ut det skadade bränslet med stora kostnader som följd. Även om skador på bränslet har minskat med de moderna designerna så förekommer de fortfarande och en ökad förståelse av skadeförloppet är av stor vikt för att hitta motåtgärder. Förloppet är oftast att en primärskada uppstår på bränslekapslingen genom nötning av någon partikel, vanligtvis skräp som cirkulerar i reaktorkretsen. Via denna primära skada kommer vatten in i bränslestavens fria inre volym och en process startar där frigjort väte tränger in i kapslingen från insidan, hydrerar denna som man säger, vilket avsevärt försvagar kapslingens fysikaliska egenskaper och gör den mindre motståndskraftig och

spröd. I vissa fall får man ett brott på kapslingen där hydreringen varit som kraftigast och en fullt utvecklad bränsleskada (sekundärskada) med stora aktivitetsutsläpp som konsekvens. Processen brukar refereras till som sekundär bränsledegradering eller som sekundär bränsleskadeutveckling. Genom att förse kapslingens insida med en så kallad liner eller genom att föroxidera kapslingen kan man motverka en sådan utveckling. Dessa åtgärder fungerar då som en barriär mot vätediffusionen in i kapslingen.

Experiment har utförts i Haldenreaktorn där man simulerat en primärskada genom att under kontrollerade former släppa in vatten i stavarna och sedan följa utvecklingen under fortsatt drift, dels genom att mäta temperaturen i stavarna och dels aktivitetsnivån i testriggen. Experimenten simulerade väl den utveckling som sker i en kommersiell bränslestav efter en primärskada i den övre delen och att massivt upptag av väte sker under de första dagarna efter en primärskada. Vid mycket höga partialtryck av väte tycks inte heller en föroxiderad inre kapslingsyta fungera som en effektiv diffusionsbarriär för väte.

References

1. F. Robelius, *Giant Oil Fields and Their Importance for Peak Oil*, Licentiate Thesis, Department of Radiation Sciences, Uppsala University (2005).
2. *Deep repository for spent nuclear fuel, SR 97 – Post Closure Safety*, Technical Report TR-99-06, Swedish Nuclear Fuel and Waste Management Company, SKB AB (1999).
3. S.T. Hsue, T.W. Crane, W.L. Talbert Jr and J.C. Lee, *Nondestructive Assay Methods for Irradiated Nuclear Fuels*, Report LA-6923 (ISPO-9), Los Alamos National Laboratory (1978).
4. A. Bäcklin, A. Håkansson, P. Björkholm, A. Dyring and K-G. Görsten, *A Gamma-Spectroscopy System for Burnup Measurements of Nuclear Fuel*, 13th ESARDA Symposium of Safeguards and Nuclear Material Management, Avignon, France, May 1991.
5. A. Håkansson and A. Bäcklin, *Non-destructive assay of spent BWR fuel with high-resolution gamma-ray spectroscopy*, Report TSL/ISV-95-0121, ISSN 0284-2769, Department of Radiation Sciences, Uppsala University (1995).
6. J. Casal, J. Krouthén and M. Albendea, *Reliable tools to model advanced SVEA fuel designs*, Proceedings from the 3rd ANS topical meeting on Advances in Nuclear Fuel Management, Hilton Head Island, SC, USA, October 5-8, 2003.
7. J. Casal, J. Krouthén and M. Albendea, *Accurate Tools to Model Advanced SVEA Fuel Designs*, Nuclear Technology, vol. 151, pp. 51-59 (2005).
8. P. Jansson, *Studies of Nuclear Fuel by Means of Nuclear Spectroscopic Methods*, Acta Universitatis Upsaliensis, Comprehensive Summaries of Uppsala Dissertations from the Faculty of Science and Technology 714, Uppsala, ISBN 91-554-5315-5 (2002).
9. S. Jacobsson Svärd, *A Tomographic Measurement Technique for Irradiated Nuclear Fuel Assemblies*, Acta Universitatis Upsaliensis, Comprehensive Summaries of Uppsala Dissertations from the Faculty of Science and Technology 967, Uppsala, ISBN 91-554-5944-7 (2004).
10. M. Dahlfors, *Studies of Accelerator-Driven Systems for Transmutation of Nuclear Waste*, Comprehensive Summaries of Uppsala Dissertations from the Faculty of Science and Technology 146, Uppsala ISBN 91-554-6462-9 (2006).
11. J.-E. Lindbäck, *STAV7.0 Calibration and validation*, ABB Atom Report BKC 96-108 (1996).
12. B. Cox, *Pellet-Cladding Interaction (PCI) Failures of Zirconium Alloy Fuel Cladding – A Review*, Journal of Nuclear Materials, vol. 172, pp. 249-292 (1990).
13. M.B. Cutrone and G.F. Valby, *Gamma Scan Measurements at Quad Cities Nuclear Power Station Unit I Following Cycle 2*, Report EPRI NP-214, Electric Power Research Institute (1976).
14. N.G. Sjöstrand, *Reaktorfysik*, Chalmers University of Technology (1992).
15. J.K. Fink, M.G. Chasanov and L. Leibowitz, *Thermodynamic Properties of Uranium Dioxide*, Journal of Nuclear Materials, vol. 102, pp. 17-25 (1981).

16. S. Glasstone and A. Sesonske, *Nuclear Reactor Engineering*, Krieger Publishing Company, Malabar, Florida (1981).
17. M.D. Freshley, D.W. Brite, J.L. Daniel and P.E. Hart, *Irradiation-induced densification of UO_2 pellet fuel*, Journal of Nuclear Materials, vol. 62 (1975).
18. D.G. Franklin et al., *Low Temperature Swelling and Densification Properties of LWR Fuels*, Journal of Nuclear Materials, vol. 125, pp. 96-103 (1984).
19. L.E. Thomas, C.E. Beyer and L.A. Charlot, *Microstructural Analysis of LWR Spent Fuels at High Burnup*, Journal of Nuclear Materials, vol. 188 (1992).
20. J.C. Killeen, *The Effect of Additives on the Irradiation Behavior of UO_2*, Journal of Nuclear Materials, vol. 58, pp. 39-46 (1975).
21. J.C. Killeen, *Fission Gas Release and Swelling in UO_2 Doped with Cr_2O_3*, Journal of Nuclear Materials, vol. 88, pp. 177-184 (1980).
22. J.A. Turnbull, *The Effect of Grain Size on the Swelling and Gas Release Properties of UO_2 During Irradiation*, Journal of Nuclear Materials, vol. 50, pp. 62-68 (1974).
23. M. Mogensen, C.T. Walker, I.L.F. Ray and M. Coquerelle, *Local Fission Gas Release and Swelling in Water Reactor Fuel During Slow Power Transients*, Journal of Nuclear Materials, vol. 131, pp. 162-171 (1985).
24. H. Devold, *Characterization of Swelling Rates of high Burnup Fuel (IFA-515)*, OECD Halden Reactor Project Report HWR-252 (1990).
25. H. Zimmerman, *Investigations on swelling and fission gas behavior in uranium dioxide*, Journal of Nuclear Materials, vol. 75 (1978).
26. M.E. Cunnigham et al., *Development and Characteristics of the Rim Region in High Burnup UO_2 Fuel Pellets*, Journal of Nuclear Materials, vol. 188, pp. 19-27 (1992).
27. C.T. Walker et al., *Concerning the Microstructure Changes that Occur at the Surface of UO2 Pellets on Irradiation to High Burnup*, Journal of Nuclear Materials, vol. 188, pp. 73-79 (1992).
28. J.H. Harding and D.G. Martin, *A Recommendation for the Thermal Conductivity of UO_2*, Journal of Nuclear Materials, vol. 166 (1989).
29. Y. Phillipponeau, *Thermal Conductivity of $(U,Pu)O_{2-x}$ Mixed Oxide Fuel*, Journal of Nuclear Materials, vol. 188, pp. 194-197 (1992).
30. S.L. Hayes and K.L. Peddicord, *Radiative Heat Transfer in Porous Uranium Dioxide*, Journal of Nuclear Materials, vol. 202, pp. 87-97 (1993).
31. C. Ronchi and G.J. Hyland, *Analysis of Recent Measurements of the Heat Capacity of Uranium Dioxide*, Journal of Alloys and Compounds, vol. 213/214, pp. 159-168 (1994).
32. W. Wiesenack, M. Vankeerberghen and R. Thankappan, *As Assessment of UO_2 Conductivity Data Based on In-Pile Temperature Data*, OECD Reactor Project Report HWR-469 (1996).
33. M. Pihlatie, Thermal *Properties of High Burnup UO_2 Fuel Rods*, OECD Halden Reactor Project Report HWR-559 (1999).
34. P.G. Lucucta, H. Matzke and R.A. Verall, *Modeling of UO_2 based SIMFUEL thermal conductivity- the effect of burnup*, Journal of Nuclear Materials, vol. 223 (1995).
35. ASTM, *Standard Test Method for Atom Percent Fission in Uranium and Plutonium Fuel (Neodymium-148 Method)*, ASTM Designation: E 321-79 (Reapproved 1990) (1990).
36. I. Matsson, *ORIGEN2 Simulations of Spent BWR Fuel with Different Burnup, Power History and Initial Enrichment*, SKI Report 95:46 (1995).

37. M. Tarvainen, A. Bäcklin and A. Håkansson. *Calibration of the TVO spent BWR reference fuel assembly*, STUK Report, STUK-YTO-TR 37 (1992).
38. G. Pfennig, H. Klewe-Nebenius and W. Seelmann-Eggebert, *Karlsruher Nuklidkarte*, Forschungszentrum Karlsruhe GmbH (1998).
39. T.R. England and B.F. Rider, *Evaluation and Compilation of Fission Product Yields 1993*, Report LA-UR-94-3106, ENDF-349, Los Alamos National Laboratory (1994).
40. C.T. Walker, C. Bagger and M. Mogensen, *Observations on the release of cesium from UO_2 fuel*, Journal of Nuclear Materials, vol. 240 (1996).
41. I. Matsson, *Gammascanning of I and Cs at KKL*, ABB Atom Report BKD 95-132 (1995).
42. A. Massih, *Fission Gas Release*, ABB Atom Report BKC 94-010 (1994).
43. R. Lorenz, *ANS-5.4 fission gas release model III, low temperature release*, Proceedings of the ANS Topical Meeting on LWR Fuel Performance, Portland, Oregon, April 1979.
44. A.H. Booth, *Method of Calculating Fission Gas Diffusion from UO_2 Fuel and its Application to the X-2 Loop Test*, CRDC-721 (1957).
45. C. Vitanza, V. Graziani, N.T. Fødestrømmen and K.O. Vilpponen, *Fission Gas Release from In-Pile Pressure Measurements*, HPR-221.10 (Paper 38) (1978).
46. V. Fidleris, *Summary of experimental results on in-reactor creep and irradiation growth of zirconium alloys*, Atomic Energy Review, vol. 13 (1975).
47. L.O. Jernkvist and A. Massih, *Models for Fuel Rod Behaviour at High Burnup*, SKI Report 2005:41 (2004).
48. J. Bai, C. Prioul, J. Pelchat and F. Barcelo, *Effect of hydrides on the ductile-brittle transition in stress-relieved, recrystallised and β-treated Zry-4*, International Topical Meeting on LWR Fuel Performance, Avignon, France, April 21-24, 1991.
49. D. Gavillet, H. Bruchertseifer, Z. Kopajtic, R. Restani, E. Schenker and P. Schleuniger, *Post Irradiation Examination of two KKL pins. Oxide thickness measurement & Crud analysis*, Paul Scherer Institut Report TM-43-95-49 (1995).
50. K-Å. Magnusson, *Qualification of a method for oxide thickness measurement on fuel rods with magnetic crud deposits*, Westinghouse Atom AB Report BTM 00-079 (2000).
51. L. Sihver, M. Limbäck and B. Andersson, *How to Achieve Zero Failure Fuel*, Enlarged HPG meeting on High Burn-up Fuel performance, Safety and Reliability and Degradation of In-core Materials and Water Chemistry Effects and Man-machine Systems Research, Loen, Norway, May 24-29, 1999.
52. A. Johansson, *MAGNACROX-measurements of Crud Thickness and Correlations to Reactor Water Chemistry at KKL and CGS*, The Fuel Technology Programme Meeting, Västerås, March 3-4, 2004.
53. I. Matsson and B. Grapengiesser, *Nondestructive gamma measurements, KKL June 1996*, ABB Atom Report BUC 97-010 (1997).
54. K. Edsinger, A *Review of Fuel Degradation in BWRs*, Proceedings of the International Topical Meeting on Light Water Reactor Fuel Performance, Park City, Utah, USA, April 10-13, 2000.
55. B. Cheng, B.C. Oberländer, W. Wiesenack, S. Yagnik and J.A. Turnbull, *An In-Reactor Simulation Test to Evaluate Root Cause of Secondary Degradation of Defective BWR Fuel Rod*, Zirconium in the Nuclear Industry: Thirteenth International Symposium, West Conshohocken, PA, USA, 2002.
56. D. Schrire and K. Renström, *Development and Verification of ABB Atom's Zr-Sn Liner Cladding*, Proceedings of Jahrestagung Kerntechnik, Germany, 1994.

57. J.H. Huang and S.P. Huang, *Effect of hydrogen contents on the mechanical properties of Zircaloy-4*, Journal of Nuclear Materials, vol. 208, pp. 166-179 (1994).
58. M. Dahlbäck, L. Hallstadius, M. Limbäck, G. Vesterlund, T. Andersson, P. Witt, J. Izquierdo, B. Remartinez, M. Díaz, J.L. Sacedon, A.-M. Alvarez, U. Engman, R. Jacobsson and A.R. Massih, *The Effect of Liner Component Iron Content on Cladding Corrosion, Hydriding and PCI Resistance*, Proceedings of Zirconium in the Nuclear Industry: Fourteenth International Symposium, Stockholm, Sweden, June 14-17, 2004.
59. W. Wiesenack and T. Tverberg, *Irradiation of the Fuel Degradation Test IFA-622*, Report NFIR III/EPRI X103-20-01 (1996).
60. I. Matsson, *Experimental Procedure for IFA-631.1 Fuel Failure Degradation Test*, OECD Halden Reactor Project, EP-1631.1 (1998).
61. A. Håkansson and A. Bäcklin, *Procedure for HRGS Measurements of Spent Nuclear Fuel*, Department of Radiation Sciences, Uppsala University (1992).
62. B. Andersson and B. Grapengiesser, *Measurements on Fuel Assemblies from Cofrentes for Determination of Relative Power Distribution, March 2002*, Westinghouse Atom AB Report BTM 02-169 (2002).
63. G.F. Knoll, *Radiation detection and measurements*, John Wiley and Sons Inc., 2nd edition (1989).
64. K. Debertin and R.G. Helmer, *Gamma- and X-ray spectrometry with semiconductor detectors*, North-Holland, Elsevier Science B.V. (1988).
65. R.M. Lieder, H. Jäger, A. Neskakis and T. Venkova, *Design of a Bismuth Germanate Anti-Compton Spectrometer and its use in Nuclear Spectroscopy*, Nuclear Instruments and Methods in Physics Research, vol. 220, pp. 363-370 (1984).
66. P.J. Nolan, D.W. Gifford and P.J. Twin, *The Performance of a Bismuth Germanate Escape Suppressed Spectrometer*, Nuclear Instruments and Methods in Physics Research, vol. A236, pp. 95-99 (1985).
67. I. Matsson,, P. Jansson, B. Grapengiesser, A. Håkansson and A. Bäcklin, *Fission Gas Release Determination Using an Anti-Compton Shield Detector*, Nuclear Technology, vol. 122, pp. 276-283 (1998).
68. W.R. Leo, *Techniques for Nuclear and Particle Physics Experiments*, Springer Verlag (1987).
69. D. Reilly, N. Ensslin, H. Smith Jr. and S. Kreiner, *Passive Nondestructive Assay of Nuclear Material*s, Reports NUREG/CR-5550 and LA-UR-90-732, US Nuclear Regulatory Commission and Los Alamos National Laboratory (1991).
70. K-G. Görsten, Private communication, June 2003.
71. B. Grapengiesser and L. Hallstadius, *Non-destructive Pool-side Methods for Fission gas Release Determination and Fuel Column Characterisation of Intact fuel Rods*, Ninth International Conference on Nondestructive Evaluation in the Nuclear Industry, Tokyo, Japan, April 25-28, 1998.
72. T.R. Blair and L.F. Van Swam, *Nondestructive Determination of Fission Gas Release at Poolside*, Transactions of the American Nuclear Society, vol. 44, pp. 237-238 (1983).
73. P.M. O'Leary and D.R. Packard, *Nondestructive Fission Gas Release Measurement and Analysis*, Transactions of the American Nuclear Society, San Diego, California, June 20-24, 1993.
74. L.F. Van Swam, G.M. Bain, W.C. Dey, D.D. Davis and H. Heckerman, *BWR and PWR Fuel Performance at High Burnup*, Proceedings from the International Topical Meeting on LWR Fuel Performance, Portland, Oregon, USA, March 2-5, 1997.

75. B. Andersson, *Fission Gas Release Measurements in KKL 2003*, Westinghouse Electric Sweden AB Report BTM 03-137 (2003).
76. H.D. Kosanke, *Gamma Scan Measurements at Quad Cities 1 Following Cycle 4*, General Electric Report NEDC-25492 (1981).
77. L.M. Shiraishi and J.E. Thompson, *Comparison of Simulated Process Computer Calculations With Gamma Scan Measurements at Hatch 1 at End of Cycle 3*, Report EPRI NP-2107, Electric Power Research Institute (1984).
78. W. Harris, *Commonwealth Edison Company Topical Report Benchmark of BWR Nuclear Design Methods Quad Cities Gamma Scan Comparisons*, Report NFSR-0085 (1991).
79. I. Matsson, *Computer Simulation of the Relative Contribution to Measurement Efficiency for Gamma Scanning of Power in KKL*, Westinghouse Atom AB Report BUA 00-015 (2000).
80. S. Jakobsson, *Computer Simulation of the Relative Pin Contribution to Measurement Efficiency in a Gamma-Scanning Campaign in Leibstadt 2003*, Westinghouse Electric Sweden AB Report BTU 03-112 (2003).
81. W. Wiesenack and V. Hustadness, *Test-Fuel-Data-Bank System User Manual*, Halden Reactor Project Report HWR-338 (1993).
82. K. Svanholm, *In-Pile Power Calibration Methodology at the HBWR*, Halden Reactor Project Report HWR-559 (1998).
83. U. Kasemeyer and W.H. Beere, *Capabilities and verification of the HELIOS lattice code for the Halden Boiling Water Reactor (HBWR)*, Halden Reactor Project Report HWR-609 (1999).
84. P. Brohan, *A Study, using Noise Analysis, of Fuel thermo-mechanical behaviour in the High Burn-up MOX Experiment IFA 648.1 and the PWR/WWER Comparison Experiment IFA 503.2*, Halden Reactor Project Report HWR-607 (1999).
85. T. Tverberg, User *manual for program pf-drift on HP work-stations*, Halden Reactor Project F-Note 1330 (1996).
86. W. Wiesenack and T. Tverberg, *Irradiation Phase II of the Fuel degradation test IFA-622: operation with Steam and Power Ramping*, Report NFIR III/EPRI X103-20-04 (1997).
87. M. Mohsen, *A Compact Compton Suppression Spectrometer Using Bismuth Germanate Scintillator*, Nuclear Instruments and Methods, vol. 212, pp. 241-244 (1983).
88. G. Lysell and S. Bengtsson, *PIE on three Fuel Rods from Oskarshamn 3*, Studsvik Report HCL-113, STUDSVIK/N(H)-95/32 (1995).
89. B. Grapengiesser and D. Schrire, *Impact of systematic stochiometric differences among BWR rods on fission gas release*, IAEA Technical Committee Meeting on fission gas release and fuel chemistry related to extended burnup, Pembroke, Ontario, Canada, April 28-May 1, 1992.
90. B. Grapengiesser and I. Matsson, *Nondestructive gamma measurements, KKL August 1998*, ABB Atom Report BUA 99-062 (1999).
91. T. Eriksson, *Resultattolkning av digitalt registrerad aktivitetsfördelning i bränslestav*, ASEA-ATOM Report UK 86-498 (1986).
92. L. von der Burg, Private communication, 2000.
93. K. Lassman, C. O'Carroll, J. van der Laar and C.T. Walker, *The radial distribution of plutonium in high burnup UO fuels*, Journal of Nuclear Materials, vol. 208, pp. 223-231 (1994).
94. K. Lassman, *TRANSURANUS: a fuel rod analysis code ready for use*, Journal of Nuclear Materials, vol. 188, pp. 295-302 (1995).

95. J. Turnbull, C. Friskey, J. Findlay, F. Johnson and A. Walter, *The diffusion coefficients of gaseous and volatile species during the irradiation of uranium dioxide*, Journal of Nuclear Materials, vol. 107 (1982).
96. J. Turnbull, R. White and C. Wise, *The Diffusion Coefficient for Fission Gas Atoms in Uranium Dioxide*, Report IAEA-TC-659/3.5.
97. J. Turnbull, *An Assessment of Fission Gas Release and the Effect of Microstructure at High Burn-up*, OECD Halden Reactor Project Report HWR-604 (1999).
98. F. Garzarolli, *Waterside Corrosion on Zircaloy Fuel Rods*, Report EPRI-NP-2789, Electric Power Research Institute (1982).

Acta Universitatis Upsaliensis

Digital Comprehensive Summaries of Uppsala Dissertations from the Faculty of Science and Technology 191

Editor: The Dean of the Faculty of Science and Technology

A doctoral dissertation from the Faculty of Science and Technology, Uppsala University, is usually a summary of a number of papers. A few copies of the complete dissertation are kept at major Swedish research libraries, while the summary alone is distributed internationally through the series Digital Comprehensive Summaries of Uppsala Dissertations from the Faculty of Science and Technology. (Prior to January, 2005, the series was published under the title "Comprehensive Summaries of Uppsala Dissertations from the Faculty of Science and Technology".)

Distribution: publications.uu.se
urn:nbn:se:uu:diva-6912

ACTA
UNIVERSITATIS
UPSALIENSIS
UPPSALA
2006